ACTA UNIVERSITATIS SZEGEDIENSIS

ACTA
MINERALOGICA-PETROGRAPHICA

Tomus XLII

Szeged, 2001

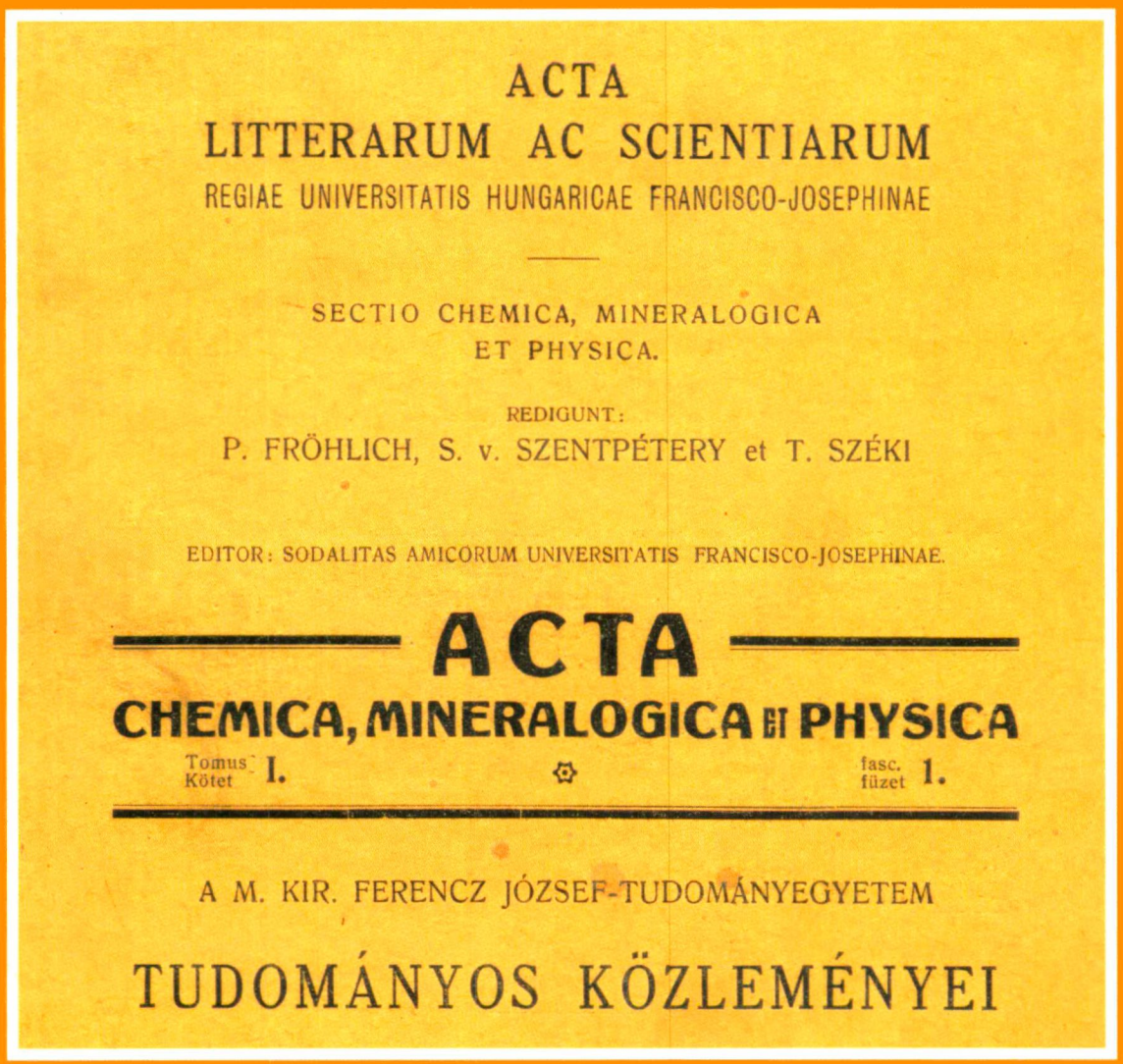

Published by the Department of Mineralogy, Geochemistry and Petrology, University of Szeged

ACTA MINERALOGICA-PETROGRAPHICA
established in 1922
HU ISSN 0365-8066

Short name of the journal:

Acta Miner. Petr., Szeged

The Acta Mineralogica-Petrographica is published by the Department of Mineralogy, Geocemistry and Petrology, University of Szeged

---

On the cover: The front page of Acta Chemica, Mineralogica et Physica (Vol. I., Part 1, 1928)

Acta Mineralogica-Petrographica, Szeged 2001, Vol. 42, pp.1-4

ACTA MINERALOGICA-PETROGRAPHICA: A PROMISING REVIVAL

ELEMÉR PÁL-MOLNÁR

AMP IN THE PAST

The Royal Hungarian Francis Joseph University [Magyar Királyi Ferencz József Tudományegyetem], that had been founded in Kolozsvár on 29th May, 1872, was closed down on 8th May, 1919 as a result of the prevailing political situation after World War I. Since Kolozsvár was lost due to the Treaty of Trianon, its university was moved temporarily to the town of Szeged following a 29th May, 1921 decision of the Hungarian Government. Here, on the fundaments laid down in Kolozsvár, the scientific work was revived, and already in 1922 the first journal of natural sciences was published by the Association of the Patrons of the University [Egyetem Barátai Egyesülete] as a section in the series of the Acta Litterarum ac Scientiarum Regiae Universitatis Hungariae Francisco-Josephinae [Scientific Bulletin of the Royal Hungarian Francis Joseph University]. The title of the section was Sectio Scientiarum Naturalium (Fig. 1). The scientific activity and capacity of the newly established Mineralogical and Geological Institute and Collection [Ásvány és Földtani Intézet és Gyűjteménytár] was proved by the fact that one of the three articles published in the first issue was dealing with magmatic petrography. This periodical was published in two volumes between 1922 and 1927, consisting of three and five parts. The first part of the first volume (1922 Tomus I. Fasc. 1) (Fig. 1) was edited by István Apáthy and Béla Pogány. The following three parts were edited by Béla Pogány, while the last four (between 1924 and 1927) were the work of István Győrffy and Rudolf Ortvay. The language of the articles was German and Hungarian.

In 1928 still as a part of the former Sectio Scientiarum Naturalium, published in the Acta Litterarum ac Scientiarum Regiae Universitatis Hungariae Francisco-Josephinae, a new section was established under the name of Sectio Chemica, Mineralogica et Physica. Its journal was the Acta Chemica, Mineralogica et Physica. The new journal (Fig. 2) started a new numbering, and consisted of articles whose subject related to chemistry, mineralogy, geology or physics. Between 1928 and 1940 seven volumes were published with sixteen parts. The language of the articles was still German and Hungarian, however, those which were written in German usually contained a summary in Hungarian, as well. Between 1928 and 1934 the journal was edited by Pál Fröhlich, Tibor Széki and petrographist Zsigmond

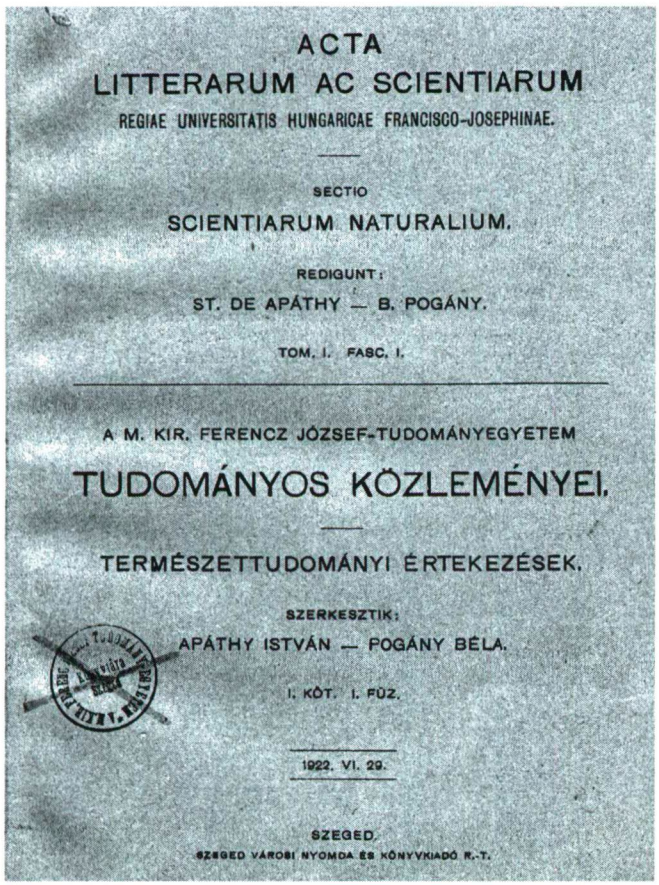
ACTA
LITTERARUM AC SCIENTIARUM
REGIAE UNIVERSITATIS HUNGARICAE FRANCISCO-JOSEPHINAE.
SECTIO
SCIENTIARUM NATURALIUM.
REDIGUNT:
ST. DE APÁTHY — B. POGÁNY.
TOM. I. FASC. I.
A M. KIR. FERENCZ JÓZSEF-TUDOMÁNYEGYETEM
TUDOMÁNYOS KÖZLEMÉNYEI.
TERMÉSZETTUDOMÁNYI ÉRTEKEZÉSEK.
SZERKESZTIK:
APÁTHY ISTVÁN — POGÁNY BÉLA.
I. KÖT. I. FÜZ.
1922. VI. 29.
SZEGED,
SZEGED VÁROSI NYOMDA ÉS KÖNYVKIADÓ R.-T.

Fig. 1. The cover of the first issue of Acta Litterarum ac Scientiarum, Sectio Scientiarum Naturalium (Vol. I., Part 1, 1922)

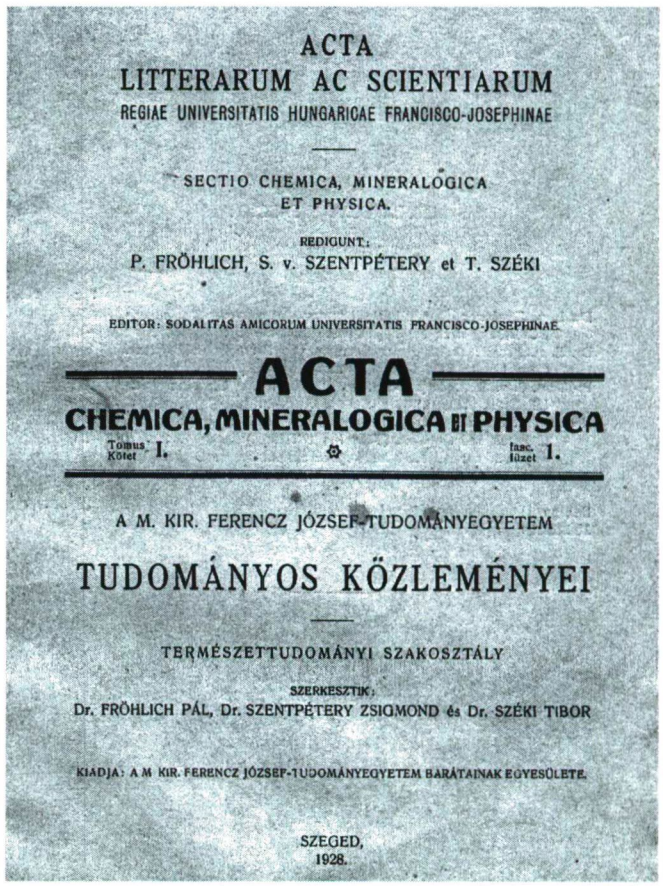
ACTA
LITTERARUM AC SCIENTIARUM
REGIAE UNIVERSITATIS HUNGARICAE FRANCISCO-JOSEPHINAE
SECTIO CHEMICA, MINERALOGICA
ET PHYSICA.
REDIGUNT:
P. FRÖHLICH, S. v. SZENTPÉTERY et T. SZÉKI
EDITOR: SODALITAS AMICORUM UNIVERSITATIS FRANCISCO-JOSEPHINAE.
ACTA
CHEMICA, MINERALOGICA ET PHYSICA
Tomus I. Fasc. 1.
A M. KIR. FERENCZ JÓZSEF-TUDOMÁNYEGYETEM
TUDOMÁNYOS KÖZLEMÉNYEI
TERMÉSZETTUDOMÁNYI SZAKOSZTÁLY
SZERKESZTIK:
Dr. FRÖHLICH PÁL, Dr. SZENTPÉTERY ZSIGMOND és Dr. SZÉKI TIBOR
KIADJA: A M. KIR. FERENCZ JÓZSEF-TUDOMÁNYEGYETEM BARÁTAINAK EGYESÜLETE.
SZEGED,
1928.

Fig. 2. The cover of Acta Chemica, Mineralogica et Physica (Vol. I., Part 1, 1928)

Szentpétery, who was a private-professor at the Mineralogical and Geological Institute and Collection. In 1935 the form of the journal significantly changed (Fig. 3), besides, a new member, Árpád Kiss was taken into the editorial board, though, in 1936 Tibor Széki quitted. Between 1939 and 1940 only some minor modifications appeared in the form.

World War II. brought changes both in the history of the university and the journal. The Royal Hungarian Francis Joseph University was placed back to Kolozsvár, while in Szeged a new institution, the Royal Hungarian Miklós Horthy University [Magyar Királyi Horthy Miklós Tudományegyetem] was established. In 1940 two new institutes evolved from the former Mineralogical and Geological Institute and Collection. These were the Mineralogical and Petrographical Institute [Ásvány-Kőzettani Intézet], the leader of which was mineralogist Sándor Koch, and the Geological Institute [Geológiai Intézet].

The series of the Acta Litterarum ac Scientiarum Regiae Universitatis Hungariae Francisco-Josephinae discontinued, and it was replaced by a new series, the Acta Universitatis Szegediensis [Bulletin of the University of Szeged]. In 1942 the journal of the Natural Science Section, the Acta Chemica, Mineraloogica et Physica was divided into two, the Acta Chemica et Physica and the **Acta Mineralogica-Petrographica**. Between 1942 and 1947 due to the war the AMP was published only once in 1943 (Fig. 3). Concerning the form, there were not any significant changes compared to the previous volumes, the language remained German and Hungarian. Mineralogist Sándor Koch became the editor-in-chief by this time.

In 1945 the name of the university changed to University of Szeged [Szegedi Tudományegyetem]. Concerning not only the name but the form and the content too, the first really novel volume of the Acta Mineralogica-Petrographica (AMP volume II.) (Fig. 4) was published in 1948. Sándor Koch remained the editor-in-chief, nevertheless, English appeared beside German as a new language of articles. From 1952 the articles written in English were sporadically followed by summaries in Russian. In 1962 the university took up the name of its former student, the famous poet, Attila József. Between 1943 and 1962 fifteen volumes of AMP were published.

In 1963 (volume 16, part 1) a new technical editor, geochemist Gyula Grasselly started his work beside Sándor Koch. The AMP applied the volume-part system again. The co-editor in chief already of two parts in volume 17 and the first part in volume 18 was Gyula Grasselly. From the second part of volume 17 (1968) till 1975 the edition work was carried out by him alone. Meanwhile, in 1967 the name of the Mineralogical and Petrographical Institute was changed to the Institute of Mineralogy, Geochemistry and Petrography [Ásványtani, Geokémiai és Kőzettani Intézet].

In 1976 with the second part of volume 22 a new editorial board was established, the members were Kálmán Balogh and József Mezősi. In 1977 Tibor Szederkényi replaced József Mezősi. In the same year the name of the Institute was

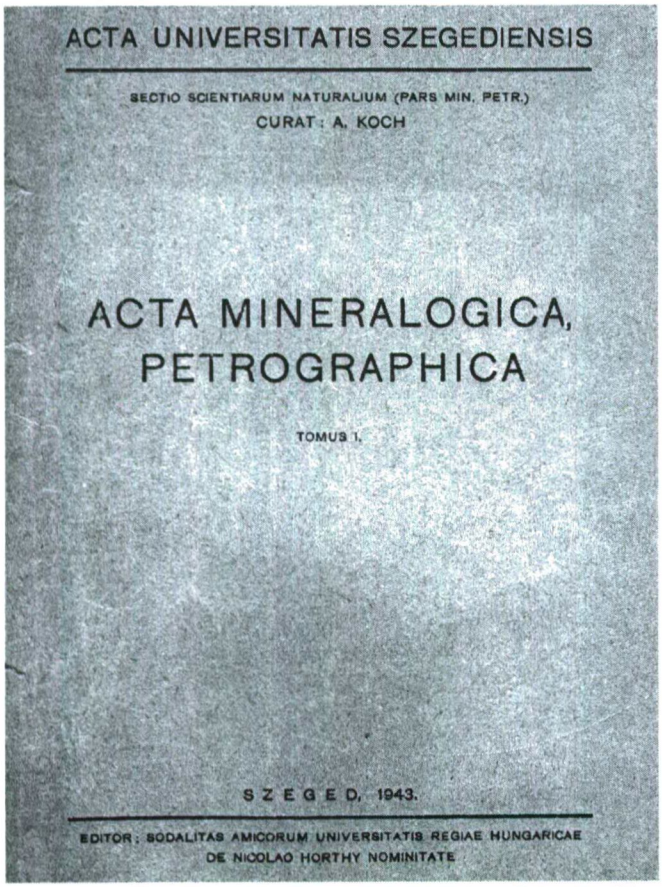

Fig. 3. The 1943 cover of Acta Mineralogica, Petrographica (Vol. I., 1943)

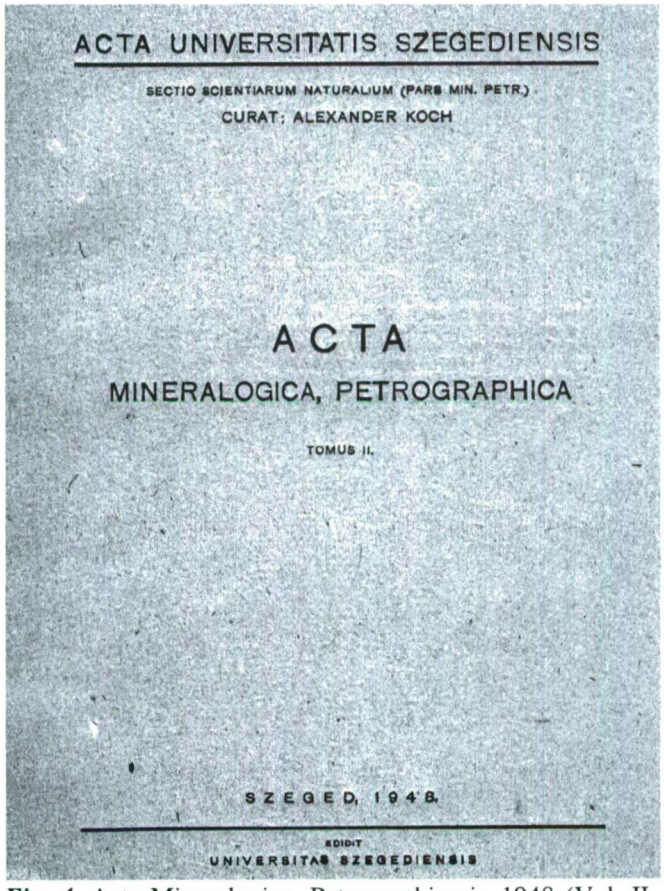

Fig. 4. Acta Mineralogica, Petrographica in 1948 (Vol. II., 1948)

changed to Department, i.e. Department of Mineralogy, Geochemostry and Petrography [Ásványtani, Geokémiai és Kőzettani Tanszék]. Since 1976 English has been the only language of AMP.

Between 1979 and 1986 the editor-in-chief was still academician Gyula Grasselly. The editorial board was formed by Tibor Szederkényi and Béla Molnár.

Between 1963 and 1986 usually each volume consisted of two parts.

In 1987 Tibor Szederkényi became the new editor-in-chief of the AMP. A new editorial board was established as well with Imre Kubovics, Frigyes Egerer, Gyula Szöőr, Béla Kleb, later Pál Gyarmati. This team edited the AMP between 1987 and 2000.

AMP IN THE FUTURE

By the unification of the institutions functioning in the town the University of Szeged [Szegedi Tudományegyetem] has been reborn in 2000. Between 1948 and 2000 the costs of the edition of the AMP was mostly covered by the Faculty of Natural Sciences. After 2000 the subsidy ceased, since the university was unwilling to support the Acta Universitatis Szegediensis, hence, the further existence of several periodicals, including the AMP, has become doubtful. The question arose: Will the publication of the nearly 80 year old AMP come to an end? In this critical situation the leadership of the Department of Mineralogy, Geochemistry and Petrology felt that something has to be done. The only Hungarian periodical of clear mineralogical and petrographical image must not die! Finally, the Department has taken on the edition of the AMP, and decided to finance the publication and the distribution as well. Of course, the decision means a huge financial burden, since the AMP has been and will be distributed mainly for free, or in exchange for other periodicals. The editor-in-chief and the new associate editor will do a voluntary work for the journal, while the Department will do its best to firmly meet the expenses of the publication and the distribution. Besides, the leadership of the Department of Mineralogy, Geochemistry and Petrology decided to reform the journal and to create a modern and up-to-date periodical. As a first step the establishment of a new editorial board was suggested, because the former one has been unchanged since 1987. The editor in chief remained Dr. Tibor Szederkényi, though, he is going to be helped by a new associate editor, Dr. Elemér Pál-Molnár. The 2001 volume was more or less edited in the former way by the old board. The members of the new editorial board in the transitional 2001 volume were Hungarian experts, however, the board of the 2002 volume is planned to involve significant representatives of the field from the whole Carpathian Basin (Rumanian, Ukrainian, Slovakian, Czech, Austrian, Slovenian, Croatian and Serbian experts).

The AMP endeavours to publish those novel scientific results that are mainly related to researches carried out in Hungary and in the Alpine-Carpathian-Dinaric region. Of course, the editorial board does accept papers dealing with other regions as well, let they be compiled either by Hungarian or foreign authors.

The new editorial board of the AMP and the Department of Mineralogy, Geochemistry and Petrology would like to thank the editorial board operating between 1987 and 2000 for their great work.

The Editorial Board between 1987 and 2000

Prof. Tibor Szederkényi University of Szeged, Szeged, Hungary	petrology, environmental geology, fissile material exploration
Prof. Imre Kubovics Eötvös Loránd University, Budapest, Hungary	petrology, geochemistry, vulcanology cosmopetrology, cosmogeochemistry
Dr. György Buda Eötvös Loránd University, Budapest, Hungary	petrology, mineralogy
Dr. Frigyes Egerer University of Miskolc, Miskolc, Hungary	mineralogy, petrology, petrophysics
Dr. Pál Gyarmati University of Debrecen, Debrecen, Hungary	geology
Dr. Szöőr Gyula University of Debrecen, Debrecen, Hungary	geochemistry
Dr. Béla Kleb Technical University of Budapest, Budapest, Hungary	environmental geology, engineering geology

ACTA
Mineralogica
Petrographica

The new Editorial Board

Acta Mineralogica-Petrographica, Szeged 2001, Vol. 42, pp. 5-20

ACTA Mineralogica Petrographica

AGE, GEOCHEMISTRY AND ORIGIN OF PERALUMINOUS A-TYPE GRANITOIDS OF THE ABLAH-SHUWAS PLUTON, ABLAH GRABEN, ARABIAN SHIELD

MOHAMMED RASHAD H. MOUFTI

Faculty of Earth Sciences, King Abdulaziz University
P.O. Box 80206, Jeddah-21589, Saudi Arabia

ABSTRACT

The A-type granitoids of the Ablah-Shuwas pluton, situated in the Ablah graben of the Asir terrane, occur as discontinuous ring complexes, cone sheets and irregular bodies. They intrude into the younger diorite and tonalite rocks of probably 744±22 Ma old. Their emplacement is contemporaneous with the movement (~610 Ma or later) along the Umm Farwah shear zone, which cuts the eastern margin of the rift-related epiclastic and volcanic complex of the Ablah group. The whole rock Rb-Sr isochrons indicate shear zone compatible ages of 617±17 and 605±5 Ma for the syenites and quartz syenites-granites, respectively. The low initial $^{87}Sr/^{86}Sr$ ratios (0.7035-0.7038) in the A-type granitoids indicate either a mantle origin or a Rb-depleted crustal source.

The granitoids show the petrological and geochemical characteristics of a typical A-type granite. They are composed of suites of cogenetic syenites, quartz syenites, and syenogranites with iron- and alkali-rich silicates, high FeO^t/MgO and Ga/Al ratios. They show the marked enrichment of high field strength elements (Zr, Nb, Y and Ga), Zn, and Na_2O+K_2O and depletion in CaO and MgO with a large negative Ba anomaly.

The origin of A-type granitoids is related with the Umm Farwah shear zone that trigger off partial melting in the volatiles and LIL-enriched metasomatized mantle. The rise of this mantle flux through reactivated; deep-seated; heat-laden shearzones/faults caused crustal fusion in the arc-related lower mafic and upper volcano-plutonic crust of intermediate to felsic compositions to produce A-type granitoids.

Key words: A-type granitoids, Ablah-Shuwas pluton, Ablah-graben, Asir terrane, Umm Farwah shear zone, ring complexes, syenites, quartz syenites, syenogranites, metasomatized mantle, crustal fusion.

INTRODUCTION

The Arabian Shield mainly developed and cratonized in the Neoproterozoic (~950-550 Ma) as a results of subduction-related volcano-plutonic arc magmatism and their related sedimentation (~950-715 Ma) followed by arc/backarc and microplate accretion and continental collision (715-640 Ma), filling of intracratonic rifts, and post-accretion magmatism and tectonism (640-550 Ma) (Stoeser, Camp, 1985; Jackson, 1986; Greene 1993).

The Arabian Shield alkali-feldspar granites of the post-accretion magmatism are considered as A-type (anorogenic) granites (Stoeser, 1986). The tectonic environment of the alkali-feldspar granites that emerge late in orogenic cycles is used as a basis of classification (Loiselle, Wones, 1979; Collins et al., 1982; Pitcher, 1982). Stoeser (1986) described that the post-orogenic magmatism of the Arabian A-type granites was continued for about 70 years after accretion. He subdivides the alkali-feldspar granite that constitutes about 7% of all plutonic rocks of the Shield into: biotite and (or) hornblende alkali-feldspar granite; alkali granite; and aluminous granites.

Detailed petrological studies of the plutonic rock associations of the post-accretion stage in the western part of the Arabian Shield (central Hijaz: Jackson et al., 1984; Jackson, 1986; Midyan region: Ramsay et al., 1986) and eastern part (southern Najd province: Dodge, 1979; Kanaan, 1979; Stuckless et al., 1982, 1983; Le Bel, LaVal, 1986; Du Bray, 1986) reveal the domination of at least three types of felsic plutonic rock associations: 1) monzogranite and granodiorite with high Ca and Mg contents; 2) syenogranite and monzogranite with moderate Ca and Mg contents; and 3) alkali-feldspar granite and quartz-alkali-feldspar syenite with very low Ca and Mg contents. The major difference found between eastern and western felsic plutonic rocks was the widespread occurrence of low-Ca, low-Mg, high FeO_t alkali granites in the western part. Jackson et al. (1984) grouped the high Ca granites of the monzogranite association with I-type rocks and the alkali granite and alkali-feldspar granite association with A-type.

The term 'A-type' was defined by Loiselle, Wones (1979) to differentiate 'mildly alkaline' rocks (A-type) from typical calc-alkaline (I-type) rocks with anhydrous character of magmas. The other geochemcial characteristics of the A-type granites, which are discussed by several workers (Loiselle, Wones, 1979; Whalen et al., 1987; King et al., 1997; Pearce et al., 1984; Hermes et al., 1981; Collins et al., 1982) are high ratios of $FeO(t)/(FeO(t)+MgO)$, F/H_2O, and Ga/Al, high contents of Na_2O+K_2O, highly charged cations such as Ga, Zr, Nb, Y, and trivalent rare earth elements (REE^{3+}) and Zn, and lower abundances of Mg, Ca, and Fe-Mg trace elements (Cr, V, Ni,Cu) and Sr with significant Ba and Eu anomalies.

A-type granitoids are typically metaluminous but peralkaline and peraluminous A-types also occur. Whalen et al. (1987) and Bonin (1988) included calc-alkaline and peralkaline rocks in their A-type group, respectively. Brown et al. (1984) included the alkaline to alkali-calcic and peralkaline rocks in their A-type category. Based on distinctive field, chemical and petrographic characteristics, King et al. (1997) strongly opposed the inclusion of

peralkaline rocks in the category of A-type granites. A-type granitoids from the southwestern part of the Indian Peninsula are designated as ultrapotassic aluminous A-type granitoids on account of high contents of $K_2O/Na_2O>2$, $K_2O>3$ wt.% (Foley et al., 1987) and Al_2O_3 (14 to 19 wt%).

A-type granitoids are reported from a variety of tectonic settings such as rift environment (e.g., Oslo graben: Sundvoll, 1978; Yemen rift: Capaldi et al., 1987); intra-continental ring complexes (e.g., the anorogenic complex of Evisa, Corsica: Boninet et al., 1978; alkaline complexes of Sudan: Black et al., 1985); hotspots or plume environment (e.g., White Mountain batholith, New Hampshire: Eby et al., 1992; Ras ed Dom ring complex, Sudan: O'Halloran, 1985); and post-collisional or post-orogenic settings (e.g., Gabo and Mumbulla suites of the Lachlan fold belt, Australia: Collins et al., 1982; Topsails complex, Newfoundland: Whalen et al., 1987b; granites of the western Adirondacks, USA: Whitney, 1992; Homrit Waggat complex, Egypt: Hassanen, 1997). Rocks classified as A-type granitoids generally include large group of rocks such as syenite, quartz syenite, granites, rapakivi granites, etc.

In the present investigation, new geochemical and Sr isotopic data are presented for the A-type granitoids of the Ablah-Shuwas pluton, situated in the Ablah graben of the Asir terrane. The results obtained from this investigations are used to determine the nature and probable origin of these A-type granitoids.

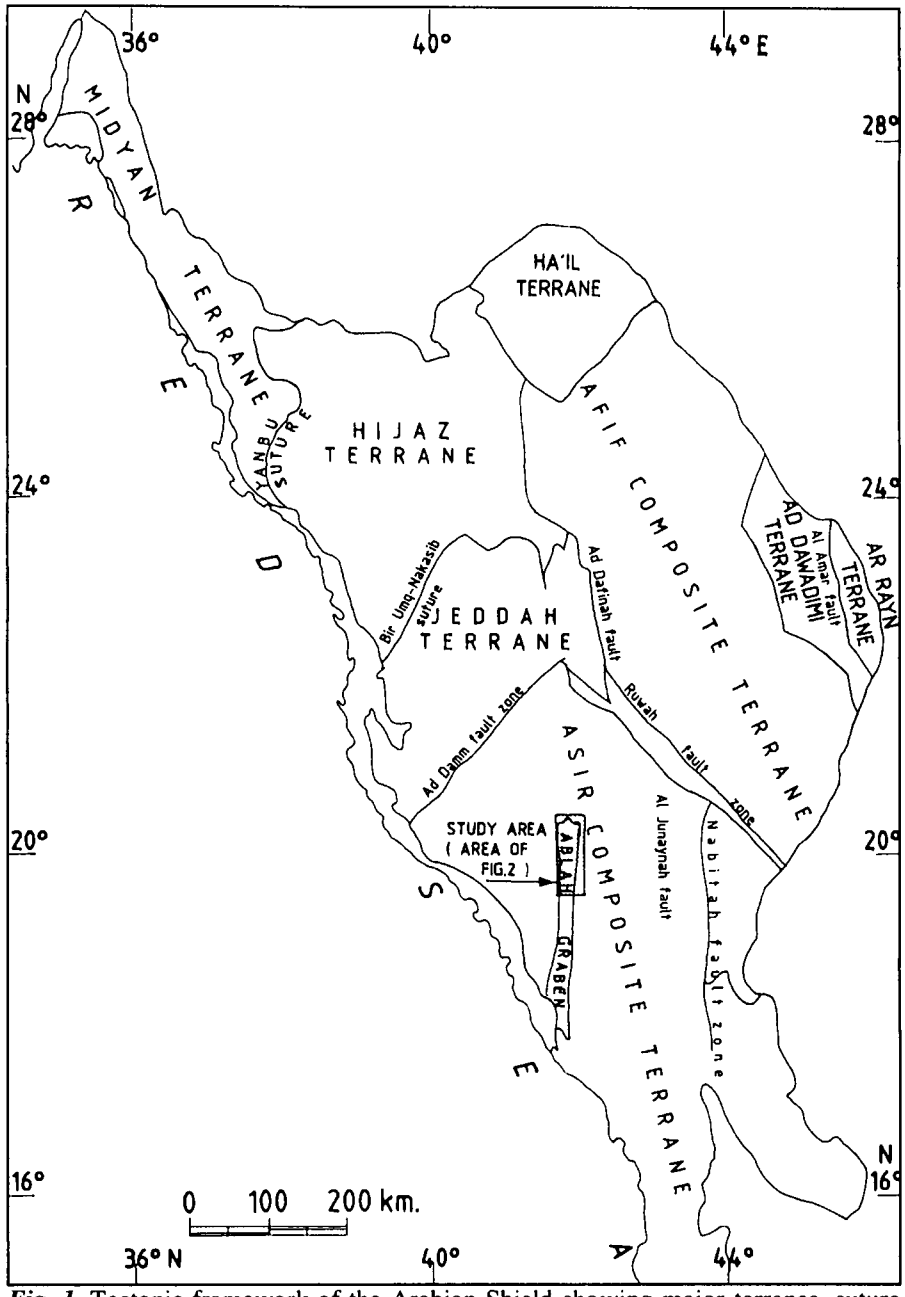

Fig. 1. Tectonic framework of the Arabian Shield showing major terranes, suture zones, location of Ablah graben and the study area (after Stoeser, Camp, 1985; Johnson, 2000).

TECTONIC AND GOLOGIC SETTING

The Arabian Shield is thought to have formed by accretion of intra-oceanic island arcs, back-arc basin complexes, and allochthonous continental blocks or microplates mainly during Pan-African time (about 680-640 Ma) (Stoeser et al., 2001; Johnson, 2000; Camp, 1984; Stoeser, Camp, 1985). This complex tectonic history formed the Neoproterozoic (about 900- ~570) Arabian Shield crystalline basement, composed of: (1)deformed and metamorphosed volcano-sedimentary assemblages of oceanic plateau, mid-oceanic-ridge, intraoceanic and continental-margin tholeiitic and calc-alkaline volcanic arcs, epicontinental volcano-sedimentary rocks, and back-arc, pull-apart and graben assemblages; (2) vast amount of orogenic plutonic rocks such as gabbro, diorite, quartz diorite, tonalite, trondjeminte and granodiorite; and (3) synorogenic, post-orogenic and anorogenic granites such as tonalite, trondhjemite, granodiorite, gabbro, granite and syenite (Johnson, 2000; Stoeser, 1986).

The latest tectonic model divides the Arabian Shield into eight distinct geological terranes separated mostly by ophiolite-decorated suture zones (Fig. 1). The four ensimatic terranes: Asir composite, Jeddah, Hijaz, and Midyan, occur in the west, whereas the four continental affinity terranes: Afif composite, Ad Dawadimi, Ar Rayn and Hail, crop out in the east.

The A-type granitoids of the Ablah-Shuwas pluton, which are exposed in the Ablah graben are part of the oceanic Asir composite terrane that forms north-trending belts of arc-related meta-volcanosedimentary and orogenic plutonic rocks. Three principle layered arc assemblages in the Ablah-Shuwas area are, from east to west, the Qirsha and Khutna formations and the Ablah group (Fig. 2).

A major submeridian fault marked by serpentinite separates Ablah group from the Khutna formation (Donzeau, Beziat, 1989).

The orogenic younger diorite-tonalite rocks, which are exposed in the Jabal Ibrahim quadrangle (GM-96 C, Sheet 20E; Cater, Johnson, 1987) are represented by at least three groups of plutons, two of them are trending in northeast direction and the third one in the northwest. They intrude at the contact between the Khutnah formation and the Ablah group.

The anorogenic (post–tectonic) A-type granitoids, which occur in three phases as successive rings, cone sheets and irregualr bodies, intrude the northeast trending Ablah-Shuwas diorite-tonalite pluton (Fig. 3). The complex forms an elliptical pluton of about 16 km long and as much as 6 km wide. Greenwood (1975) classified the A-type granitoids into late- to post-tectonic, granodiorite and monzogranite. Fleck et al. (1980) reported a Rb-Sr whole rock age of 636±21 Ma (initial $^{87}Sr/^{86}Sr$=0.7035) for this A-type granitoids. The same rocks, which occur about 3 km southwest of the studied pluton, produced Rb-Sr ages of 617±10 Ma and 630±10 Ma (Brown et al., 1978; Greenwood, 1975).

The Qirsha and Khutnah formations and their related diorite-tonalite intrusive rocks represent an island-arc complex, which is probably developed between 750 and 720 Ma (Cater and Johnson, 1986). They consist of sheared and altered volcanic and volcaniclastic rocks of tholeiitic and calc-alkalic composition (Bokhari, Kramers, 1981). Donzeau, Benziat (1989) assigned the Qirsha and Khutna formations to the Jeddah group (> 800 Ma). The 11-point errochron Rb-Sr age of 721±55 Ma and a Nd-Sm age of 757±256 are reported for metavolcanic rocks of Qirsha (Surgah) formation (Bokhari, Kramers, 1981). A Rb-Sr age of 744±22 Ma is determined (Marzouki et al., 1982) for the younger diorite-tonalite rocks of the Tharad pluton, which occurs northwest of the Ablah-Shuwas pluton.

The Ablah group consists mainly of epiclastic sedimentary and volcanic complex, deposited unconformably on the adjacent volcanic arc complex. The

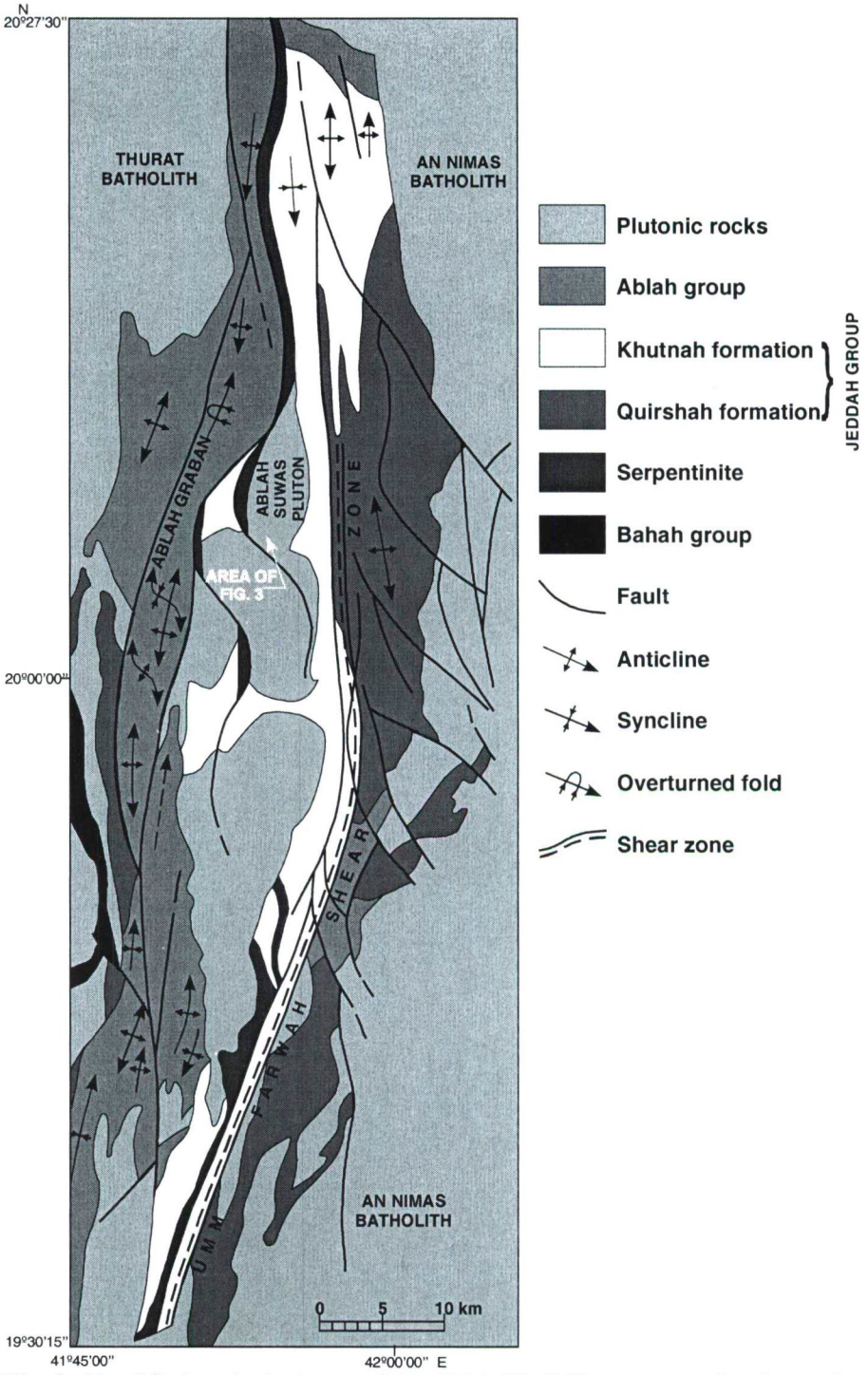

Fig. 2. Simplified geological map of the Ablah-Wadi Shuwas area showing major geologic units and Umm Farwah dextral shear zone (after Donzeau, Beziat, 1989; Johnson, 2000).

bimodal volcanism in the Ablah graben indicates a continental-rift or back-arc environment in relation to adjacent Qirsha and Khutnah volcanic arc, which is characterized by mafic to felsic volcanism (Donzeau, Beziat, 1989). The Ablah-belt or Ablah volcanic rift (Greenwood et al., 1982) is about 150 km long, north-south trending graben of extensional tectonic regimes in the Arabian Shield (Fig.1). The rocks of the Ablah group are strongly folded about north-south axes, and are strongly metamorphosed to greenschist and amphibolite facies. They were intruded by 778 and 746 Ma (Cooper et al., 1979) tonalite gneiss in the south, while the volcanic unit of the belt in the north produced an age of 721 Ma (Bokhari, Kramers, 1981).

The volcanic Jerub formation of Ablah group in the north yielded a Pb/Pb zircon depositional age of 641±1 Ma (Johnson, 2000).

PETROGRAPHY

The model abundances of the Shuwas A-type granitoids are given in Table 1. The model quartz-alkali feldspar-plagioclase (QAP) data plotted on the diagram (Fig. 4a) shows syenite, quartz-syenite and syenogranite rock compositions.

Quartz syenite and syenogranite

The quartz syenite is a holocrystalline rock with hypidiomorphic granular texture. It is composed of alkali feldspar (50-55%), plagioclase (10-25%), quartz (9-15%), hornblende (4-7%), and biotite (5-8%), with accessory sphene, apatite, magnetite and iron oxides. Alkali feldspar is represented by subhedral to anhedral orthoclase perthite and microcline perthite. Perthitic intergrowth and carlsbad and cross-hatch twinning is common in alkali feldspar. K-feldspar is slightly altered to clay minerals. Plagioclase feldspar (~14 An%) is mainly subhedral to anhedral in form and is dominated by oligoclase. It is mainly found as intergrowths within the orthoclase and microcline. Quartz is present as subhedral crystals containing inclusions of perthite. The prismatic or rhombic hornblende crystals are euhedral to subhedral in form and are locally altered to chlorite and epidote. It is strongly pleochroic with X=yellowish green and Y=Z= olive green, and shows simple twinning. Biotite occurs as prismatic crystals. It is also strongly pleochroic with X=yellowish brown and Y=Z= dark brown. Sphene occurs as rhombic or granular shape, subhedral to anhedral and light brown in color. Apatite forms euhedral to subhedral grains with prismatic or six-sided shape. It is found as inclusions in biotite, hornblende and even sphene.

The major difference between quartz syenite and syenogranite is the high contents of quartz (15-25%) at the expense of alkali feldspar (45-50%), domination of biotite over hornblende and the presence of muscovite and rutile as additional accessories in the syenogranite.

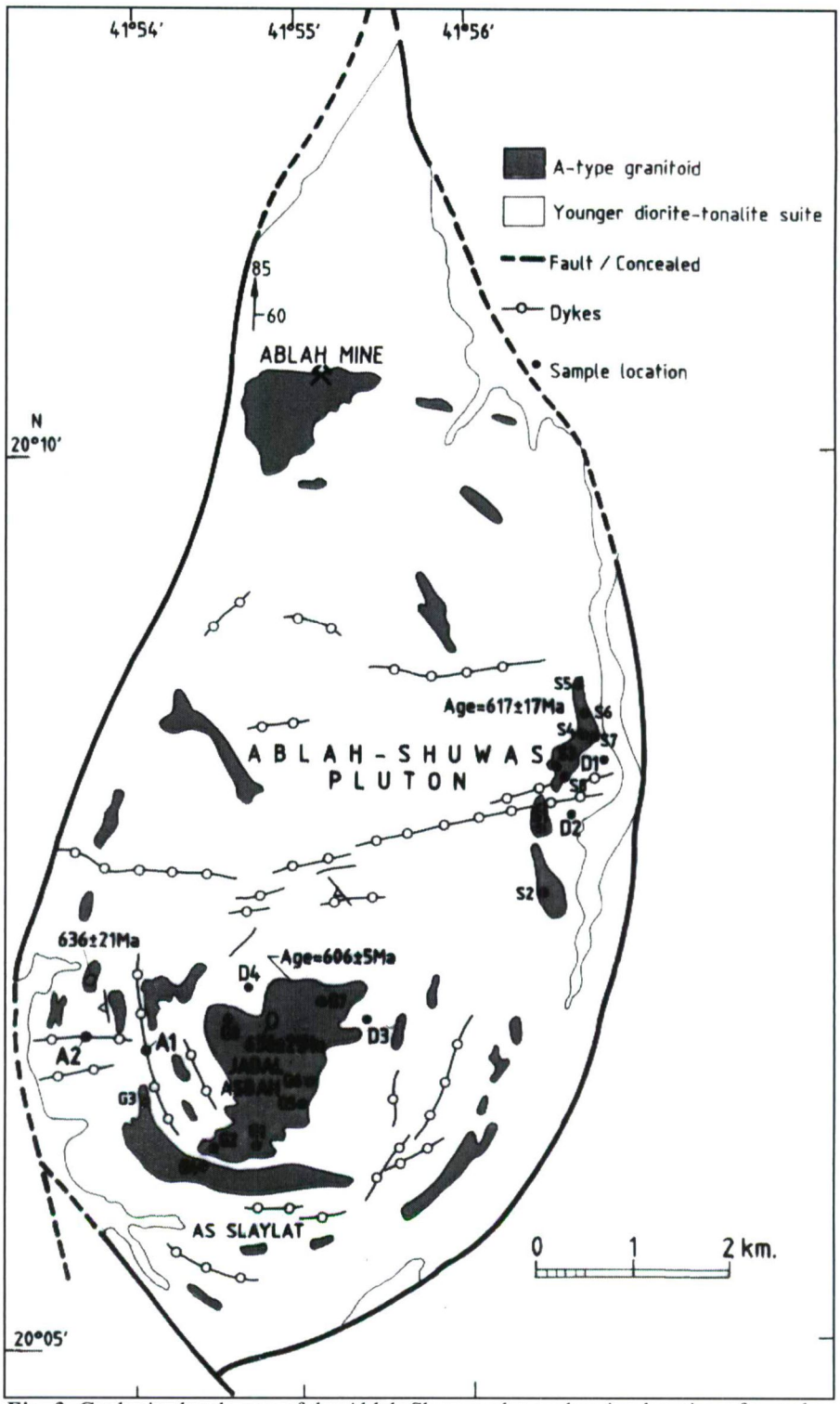

Fig. 3. Geologic sketch map of the Ablah-Shuwas pluton showing location of samples, discontinuous ring dike structure and irregular bodies of A-type granitoids (after Greenwood, 1975).

The syenite

The syenite consists mainly of alkali feldspar (55-69%), plagioclase (15-21%), hornblende (2-8%; average (n=8)=5.9%), biotite (1-10%; average (n=8)=3.75), and quartz (2-5%) with accessory sphene, rutile, apatite, zircon, iron oxides and opaque minerals. The syenites are holocrystalline with hypidomorphic granular texture; dominated by perthitic orthoclase and microcline; sodic plagioclse altered slightly to sericite and twinned on the albite law; and hornblende.

Table 1. Model analyses (volume percent) of A-type granitoids of the Ablah-Shuwas pluton.

Minerals	Syenite								Quartz Syenite					Syenogranite		
	S-1	S-2	S-3	S-4	S-5	S-6	S-7	S-8	G-1	G-4	G-5	G-6	G-7	G-2	G-3	G-8
Orthoclase	30	31	25	30	26	25	30	30	30	20	20	20	20	25	20	30
Microcline	30	30	35	35	40	36	34	39	20	35	30	30	34	20	31	20
Plagioclase	20	19	20	21	19	19	21	15	20	20	20	20	23	25	18	10
Quartz	3	3	5	4	5	5	3	2	15	14	14	10	9	15	22	25
Hornblende	8	2	8	7	5	8	8	7	7	4	6	6	4	3	2	5
Biotite	5	10	2	1	1	5	3	3	4	3	5	8	5	8	5	6
Sphene	2	-	2	1	2	2	2	1	3	3	3	4	2	3	2	3
Apatite	-	-	-	-	-	-	-	-	1	1	1	2	1	1	1	1
Iron oxides	2	5	3	3	2	3	2	2	-	-	-	-	-	-	-	-
Rutile	1	1	1	-	-	-	-	1	-	-	-	-	-	-	-	-
Zircon	-	-	-	-	2	-	-	-	-	-	-	-	-	-	-	-

GEOCHEMISTRY AND GEOCHRONOLOGY

Analytical methods

Major and trace element and Sr isotopic ratios were determined at the Faculty of Earth Sciences, King Abdulaziz University by XRF on pressed powder pellets. Accuracy is estimated as better than 3% for major elements and 5 to 8% for most of the trace elements. Rb and Sr concentrations for geochronological work were determined by XRF following the method of Pankhurst, O'Nions (1973).

Sr isotopic ratios were determined on a Isomass 54 E mass spectrometer. Standard value obtained during the course of this investigation is: $^{87}Sr/^{86}Sr = 0.710260 \pm 0.00004$ (n=16) for NBS 987 normalized to a $^{87}Sr/^{86}Sr=0.1194$. Isochron/errochron was calculated by the regression analysis of York (1969). Errors are

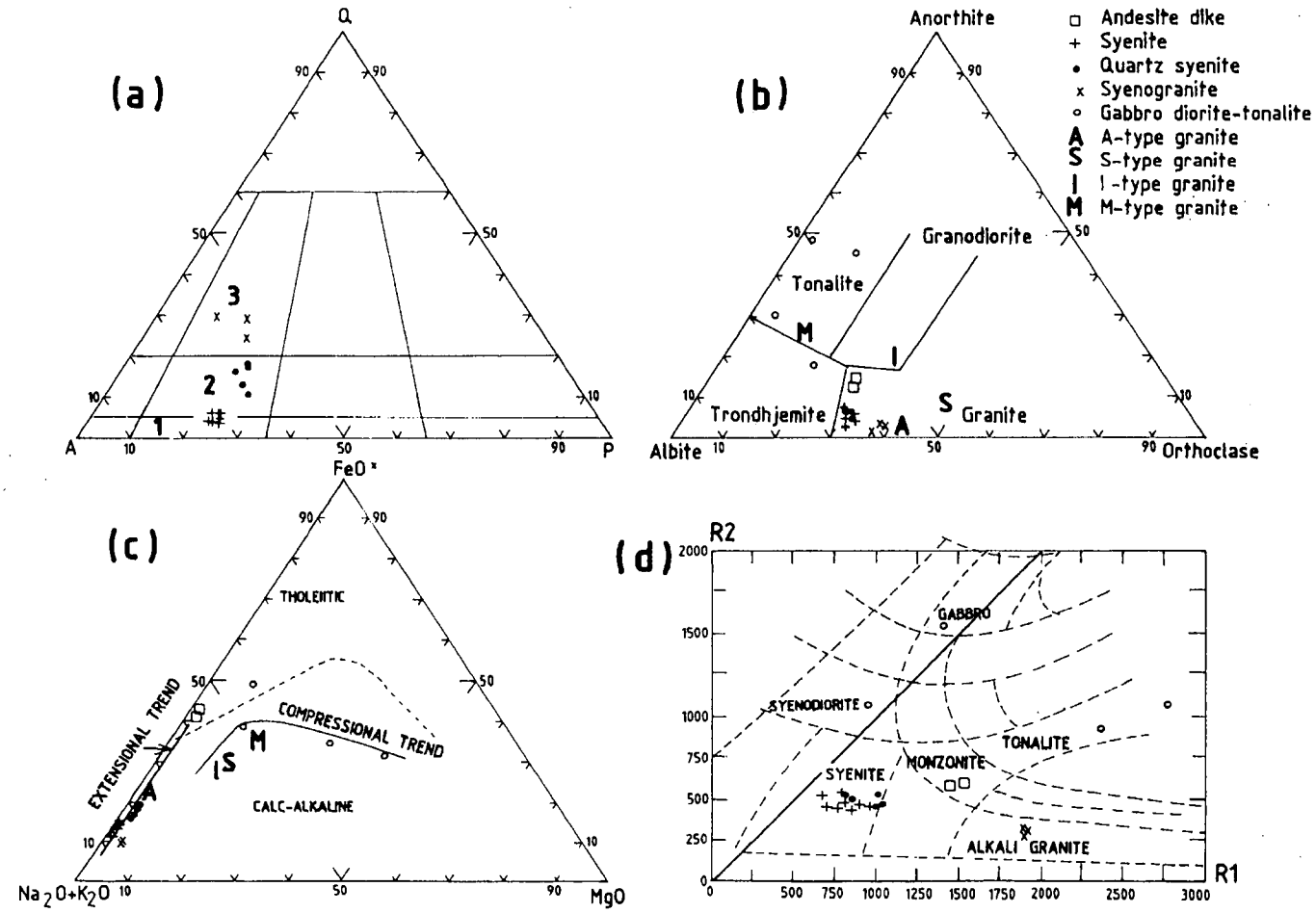

Fig. 4. The plutonic rocks of the Ablah-Shuwas pluton including A-type granitoids are plotted in : **(a)** Modal quartz-alkali feldspar-plagioclase (QAP) ternary diagram (Streckeisen, 1976), fields and petrographic nomenclature are as follows: 1=syenite; 2=quartz syenite; 3=syenogranite; **(b)** Normative An-Ab-Or diagram (Barker, 1979); **(c)** AFM diagram (Irvine, Baragar, 1971) showing trends of extensional and compressional plate boundaries (Petro et al., 1979) and **(d)** R1-R2 multicationic diagram (De La Roche et al., 1980) showing classification of granitoid rocks. The average values of A-, S- and I-type (Lachlan fold belt; Whalen et al., 1987) and M-type (Uasilau-Yau Yau complex, New Britain; Whalen, 1985) are used for comparison purposes.

quoted at the 2-sigma level. The ^{87}Rb decay constant used is $1.42\times10^{-11}\times$ a -1 (Steiger, Jager, 1977). The goodness of fit of the regression line is quoted as the MSWD (Mean Square of Weighted Deviates) of McIntyre et al. (1966), calculated here as the ratio of "chi-squared to degree of freedom" (chi-squared/(N-2). The cut-off point between isochron (MSWD <2.5) and errochron (MSWD >2.5) was made following the methods of Brook et al. (1972).

A total of 22 samples have been analyzed for major and trace elements. Out of these, 16 samples are from the A-type granitoids, 4 from the host orogenic diorite-tonalite complex, and 2 from the trachytic andesite dyke. The results are listed in Table 2. The comparison data of the studied average A-type granitoids with M-, A-, I-, and S-type granites from the Uasilau-Yau Yau complex, New Britain, PNG and the Lachlan fold belt of Australia are given in Table 3.

Geochemistry

All A-type granitoids (syenite, quartz syenite and syenogranite) of the Ablah-Shuwas pluton show restricted range of SiO_2 content from 63.90 to 65.71 wt.% in the syenite and quartz syenite and 71.46 to 72.16 wt.% in the syenogranite. All rock samples fall within the granite field on an An-Ab-Or diagram (Fig. 4b) The host gabbro-diorite-tonalite plots mostly in the tonalite field. The average compositions of the S-, I-, M-, and A-type granitoids plotted on an An-Ab-Or diagram are from data cited in Whalen et al. (1987). The host rocks are plotted as M-type and the Wadi Shwas A-type granitoids are plotted close to the average A-type granites.

The syenites and quartz syenites are characterized by high Na_2O/K_2O values (average 1.37) and Al_2O_3 content (average 18.49 and 17.36, respectively), and can be considered as high Al_2O_3 A-type granitoids. The syenogranites have average $Na2O/K_2O$ and Al_2O_3 values of 1.07 and 15.18, respectively.

On the AFM diagram (Fig. 4c), the A-type granitoids and dyke rocks are plotted very close to AF-side with parallel trend, which is a characteristic feature of the rocks developed in

Table 2. Major (in wt.%) and trace (in ppm) element concentrations for A-type granitoids, host diorite-tonalite and dyke rocks from the Ablah-Shuwas pluton.

Sample No.	S-1	S-2	S-3	S-4	S-5	S-6	S-7	S-8
				Syenites				
SiO_2	63.74	63.93	65.88	64.04	65.82	64.66	64.14	64.53
TiO_2	0.45	0.53	0.31	0.34	0.37	0.38	0.58	0.47
Al_2O_3	18.38	18.53	18.41	18.55	18.68	18.83	18.35	18.15
Fe_2O_3	2.09	2.12	1.62	2.23	1.74	1.82	2.07	1.89
MnO	0.04	0.03	0.03	0.05	0.05	0.03	0.04	0.04
MgO	0.06	0.07	0.06	0.08	0.07	0.07	0.07	0.07
CaO	1.81	0.98	0.67	1.07	0.98	0.96	1.27	0.89
Na_2O	6.60	6.41	6.64	6.53	6.44	6.56	6.56	6.51
K_2O	4.54	4.77	4.80	4.84	4.54	4.81	5.07	5.13
P_2O_5	0.08	0.10	0.06	0.06	0.06	0.06	0.09	0.08
H_2O^+	0.70	0.48	0.12	0.18	0.20	0.09	0.50	0.27
H_2O^-	0.07	0.07	0.07	0.07	0.06	0.08	0.07	0.10
Total	98.56	98.02	98.67	98.04	99.01	98.35	98.81	98.13
				Trace elements (ppm)				
Rb	140	136	132	137	127	138	129	133
Sr	197	70	35	130	57	68	147	61
Y	31	25	38	47	35	18	36	35
Ga	-	26	20	22	-	-	14	32
Zr	329	554	933	1085	876	956	815	943
Nb	12	17	12	12	12	12	20	12
Ba	-	456	194	285	457	-	0	680
Cr	9	7	9	6	6	8	9	9
Ni	6	8	8	8	8	8	8	8
Co	9	8	9	7	9	8	8	8
Sc	3	5	4	4	4	3	4	4
Cu	22	23	17	31	24	23	18	66
Zn	99	74	73	117	75	116	94	122
Mo	1.8	1.2	1.06	1.87	1.87	1.87	1.14	1.36
K/Rb	269	291	302	293	297	289	326	320
Rb/Sr	0.71	1.94	3.77	1.05	2.23	2.03	0.88	2.18
Ga/Al	-	2.65	2.05	2.24	-	-	1.44	3.33
Rb/Ba	-	0.30	0.68	0.48	0.27	-	-	0.20
Y/Nb	2.58	1.47	3.17	3.92	2.92	1.50	1.80	2.92
ZNY	372	596	983	1144	923	986	871	990

(- = not determined)

Table 2. continued

Sample No.	G-1	G-4	G-5	G-6	G-7	G-2	G-3	G-8
		Quartz syenite				Syenogranite		
SiO_2	65.24	64.37	64.80	64.32	65.71	71.66	71.46	72.16
TiO_2	0.54	0.62	0.54	0.55	0.50	0.21	0.21	0.26
Al_2O_3	17.45	17.38	18.06	17.88	16.82	15.24	15.63	14.66
Fe_2O_3	2.31	2.73	2.46	2.48	2.98	1.24	1.30	1.43
MnO	0.06	0.08	0.07	0.06	0.04	0.04	0.04	0.04
MgO	0.42	0.42	0.41	0.42	0.42	0.44	0.46	0.42
CaO	1.17	1.37	1.29	1.37	1.15	0.45	0.52	0.37
Na_2O	6.22	6.22	6.20	6.47	6.14	4.81	4.93	5.18
K_2O	4.40	4.56	4.45	4.47	4.69	4.73	4.71	4.49
P_2O_5	0.06	0.09	0.08	0.08	0.07	0.04	0.04	0.04
H_2O^+	0.34	0.34	0.25	0.30	0.37	0.15	0.34	0.26
H_2O^-	0.08	0.05	0.07	0.07	0.08	0.08	0.04	0.06
Total	98.29	98.23	98.68	98.47	98.97	99.09	99.68	99.37

Table 2. continued

Sample	G-1	G-4	G-5	G-6	G-7	G-2	G-3	G-8
Trace elements (ppm)								
Rb	127	128	126	144	139	134	139	131
Sr	304	234	364	277	202	159	164	57
Y	35	39	34	36	32	32	34	26
Ga	33	-	26	25	29	16	43	26
Zr	669	683	711	740	606	415	378	317
Nb	22	27	12	25	12	17	19	13
Ba	526	515	144	205	51	508	-	719
Cr	8	8	7	8	7	7	6	6
Ni	8	8	8	8	8	8	8	8
Co	7	5	7	6	7	9	8	8
Sc	4	3	5	4	2	5	3	3
Cu	40	46	37	33	38	15	26	31
Zn	155	201	136	166	107	115	150	129
Mo	1.4	1.3	1.5	1	108	1.3	1.3	1.3
K/Rb	288	296	293	258	280	293	281	285
Rb/Sr	0.42	0.55	0.35	.052	0.69	0.84	0.85	2.30
Ga/Al	3.57	-	2.72	2.64	3.26	1.98	5.20	3.35
Rb/Ba	0.24	0.25	0.88	0.70	2.72	0.26	-	0.18
Y/Nb	1.59	1.44	2.83	1.44	2.67	1.88	1.79	2.0
ZNY	726	749	757	801	650	464	421	356

Table 3. Comparison of average major and trace element concentrations of Ablah-Shuwas A-type granitoids with M-type (1-Uasilau-Yau Yau complex, New Britain; Whalen, 1985) and A-, I-, and S-type granites (2-Lachlan fold belt of Australia; Whalen et al., 1987).

Sample	Average A-type granites (this Study)	(1) Average M-type granites (17)	(2) Average A-type granites (148)	(2) Average I-type granites (991)	(2) Average S-type granites (578)
SiO_2	66.03	67.24	73.81	69.17	70.27
TiO_2	0.43	0.49	0.26	0.43	0.48
Al_2O_3	17.56	15.18	12.40	14.33	14.10
Fe_2O_3	2.03	1.94	1.24	1.04	0.56
FeO	1.42	2.35	1.58	2.29	2.87
MnO	0.05	0.11	0.06	0.07	0.06
MgO	0.25	1.73	0.20	1.42	1.42
CaO	1.02	4.27	0.75	3.20	2.03
Na_2O	6.15	3.97	4.07	3.13	2.41
K_2O	4.69	1.26	4.65	3.40	3.96
P_2O_5	0.07	0.09	0.04	0.11	0.15
Trace elements (ppm)					
Rb	134	17.5	169	151	217
Sr	158	282	48	247	120
Y	33	22	75	28	32
Ga	20	15	25	16	17
Zr	688	108	528	151	165
Nb	16	1.3	37	11	12
Ba	296	263	352	538	468
Ni	8	2	<1	7	13
Sc	4	15	4	13	12
Cu	31	42	2	9	11
Zn	121	56	120	49	62
K/Rb	290	598	229	187	151
Rb/Sr	0.85	0.06	3.52	0.61	1.81
Ga/Al	0.60	1.87	3.75	2.10	2.28
Rb/Ba	0.45	0.07	0.48	0.28	0.46

extensional plate margins (Petro et al., 1979). The host gabbro-diorite-tonalite rocks show compressional trend, which is nearly perpendicular to the FM-side.

Chemical data of the Ablah-Shuwas pluton plotted in the multi-cationic R1-R2 [4Si - 11(Na+K) - 2(Fe+Ti) - 6Ca + 2Mg + Al] diagram (Fig. 4d; De La Roche et al., 1980) show a broad chemical range of plutonism from mafic to felsic. The host rocks are plotted in the gabbro-syenodiorite-tonalite fields and the A-type rocks in the syenite/quartz syenite and alkali granite fields. The dyke rocks show quartz monzonite composition.

Major and trace element data have been plotted in Harker diagrams (Fig. 5A-B). The Ablah-Shuwas pluton ranges from gabbro to granite (51-72 wt% SiO_2). The host gabbro-diorite-tonalite rocks show scatter on the variation diagram, whereas A-type granitoids show two different restricted ranges of SiO_2 contents: syenite (63.9-65.7) and syenogranite (71.46-72.16). The A-type granitoids are characterized by high contents of Na_2O, K_2O, Al_2O_3, Zr, Nb, Y and Zn compared to host rocks, which are enriched only in the Fe, CaO, Mg and Sr contents. The A-type granitoids do not show any statistically significant correlation between SiO_2 and Na_2O, K_2O, Mg, Al_2O_3, TiO_2, MnO, Zr, Ga, Nb, Y, Zn, Ba and Rb. The Fe and Sr in the syenite and the CaO in the quartz syenite display statistically significant negative correlation with SiO_2 (Fig. 5A-B). In the Harker diagram, the average M-type granites from New Britain (Whalen, 1985) and the I-, S-, and A-type granites from Lachlan fold belt of Australia (Whalen et al., 1987 and unpublished data of B.W.Chappell) are plotted for comparison. The Ablah-Shuwas A-type granitoids are high in Na_2O, Al_2O_3, TiO_2, CaO, Zr and Sr, low in SiO_2, Fe, Y, Nb and almost identical in K_2O, Mg, MnO, Rb, Ga, Ba and Zn compared to average A-type granitoids. They overlap in composition with average I- and S-types granitoids with respect to TiO_2, MnO, Nb, Y, Ba, Sr and Rb and M-type with respect to Sr, Ba and TiO_2.

In the FeO(T)/(FeO(T)+MgO versus SiO_2 plot (Fig. 6) of Maniar and Piccoli (1989), the Ablah-Shuwas A-type granitoids (syenite and quartz

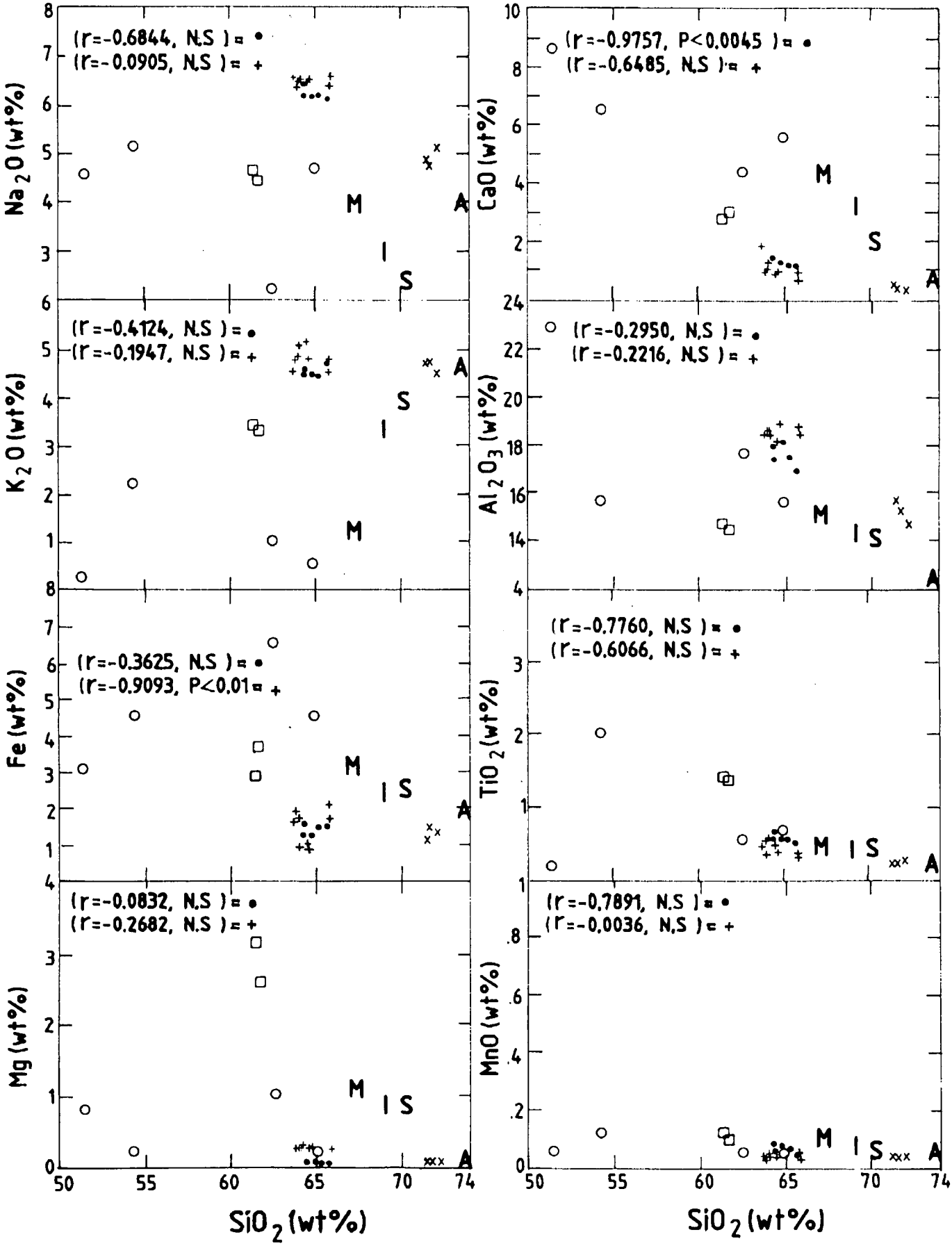

Fig. 5A. Harker variation diagrams for major element compositions. Symbols as in Fig. 4.
(r = Correlation Coefficient, N.S. = Not Significant, p= Level of Significance =< 0.05)

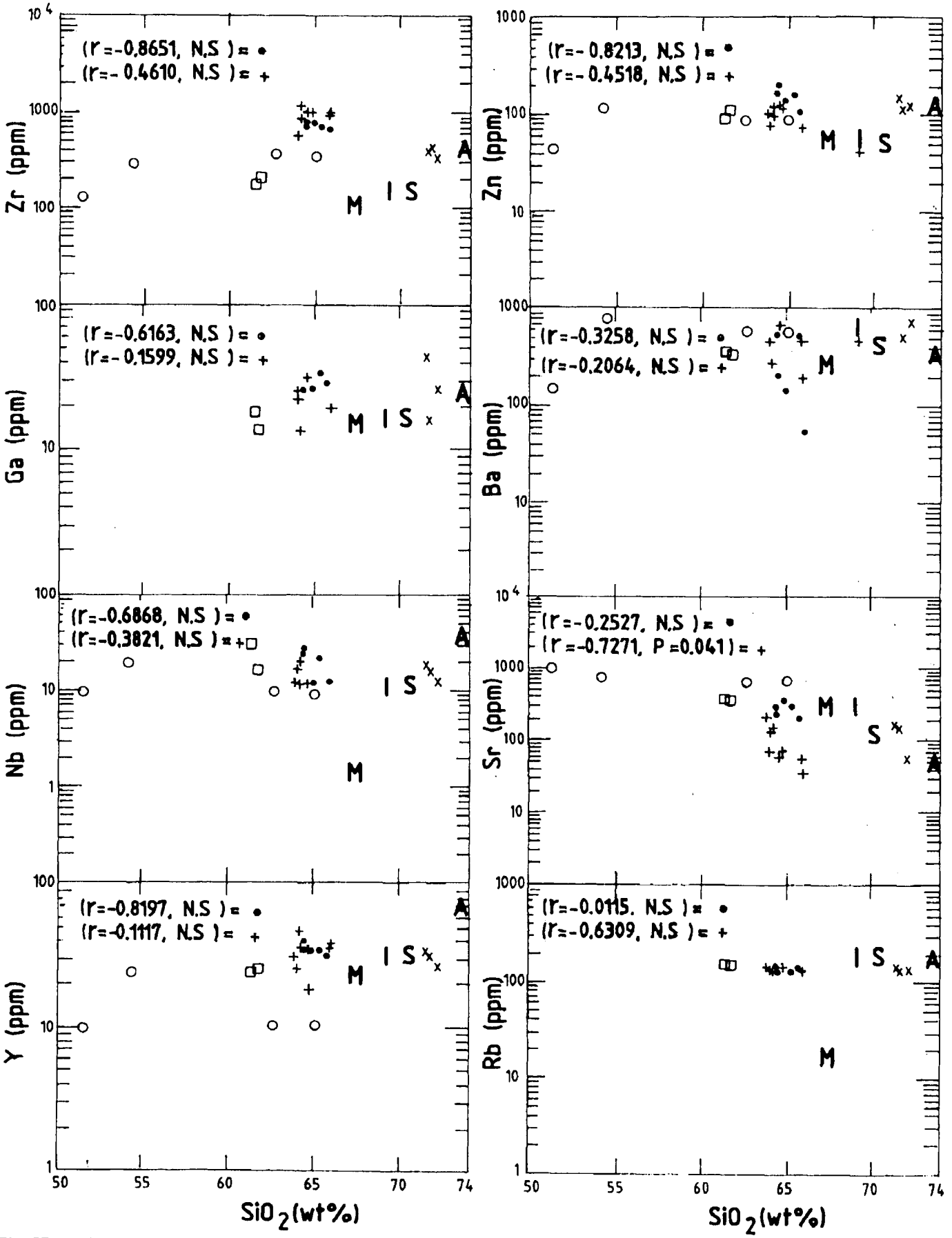

Fig. 5B. Harker variation diagrams for some trace element compositions. Symbols as in Fig. 4.
(r = Correlation Coefficient, N.S. = Not Significant, p= Level of Significance =< 0.05)

syenite) plot in the field of anorogenic rift-related or continental epiorogenic granitoids. The average values of M-, I-, and S-type granitoids (Whalen et al., 1987), are similar in composition to orogenic granitoids, whereas the average A-type granites exhibit anorogenic or rift-related setting.

In a ZNCY (Zr+Nb+Ce+Y) versus FeO^*/MgO and $(K_2O+Na_2O)/CaO$ granite discrimination diagrams (Fig. 7A-B; Whalen et al., 1987), the granitoids plot in the field of A-type granites. The average values of orogenic granites (M-, I- and S-types) are clearly discriminated in these diagrams. The Ablah-Shuwas A-type granitoids range from slightly metaluminous to peraluminous and do not show any correlation between the A/CNK (molar $Al_2O_3/CaO+Na_2O+K_2O$) and ZNCY indices (Fig. 7C). The highest concentration of ZNCY is found in the syenites followed by quartz syenite and syenogranite.

Whalen et al. (1987) found the good discrimination between A-type granites and the M-, I- and S-type by using Ga/Al versus Zr diagram (Fig. 7D). In this diagram, the studied granitoids plot in the A-type field and away from the I- and S-type field boundaries. The peraluminous nature of the granitoids lowered the Ga/Al ratios, so many samples are plotted well over the 10000*Ga/Al boundary of I- and S-type granites.

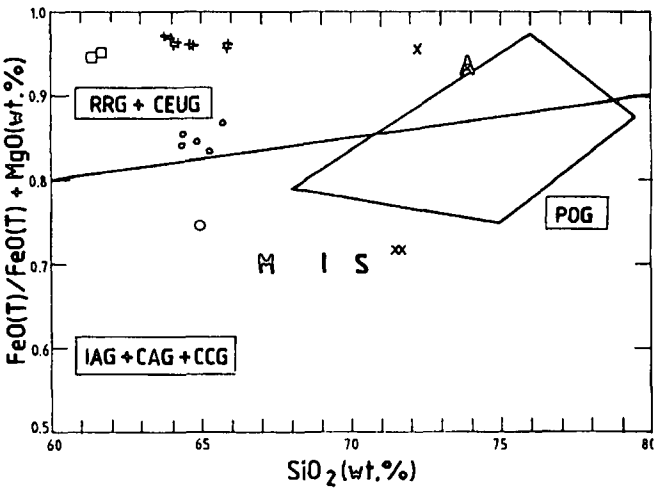

Fig. 6. FeO(T)/(FeO(T)+MgO) versus SiO_2 granitoid tectonic discrimination diagram (Maniar, Piccoli, 1989). RRG=rift-related granitoids; CEUG=continental epirogenic uplift granitoids; IAG=island arc granitoids; CAG=continental arc granitoids and; CCG=continental collision granitoids. Symbols as in Fig. 4.

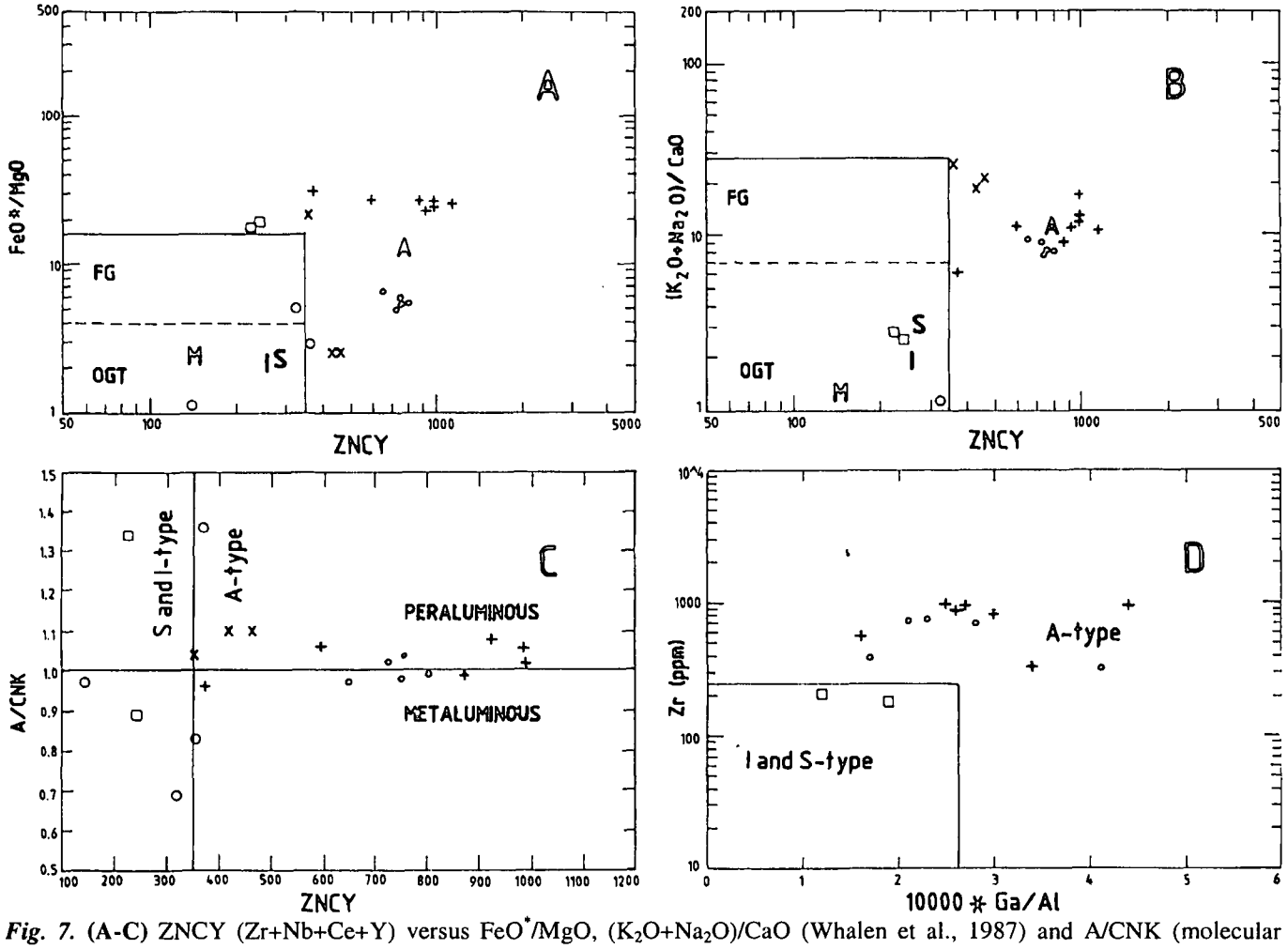

Fig. 7. **(A-C)** ZNCY (Zr+Nb+Ce+Y) versus FeO^*/MgO, $(K_2O+Na_2O)/CaO$ (Whalen et al., 1987) and A/CNK (molecular values of $Al_2O_3/(CaO+Na_2O+K_2O)$; Condie 1991) plots showing the A-type characteristics for the syenite, quartz syenite and syenorgranite rocks of the Ablah-Shuwas pluton. **(D)** 10000*Ga/Al versus Zr plot for various phases of the Ablah-Shuwas pluton. Symbols as in Fig. 4.

Eby (1992) divided the A-type granitoids into A_1 and A_2 chemical groups, based on tectonic affiliations (A_1=truly anorogenic rifting; A_2=post-orogenic) and the Y/Nb ratios to differentiate between mantle (Y/Nb <1.2) and crustal (Y/Nb>1.2) origin. The studied A-type granitoids have Y/Nb ratios ranging from 1.4 to 3.92, and they plot clearly in the A_2 granite field in the Rb/Nb-Y/Nb binary and Nb-Y-Ga*3 ternary diagrams (Fig. 8A-B). This affiliation is consistent with the studied A-type granitoids' postcollisional or postorogenic environment and the derivation of the magma largely from arc-derived Pan-African mafic to intermediate continental crust.

In Rb-Y+Nb and Nb-Y granite discrimination diagrams (Fig. 9A-B; Pearce et al., 1984), the studied A-type granitoids show a limited distribution in the field of within plate granites (i.e. A-type granite, Whalen et al., 1987). This reflects the depletion of Y and Na elements compared to A-type granites from the Lachlan fold belt of Australia (Whalen et al., 1987).

All three rock types (syenite, quartz syenite, and syenogranite) of the A-type suite and the host rocks of the Ablah-Shuwas pluton normalized to ocean ridge granite values (ORG; Pearce et al., 1984), are shown in Fig. 10. All three rock type of the A-type suite exhibit almost identical patterns of elements distribution. They are enriched in LIL-elements (K_2O, Rb and Ba) relative to HFS-elements (Nb, Zr, Y). The most characteristic features of the A-type granitoids are a large negative Ba anomaly especially in the quartz syenites, Ba apart, significantly enriched Zr and Sr abundances, and a lesser values of Nb and Y.

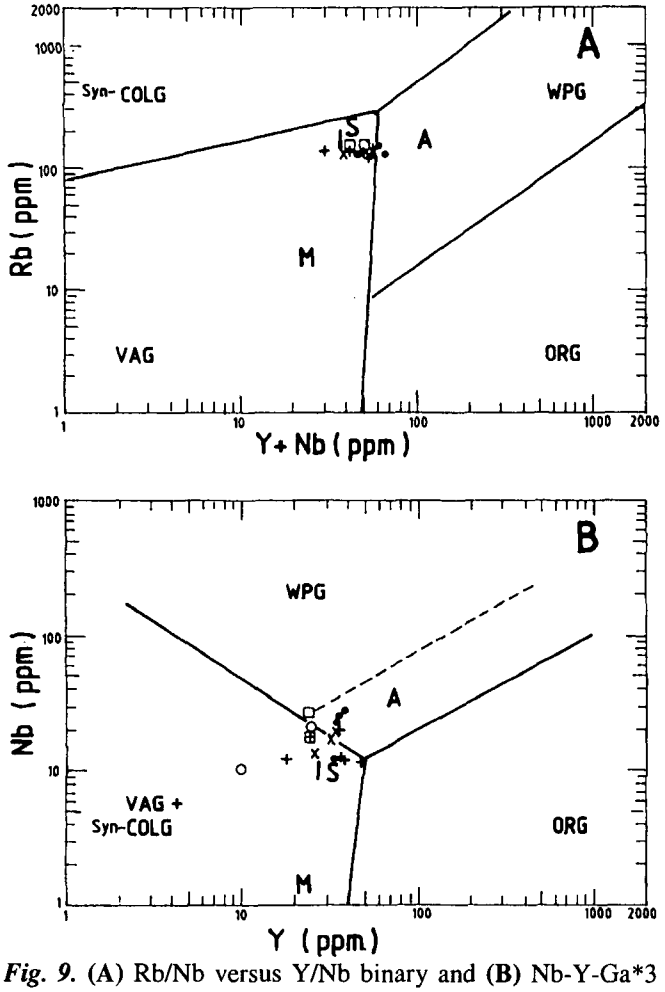

Fig. 9. (**A**) Rb/Nb versus Y/Nb binary and (**B**) Nb-Y-Ga*3 ternary diagrams (Eby, 1992) to distinguish between A_1 and A_2 granitoids. Symbols as in Fig. 4.

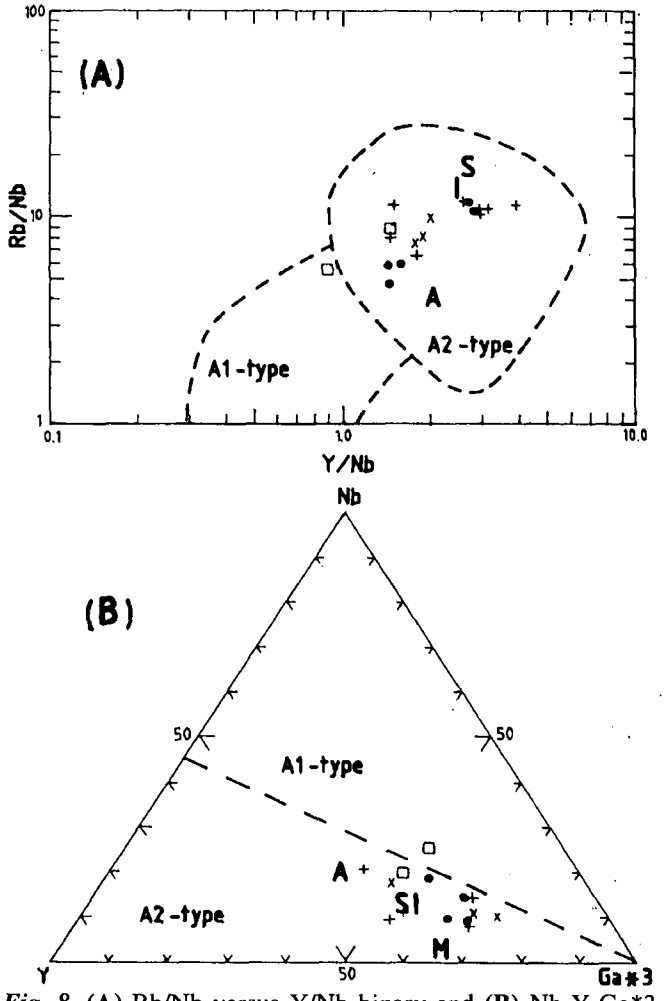

Fig. 8. (**A**) Rb/Nb versus Y/Nb binary and (**B**) Nb-Y-Ga*3 ternary diagrams (Eby, 1992) to distinguish between A_1 and A_2 granitoids. Symbols as in Fig. 4.

The patterns for average A-type granite of Whalen et al. (1987) are compared and shown in Fig. 10A-C. The Wadi Shuwas A-type granitoids exhibit almost identical abundances of K_2O, Rb and Ba, depletion of Nb and Y, and a significant enrichment of Sr and Zr. Compared to average I-, and S-type granite patterns (Fig. 10E; Whalen et al., 1987), the rocks exhibit slighlty higher Nb and Y abundances, high and approximately equal Sr contents and almost overlapping patterns with K_2O, Rb and Ba. The abundances of Ba, Sr and Y closely resemble with M-type granites. The patterns for the host gabbro-syenodiorite-tonalite are shown in Fig. 10D. Most of the patterns (e.g., K_2O, Ba, Zr, Y) resemble with M-type granites with significant enrichment in Nb and Sr.

Rb-Sr isotopic studies

Syenites: Rb-Sr data for the A-type granitoids are given in Table 4. The Rb/Sr isotopic data for six whole-rock samples from A-type syenites that cut the east-central part of the Ablah-Shuwas pluton yield an errochron age of 617±17

Table 4. Rb-Sr data for the A-type granitoids from the Ablah-Shuwas pluton.

Sample No.	Rb ppm	Sr ppm	$^{87}Rb/^{86}Sr$	$^{87}Sr/^{86}Sr$
S-1	140	197	2.0555	0.721052
S-3	132	35	11.1466	0.801880
S-4	137	130	3.0561	0.731370
S-6	138	68	5.9143	0.755850
S-7	129	147	2.5440	0.727146
S-8	133	61	6.3050	0.757808
G-3	139	164	2.46673	0.724920
G-5	126	364	1.0056	0.712130
G-6	144	277	1.5056	0.716650
G-7	139	202	1.9934	0.720611
G-8	131	57	6.7067	0.761270

Ma (MSWD=9.39) and an initial $^{87}Sr/^{86}Sr$ ratio of 0.70380±0.0008 (2σ) (Fig. 11A).

Quartz syenite/syenogranite: whole rock Rb/Sr data for the five samples from A-type quartz syenite/syenogranite that cut the southwestern part of the Ablah-Shuwas pluton define a 606±5 Ma isochron age (MSWD=0.49) with an initial $^{87}Sr/^{86}Sr$ ratio of 0.70350±0.00012 (2σ) (Fig. 11B).

The low initial $^{87}Sr/^{86}Sr$ ratios of 0.7035 and 0.7038 obtained for the A-type granitoids are within the range (0.701-0.706) expected for rocks derived from mantle-like protoliths. The Rb-Sr ages obtained in this study are compatible with post tectonic granitic rocks that intrude the Shuwas pluton. Fleck et al. (1980) reported an Rb-Sr isochron age of 636±21 for the granitic rocks which intrude the Ablah-Shuwas puton. The Rb-Sr ages of 617±10 Ma and 630±10 Ma are also reported for post-tectonic granites, that cut the diorite-tonalite pluton of similar age in the south west of the studied area (Brown et al., 1978; Greenwood, 1975).

Discussion

A-type granitoids of the Arabian Shield have not been given much attention. Stoeser (1986) labeled the post-tectonic alkali-feldspar granites of the Arabian Shield as "A-type granites (anorogenic)". He suggested that vast amount (7% of all plutonic rocks of the Shield) of A-type granites was being generated for about 70 years after accretion of the Shield (~630–560 Ma) as a result of crustal thickening due to continental collision. On the basis of some trace-element and major-oxide composition, Jackson et al. (1984) suggested that the late Precambrian younger (686-517 Ma) granitic associations of the alkali granite and alkali-feldspar granites can be grouped as "A-type granites". The above authors did not discuss about the distinctive chemical, mineralogical and textural characteristic of the A-type granites. They simply used the tectonic definition of A-type granites such as anorogenic, within-plate, post-collision or post-orogenic. King et al. (1997) suggested that A-type granites can be emplaced at any time during a tectonic-magmatic episode. They found the occurrence of coeval I- and A-type granitoids adjacent to each other with similar field relations in the Lachlan fold belt of southeastern Australia. Thus, the tectonic setting is not a good discriminator to classify the A-

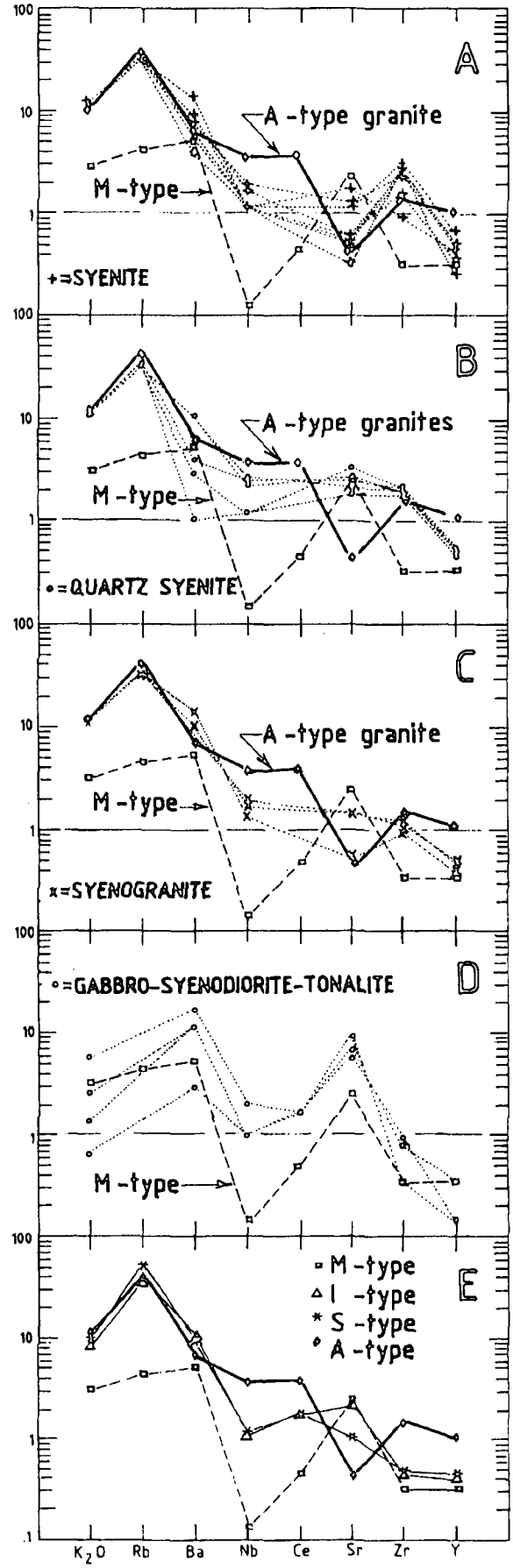

Fig. 10. ORG-normalized multi-element patterns for the Ablah-Shuwas granitoid pluton. Normalization values are from Pearce et al. (1984).

type granites, which occur in a variety of tectonic setting such as extensional, hotspots or plume, plate margins, post-collisional or post-orogenic. Various petrogenetic models have been proposed for the A-type granitoids such as mantle-derived fractionation of mafic (basaltic) magma (e.g., Turner et al., 1992; Loiselle, Wones, 1979), melting of I-type granites or their residual sources and (e.g., Clemens et al., 1986; Whalen et al., 1987; Sylvester, 1989; Anderson 1983), remelting of hybridized lithospheric mantle generated during arc-continent collision (e.g., Whalen et al., 1996). The thickened crustal source (Stoeser, 1986) is not a major mechanism, which generates the A-type granitoids.

The Wadi Shuwas A-type granitoids have distinctive chemical signatures such as high Al_2O_3, Zr, and Sr and low range of SiO_2 (~63-72%) relative to a typical A-type granitoids. The high content of Zr in the A-type granitoids implies their derivation from a significantly high temperature melt (King et al., 1997). The Wadi Shuwas A-type syenites and quartz syenites units are clearly peraluminous (~17-19 wt.%) with high contents of Na_2O (6.0-6.6 wt.%) and Zr (329-1095 ppm) and restricted range of SiO_2 (64-66 wt%), whereas A-type synogranites with high contents of SiO_2 (71-72 wt.%) are weakly peraluminous (14.6-15.6) with low Na_2O (4.8-5.2 wt.%) and Zr (317-415 ppm) contents, probably as a result of fractionation and low temperature melts.

In my opinion, the A-type granitoids should be classified into primitive or A-type$_p$ and evolved or A-type$_e$ granitoids based on their field associations with the primitive or evolved crustal rocks. Crustal rocks, especially felsic rocks play a major role in modifying the chemical signatures of the intrusive rocks. The A-type$_p$ granitoids, such as those of the Wadi Shuwas, are associated with the M-type or primitive crustle rocks, whereas A-type$_e$ are associated with the evolved and highly fractionated I-type crustal rocks. Both varieties of the A-type granitoids are present in the Lachlan fold belt of Australia (Whalen et al., 1987) and elsewhere.

The Wadi Shuwas A-type granitoids are depleted to a lesser extent in Y (33 ppm) and Nb (16 ppm), which is somewhat different from typical A-type granitoids. This type of difference is attributed to the different crustal source composition (Condie, 1991). The low Nb content is a distinctive feature of some continental rift tectonic settings. The low Nb content is reported from the Arbaat volcanic rocks of Sudan (Abdelsalam, Stern, 1993), Shadli rift volcanic of the south Eastern Desert of Egypt (Stern et al., 1991) and within-plate dykes of Sinai (Friz-Toppfer, 1991). The low Nb content in the Wadi Shuwas A-type granitoids and their intrusion into the rift-related Ablah group of rocks may indicate the presence of subduction-related volcanic arc material in the subcontinental lithosphere, which played a major role in inheriting the arc signature, represented by low Nb. The seismic-refraction crustal model of western Saudi Arabia (Mooney et al., 1985; Badri, 1991), divides the horizontal layered structure of the Arabian Shield into four layers. The upper two layers, 5-15 km below the surface, are made up of deformed Precambrian rocks, while the two lower layers, 20-45 km below the surface are mafic in composition, derived entirely from mantle-derived magmas. They are similar to calc-alkaline island arc and low-K tholeiitic basalts (McGuire, Stern, 1993).

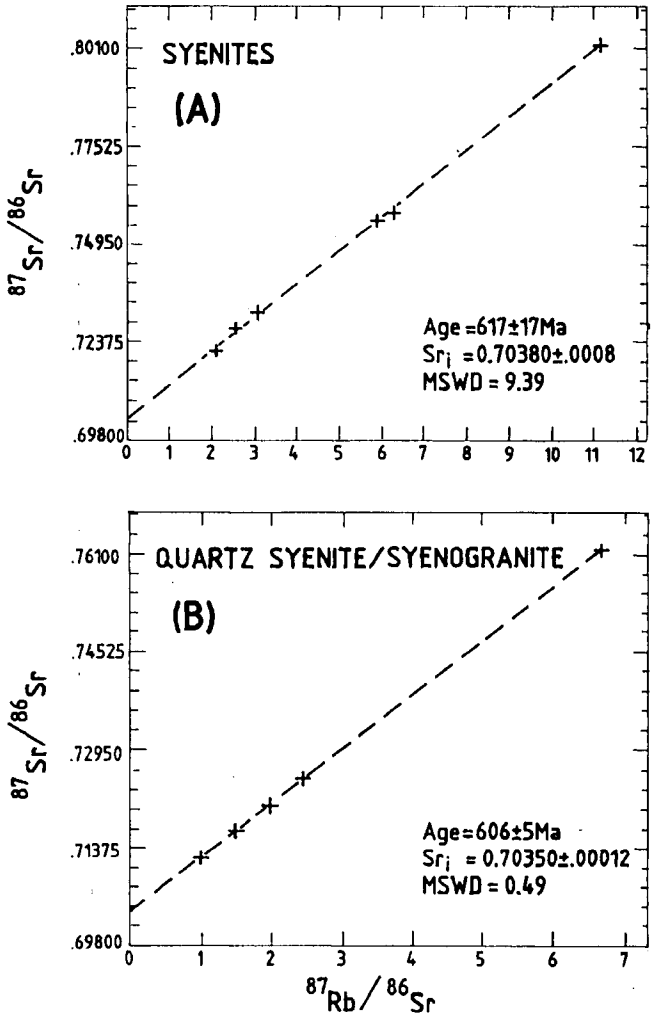

Fig. 11. Rb-Sr isochron plots of A-type **(A)** syenites and **(B)** quartz-syenites and syenogranites rocks of the Ablah-Shuwas pluton.

The 150 km long north-trending Ablah graben of the Asir terrane, situated in the southwest corner of the Arabian Shield, was developed at different times as a result of continuous extensional tectonic activity. The presence of calc-alkaline volcanic rocks at the base of the Ablah group rocks in the south indicate initialization of oceanic rifting in the south. The metamorphosed clastic and carbonate units found in the belt show deep water sedimentation in the south, shallow water marine origin sedimentation towards northward, and deltaic, marginal continental environment in the north (Parker, Smith, 1980). The island arc complex represented by Qirsha and Khutnah formations occurs in the proximity of the continental-deltaic environment. Donzea, Beziat (1989) suggested a rift environment (back-arc) for the Ablah group. The Wadi Baqarah granodiorite gneiss, which intrudes the Ablah group in the south, yielded a U/Pb zircon age of 763±4 Ma. Thus Ablah group must be older than at least 763 Ma (Cooper et al., 1979), whereas in the north Ablah group rocks yielded a Pb/Pb zircon age of 641±1 Ma (Johnson, 2000) and a Rb/Sr age of 721 ±55 Ma (Bokhari, Kramers, 1981). This variability indicates that the Ablah graben was probably developed progressively from south to north. If the age of 641±1 Ma for the Ablah group is accepted, then the younger diorite-tonalite rocks which

intrude the Ablah group must be younger than the 641 Ma and cannot be correlated with the 744±22 Ma Tharad pluton (Marzouki et al., 1982), which occurs northwest of the Ablah-Shuwas pluton.

The A-type granitoids, which intrude the Ablah-Shuwas younger diorite-tonalite pluton, are believed to be contemporaneous with the movement (610 Ma or later) on the Umm Farwah strike-slip shear zone, which cuts the eastern margin of the Ablah group. The Ablah group rhyolite, which intrudes the Umm Farwah shear zone, gave an age of 613±7 Ma (SHRIMP-RG analyses on zircons; Johnson et al., 2001). The Rb-Sr ages of 617±17 and 605±5 Ma obtained from this study for the A-type granitoids are almost compatible with the young shearing event. The out cropping of alkaline rocks along zones of lithospheric fractures, deep-seated tectonic zones, shear zones, and transform faults in Africa (Bowden, 1985) and Egypt (Schandelmeier et al., 1987; Schandelmeier, Pudlo, 1990; Mohamed et al., 1999) imply that the reactivation of lithospheric structures played an important role in the generation of alkaline magmatism of mostly A-type granitoids.

The reactivation stage (670-550 Ma) in the Arabian Shield formed the Najd system of transcurrent faults, deposition of volcanic and sedimentary rocks in pull-apart basins or grabens, and intraplate S- and A-type magmatism (Johnson et al., 1987). The origin of the Wadi Shuwas A-type granitoids can be related to the Umm Farwah strike-slip shear zone, that facilitated the partial melting in the volatiles and LIL-enriched matasomatized mantle, which was developed due to long history of 200 to 300 Ma subduction related magmatism (Pearce, 1982). The rise of volatiles and F-rich flux through reactivated weak lithospheric structures caused anhydrous high temperature partial melting in the homogeneous mafic lower crust and early formed intermediate composition host diorite-tonalite rocks to form primitive A-type granitoids. The presence of regional dyke swarms in the study area may indicate the presence of deep-seated faults or zones of lithospheric weakness through which mantle flux rised to the surface.

Conclusions

All post-orogenic alkali-feldspar or alkali granites of the Arabian Shield do not define a distinctive character of A-type granites as proposed by Stoeser (1986) and Jackson (1986). The classification presented by the authors is too broad. Based on chemical, mineralogical and tectonic criteria, a clear distinction should be made between post-tectonic and anorogenic A-type granitoids.

About 610 Ma old granitoids, which intrude the young arc-related diorite-tonalite rocks of the Ablah-Shuwas pluton show 'A-type', peraluminous to slightly metaluminous character rich in total alkalies and Fe, high field strength elements, Ga and Zn and low in CaO and MgO with a large negative Ba anomaly. The low initial $^{87}Sr/^{86}Sr$ values (0.7035-0.7038) of the granitoids indicate their derivation from mantle-like protoliths.

The A-type granitoids can be classified into primitive (A-type$_p$) and evolved (A-type$_e$) granitoids, based primarily on their field associations with the primitive or evolved crustal rocks in which they intrude.

The low Nb content in the Wadi-Shuwas A-type granitoids reflects the presence of arc-related mafic material in the subcontinental lithosphere.

The studied A-type granitoids are believed to be contemporaneous (610 Ma or later) with the movement on the Umm Farwah strike-slip shear zone that cuts the eastern margin of the Ablah group of rocks.

The origin of the studied granitoids is related with the Umm Farwah shear zone, that trigger off partial melting in the volatiles and LIL-enriched mantle and brought the mantle flux with advect heat into higher level of the crust. The ascent of this mantle flux through the deep-seated shear zone initiated partial melting in the lower mafic and upper crustal rocks of dominantly intermediate to felsic composition to generate A-type granitoids.

References

Abdelsalam, M. G., Stern, R. J. (1993): Tectonic evolution of the Nakasib suture, Red Sea Hills, Sudan: evidence for a late Precambrian Wilson Cycle. Jour. Geol. Soc. Lond., **150**, 393-404.

Anderson, J. L. (1983): Proterozoic anorogenic granite plutonism of North America. Geol. Soc. Am. Mem., **161**, 133-154.

Badri, M. (1991): Crustal structure of central Saudi Arabia determined from seismic refraction profiling. Tectonophysics, **185**, 357-374.

Barker, F. (1979): Trondhjemite- definition, environment and hypothesis of origin. In: Barker, F. (ed.) Trondhjemites, Dacites and Related Rocks, 1-12. Elsevier, Amsterdam.

Black, R., Lameyre, J., Bonin, B. (1985): The structural setting of alkaline complexes. J. Afr. Earth Sci., **3**, 5-16.

Bokhari, F. Y., Kramers, J. D. (1981): Island arc character and later Precambrian age of volcanic at Wadi Shuwas, Hijaz, Saudi Arabia-Geochemical and Sr and Nd isotopic evidence. Earth Planet. Sci. Lett., **54**, 409-422.

Bonin, B. (1988): Peralkaline granites in Corsica: some petrological and geochemical constraints. Rendiconti della Societa Italiana di Mineralogia et Petrologia, **43-2**, 281-306.

Bonin, B., Grelov-Orsini, C., Vialette, Y. (1978): Ages, origin and evolution of the anorogenic complex of Evisa (Corsica): a K-Li-Rb-Sr study. Contib. Mineral. Petrol., **65**, 425-432.

Bowden, P. (1985): The geochemistry and mineralization of alkaline ring complexes in Africa (a review). J. Afr. Earth Sci., **3**, 17-39.

Brooks, C., Hart, S. R., Wendt, I. (1972): Realistic use of two-error regression treatments as applied to rubidium strontium data. Rev. Geophys. Space Phys., **10**, 551-577.

Brown, G. F., Hedge, C. E., Marvin, R. F. (1978): Tabulation of Rb-Sr and K-Ar ages given by rocks of the Arabian Shield, in Geochronologic data for the Arabian Shield, Section 2: U.S. Geological Survey Saudi Arabian Project Report, **240**, 20 pp.

Brown, G. C., Thorpe, R. S., Webb, P. C. (1984): The geochemical characteristics of granitoids in contrasting arcs and comments on magma sources. J. Geol. Soc. Lond, **141**, 413-426.

Camp, V. E. (1984): Island arcs and their role in the evolution of the western Arabian Shield. Geol. Soc. Amer. Bull., **95**, 913-921.

Capaldi, G., Chiesa, S., Manetti, P., Orsi, G., Peli, G. (1987): Tertiary anorogenic granites of the western border of the Yemen Plateau. Lithos, **20**, 433-444.

Cater, F. W., Johnson, P. R. (1987): Geologic map of the Jabal Ibrahim quadrangle, sheet 20E, Kingdom of Saudi Arabia. Saudi Arabian Deputy Ministry for Mineral Resources Geologic Map GM-96C: scale 1:250,000, 32 pp.

Clemens, J. D., Holloway, J. R., White, A. J. R (1986): Origin of A-type granites: Experimental constraints. American Mineralogist, **71**, 317-324.

Collins, W. J., Beams, S. D., White, A. J. R., Chappel, B. W. (1982): Nature and origin of A-type granites with particular

reference to southwestern Australia. Contrb. Miner. Petrol., **68**, 429-439.

CONDIE, K. C. (1991): Precambrian granulites and anorogenic granites: are they related? Precamb. Res., **51**, 161-172.

COOPER, J. A., STACEY, J. S., STOESER, D. B., FLECK, R. J. (1979): An evaluation of the zircon method of isotopic dating in the southern Arabian Craton. Contrib. Mineral. Petrol., **68**, 429-439.

DE LA ROCHE, H., LETERRIER, J., GRANCLAUDE, P., MARCHAL, M. (1980): A classification of volcanic and plutonic rocks using R_1-R_2 diagram and major element analyses--its relationship with current nomenclature. Chem. Geol., **29**, 183-210.

DODGE, F. C. W. (1979): The Uyaijah ring structure, Kingdom of Saudi Arabia. U.S. Geol. Survey Prof. Paper, 774-E.

DONZEAU, M. AND BEZIAT, P. (1989): The Ablah-Wadi Shwas mineral belt, geology and mineral exploration. Ministry of Petroleum and Mineral Resources, Directorate General of Mineral Resources, Jeddah, Kingdom of Saudi Arabia. Open-File Report BRGM-OF-09-1.

DU BRAY, E. A. (1986): Specialized granitoids in the southeastern Arabian Shield-case history of a regional assessment. J. Afr. Earth Sci., **4**, 169-176.

EBY, G. N., KRUEGFER, H. W., CREASY, J.W. (1992): Geology, geochronology, and geochemistry of the White Mountain batholith, New Hampshire. In: Puffer, J. H., and Ragland, P. C. (eds.): Eastern North America Mosozoic magmatism. Geological Society of America Special Paper, **268**, 379-398.

FLECK, R. J., GREENWOOD, W. R., HADLEY, D. G., ANDERSON, R. E., SCHMIDT, D. L. (1980): Rubidium strontium geochronology and plate-tectonic evolution of the southern part of the Arabian Shield. U.S Geological Survey Professional Paper 1131, 39 pp.

FOLEY, S. F., VENTURELLI, G., GREEN, D. H., TOSCANI, L. (1987): The ultrapotassic rocks: characteristics, classification, and constraints for petrogenetic models. Earth-Sci. Rev., **24**, 81-134.

FRIZ-TOPFER, A. (1991): Geochemical characteristics of Pan-African dyke swarms in southern Sinai: from continental margin to intraplate magmatism. Precamb. Res., **49**, 281-300.

GREENE, R.C. (1993): Stratigraphy of the late Proterozoic Murdama group, Saudi Arabia. U.S. Geological Survey Bulletin 1976, 59 pp.

GREENWOOD, W. R., STOESER, D. B., FLECK, R. J., STACEY, J. S. (1982): Late Proterozoic island-arc complexes and tectonic belts in the southern part of Arabian Shield, Kingdom of Saudi Arabia. Saudi Arabian Deputy Ministry for Mineral Resources Open-File Report USGS-OF-02-8, 46 pp.

GREENWOOD, W. R. (1975): Geology of the Al Aqiq quadrangle, sheet 20/41 D, Kingdom of Saudi Arabia. Saudi Arabian Directorate General of Mineral Resources Geologic Map GM-23: scale 1:100,000

HASSANEN, M. A. (1997): Post-collision, A-type granites of Homrit Waggat complex, Egypt: petrological and geochemical constraints on its origin. Precamb. Res., **82**, 211-236.

HERMES, O. D., GROMET, L. P., ZARTMAN, R. E. (1981): Zircon geochronology and petrology of plutonic rocks in Rhode Island. In: Boothroyd J. C. (ed): Guidebook to geologic field studies in Rhode Island and adjacent areas. Annual Meeting, New England Intercollegiate Geological Conference. 315-338.

IRVINE, T. N., BARAGAR, W. R. B (1971): A guide to the chemical classification of the common volcanic rocks. Can. J. Earth Sci., **8**: 523-548.

JACKSON, N. J. (1986): Petrogenesis and evolution of Arabian plutonic rocks. J. Afr. Earth Sci., **4**, 47-59.

JACKSON, N. J., WALSH, J. N., PEGRAM, E. (1984): Geology, geochemistry and petrogenesis of late Precambrian granitoids in the central Hijaz region of the Arabian Shield. Contr. Miner. Petrol., **87**, 205-219.

JOHNSON, P. R. (2000): Proterozoic geology of Saudi Arabia: Current concepts and issues. Contribution to a workshop on the geology of the Arabian Peninsula, 6th meeting of the Saudi Society for Earth Science, King Abdulaziz City for Science and Technology, Riyadh, Saudi Arabia. 32 pp.

JOHNSON, P. R., KATTAN, F. H. AND WOODEN, J. L. (2001): Implications of SHRIMP and microstructural data on the age and kinematics of shearing in the Asir terrane, southern Arabian Shield, Saudi Arabia. (Abstract). International Geoscience Journal, Gondwana Research 4: No. 2, 172-173.

JOHNSON, P. R., SCHEIBNER, E., SMITH, E. A. (1987): Basement fragments, accreted tectonostratigraphic terranes, and overlap sequences; elements in the tectonic evolution of the Arabian Shield. American Geophysical Union Geodynamics Series, **19**, 323-343.

KANAAN, F. M. (1979): The geology, petrology and geochemistry of the granitic rocks of Jabal Al Hawshah and vicinity, Jabal Al Hawshah quadrangle, Kingdom of Saudi Arabia. Saudi Arabian Directorate General of Mineral Resources Bull. 23.

KING, P. L., WHITE, A. J. R., CHAPPELL, B. W., ALLEN, C. M. (1997): Characteristics and origin of aluminous A-type granites from the Lachlan Fold Belt, southeastern Australia. Jour. Petrol., **38**, 371-391.

LE BEL, L., LAVAL, M. (1986): Felsic plutonism in the 'Al-Amar-Idsas area, Kingdom of Saudi Arabia. J. Afr. Earth Sci., **4**, 87-98.

LOISELLE, M. C, WONES, D. R. (1979): Characteristics of anorogenic granites. Abstr. With programs. Geological Society of America Annual General Meeting. 539 pp.

MANIAR, P. D., PICCOLI, P. M. (1989): Tectonic discrimination of granitoids. Geol. Soc. Am. Bull., **101**, 635-643.

MARZOUKI, F. H. M., JACKSON, N. J., RAMSAY, C. R., DARBYSHIRE, D. P. F. (1982): Composition, age and origin of two Proterozoic diorite-tonalite complexes in the Arabian Shield. Precamb. Res., **19**, 31-50.

MCGUIRE, A. V., STERN, R. J. (1993): Granulites xenoliths from western Saudi Arabia: the lower crust of the late Precambrian Arabian-Nubian Shield. Contrib. Miner. Petrol., **114**, 395-408.

McIntyre, G. A. Brooks, C., Compston, W., Turek, A. (1966): The statistical assessment of Rb-Sr isochrons. J. Geophyus. Res., **71**, 5459-5468.

MOHAMED, F. H., MOGHAZI, A. M., HASSANEN, M. A. (1999): Petrogenesis of Late Proterozoic granitoids in the Ras Gharib magmatic province, northern Eastern Desert, Egypt: petrological and geochemical constraints. N. Jb. Miner. Abh., **174: 3**, 319-353.

MOONEY, W. D., GETTINGS, M. E., BLANK, H. R., HEALY, J. H. (1985): Saudi Arabian seismic-reflection profile: a traveltime interpretation of crustal and upper mantle structure. Tectonophysics, **111**, 173-246.

O'HALLORAN, D. A. (1985): Ras ed Dom migrating ring complex: A-type granites and syenites from the Bayuda Desert, Sudan. J. Afr. Earth Sci., **3**, 61-75.

PANKHURST, R. J., O'NIONS, R. K. (1973): Determination of Rb/Sr and $^{87}Sr/^{86}Sr$ ratios of some standard rocks and evaluation of X-ray fluorescence spectrometry in Rb-Sr geochemistry. Chem. Geol., **12**, 127-136.

PARKER, T. W. H., SMITH, G. H. (1980): An assessment of the stratiform copper potential of the Ablah synform. Ministry of Petroleum and Mineral Resources, Directorate General of Mineral Resources, Kingdom of Saudi Arabia. Riofinex Geological Mission Techical Record RF-TR-01-1.

PEARCE, J. A (1982): Trace element characteristics of lavas from destructive plate boundaries. In: Thorpe, R.S. (ed.) Andesites 525-547. Wiley, Chichester.

PEARCE, J. A. HARRIS, N. B. W. AND TINDLE, A. G. (1984): Trace elements discrimination diagrams for the tectonic interpretation of granitic rocks. J. Petrol., **25**, 956-983.

PETRO, W. L., VOGEL, T. A., WILLBORD, J. T. (1979): Major element chemistry of plutonic rock suites from compressional and extensional plate boundaries. Chem. Geol., **26**, 217-235.

PITCHER, W. S. (1982): Granite type and tectonic environment. In: Hsu, K. J. (ed): Mountain Building Process, 19-40. Academic Press, London.

RAMSAY, C. R., DRYSDALL, A. R., CLARK, M. A. (1986): Felsic plutonic rocks of the Midyan region, Kingdom of Saudi Arabia-I. Distribution, classification and resources potential. J.Afr. Earth Sci., **4**, 63-77.

SCHANDELMEIER, H., PUDLO, D. (1990): The central-African Fault zone in Sudan-a possible continental transform fault. Berliner Geowiss. Abh., **120**, 31-44.

SCHANDELMEIER, H., RICHTER, A., HARMS, U. (1987): Proterozoic deformation of the East Saharan craton in southeast Libya, south Egypt and north Sudan. Tectonophysics, **140**, 233-246.

STEIGER, R. H., JAGER, E. (1977): Subcomission on geochronology: convention on the use of decay constants in geo- and cosmochronology. Earth Planet. Sci. Lett., **36**, 359-362.

STERN, R. J., KRONER, A., RASHWAN, A. A. (1991): A late Precambrian (~710 Ma) high volcanicity rift in the southern Eastern Desert of Egypt. Geologische Rundschau, **80**, 155-170.

STOESER, D. B. (1986): Distribution and tectonic setting of plutonic rocks of the Arabian Shield. J. Afr. Earth Sci., **4**, 21-46

STOESER, D. B., CAMP, V. E. (1985): Pan-African microplate accretion of the Arabian Shield. Bull. Geol. Soc. Am., **6**, 817-826.

STOESER, D. B., WHITEHOUSE, M. J., STACEY, J. S. (2001): The Khida terrane-geology of Paleoproterozoic rocks in the Muhayil area, Eastern Arabian Shield, Saudi Arabia (Abstract). International Geoscience Journal, Gondwana Research 4: No. 2, 192-194.

STRECKEISEN, A. (1976): To each plutonic rocks its proper name. Earth Science Reviews **12**, 1-33.

STUCKLESS, J. VANTRUMP, G., JR., BUNKER, C. M. S., BUSH, C.A. (1982): Preliminary report on the geochemistry and uranium favourability of the postorogenic granites of the northeastern Arabian Shield, Kingdom of Saudi Arabia. Saudi Arabian Deputy Ministry for Mineral Resources Open-File Report USGS-OF-02-38.

STUCKLESS, J. S., VANTRUMP, G., JR., CHRISTIANSEN, E. U., BUSH, C. A., BUNKER, C. M., BARTEL, A. J. (1983): Preliminary assessment of the geochemistry and mineral favourability of the postorogenic granites of the southeastern Arabian Shield, Kingdom of Saudi Arabia. Saudi Arabian Deputy Ministry for Mineral Resources Open-File Report USGS-OF-03-64.

SUNDVOLL, B. (1978): Rb/Sr relationship in the Oslo igneous rocks. In: E.-R.. Neumann and I.B. Ramberg (Eds.), Petrology and Geochemistry of Continental Rifts. Reidel, Dordrecht. 181-184.

SYLVESTER, P. J. (1989): Post-collisional alkaline granites. Jour. Geol., **97**, 261-280.

TURNER, S. P., FODEN, J. D., MORRISON, R. S. (1992): Derivation of some A-type magmas by fractionation of basaltic magma: An example from the Padthaway Ridge, South Australia. Lithos., **28**, 151-179.

WHALEN, J. B. (1985): Geochemistry of an island-arc plutonic suite: the Uasilau-Yau Yau intrusive complex, New Britain, PNG. J. Petrol., **26**, 603-632.

WHALEN, J. B., CURRIE, K. L., BREEMAN, O. (1987b): Episodic Ordovician-Silurian plutonism in the Topsails igneous terrane, western Newfoundland. Trans. R. Soc. Edinburgh, Earth Sci., **78**, 17-28.

WHALEN, J. B., CURRIE, K. L., CHAPPELL, B. W. (1987): A-type granites: geochemical characteristics, discrimination and petrogenesis. Contrib. Mineral. Petrol., **95**, 407-419.

Whalen, J. B., Jenner, G. A., Longstaffe, F. J., Robert, F. and Gariepy, C. (1996): Geochemical and isotopic (O,Nd, Pb and Sr) constraints on A-type granite petrogenesis based on the Topsails igneous suite, Newfoundland Appalachians. Jour. Petrol., **37**: 6, 1463-148

WHITNEY, P. R. (1992): Charnockites and granites of the western Adirondacks, New York, USA: a differentiated A-type suite. Precamb. Res., **57**, 1-19.

YORK, D. (1969): Least-square fitting of a straight line with correlated errors. Earth Planet. Sci. Lett., **5**, 320-324.

Received: October 6, 2001; accepted: January 19, 2002

Acta Mineralogica-Petrographica, Szeged 2001, Vol. 42, pp. 21-31

ACTA
Mineralogica
Petrographica

PETROGRAPHICAL CHARACTERISTICS OF VARISCAN GRANITOIDS OF BATTONYA UNIT BOREHOLES (SE HUNGARY)

ELEMÉR PÁL-MOLNÁR[1], GÁBOR KOVÁCS[1], ANIKÓ BATKI[1]

[1] Department of Mineralogy, Geochemistry and Petrology, University of Szeged
H-6701 Szeged, P. O. Box 651, Hungary
e-mail: palm@geo.u-szeged.hu

ABSTRACT

The Tisia Composite Terrane Alpine megatectonic unit forms the pre-Neogene crystalline basement of South, Southeast Hungary. As an independent unit the Tisia Composite Terrane existed from the Late Cretaceous, when its rotation began, till the Early Miocene. Concerning the territory of Hungary it involves three large Variscan Terranes (Slavonia-Dravia Terrane, Kunságia Terrane and Békésia Terrane), all of which are covered by an Alpine overstep sequence. The Békésia Terrane can be divided into four units: Kelebia Unit, Csongrád Unit, Battonya Unit and the Sarkadkeresztúr Unit. The crystalline mass of the Tisia Composite Terrane is characterised by granitoid ranges and anticline wings of middle and high grade metamorphites. This paper presents the results of a petrological analysis on granitoid rocks originating from boreholes that were deepened in the axis zone of the crystalline dome (Battonya High) of the Battonya Unit. The available granitoid rocks, on the basis of their composition can be considered of similar character. The main rock forming minerals of the studied samples are: quartz ± orthoclase + microcline + plagioclase feldspar (albite-oligoclase) ± biotite + muscovite. Accessory components are apatite, zircone, monacite and less frequently titanite. Considering the modal composition of the rocks, they are syenogranites, monzogranites and granodiorites. Based on their chemical composition, the rocks are syenogranites, monzogranites and granodiorites they are subalkaline, calcic with a peraluminous character. Tectonically they are orogenous, syn-collisional or continental collisional granitoids. Most of the characteristics featuring the Battonya Unit samples indicate that they are S-type granitoids.

Key words: S-type syn-collisional CC granitoids, geochemistry, crystalline basement, Battonya Unit, Tisia Composite Terrane, Pannonian Basin, Hungary

INTRODUCTION

The present geology and tectonical setting of the Carpathian Basin (Pannonian Basin) (Fig. 1A) and that of Hungary is a result of a compound, multi-step evolution of geological structures. The complexity is reasoned first of all by the megatectonic location of the territory, since it is the actual collision zone of the European and African continental plates with oceanisation and the series of collisions, which lead here to the splintered fragmentation of the lithosphere. During the Alpine Orogenesis the nappe formation and folding processes were accompanied by the drifting and detachment of the fragments. At the end of the Miocene the attenuation of the crust (anticlines of the mantle) launched the development of large basins, that determine the present structural setting of the area.

The greatest proportion of the Pre-Neogene basement of the Pannonian Basin is built up by two Alpine megatectonic units, namely, the Pelsoian Composite Terrane in the North (comprising the Southern part of the ALCAPA Composite Terrane), and the Tisia Composite Terrane in the South (Kovács et al., 2000).

The crystalline mass of the Tisia Composite Terrane is characterised by granitoid ranges and anticline wings of middle and high grade metamorphites. This paper presents the results of a petrological analyses on the granitoid rocks located in the characteristic uplift (Mezőhegyes-Battonya) of the basement of the Békésia Terrane (Battonya Unit) – Tisia Composite Terrane (Fig. 1B).

GEOLOGICAL SETTING

The Tisia Composite Terrane (Fig. 1A) comprises the crystalline basement of South Hungary, East Croatia, North Yugoslavia and that of the Western part of Transylvania (Romania). It is bordered by the Mid Hungarian lineament, the Száva-Moslavima-Zombor-Bečej-Lipova line (the Northern border of the Srem - Mureş ophiolite belt) and the Someş lineament in the Northwest, South and Northeast, respectively. As a consequence of the fact that at the present the basement is covered by Miocene-Pliocene sediments at a depth of 2500-6500 m, its structure and petrology can only be investigated with geophysical methods and borehole samples. The seismic research of the past decades has shown that during the Neogene the Pannonian Basin has gone under a complex tectonic evolution, that has principally modified the original Variscan structures of the area (Albu et al., 1992; Tari et al., 1999; Csontos, Nagymarosi, 1999). As an independent unit the Tisia Composite Terrane existed from the Late Cretaceous, when its rotation began, till the Early Miocene. Concerning the territory of Hungary it involves three large Variscan Terranes (Slavonia-Dravia Terrane, Kunságia Terrane and Békésia Terrane), all of which are covered by an Alpine overstep sequence. From the beginning of the Late Triassic up to the Early Cretaceous a characteristic separation is recorded by sedimentary successions. Although, these units thrusted, and formed nappe zones during the Middle-Late Cretaceous, sometimes lateral transitions can be detected as well (Kovács et al., 2000).

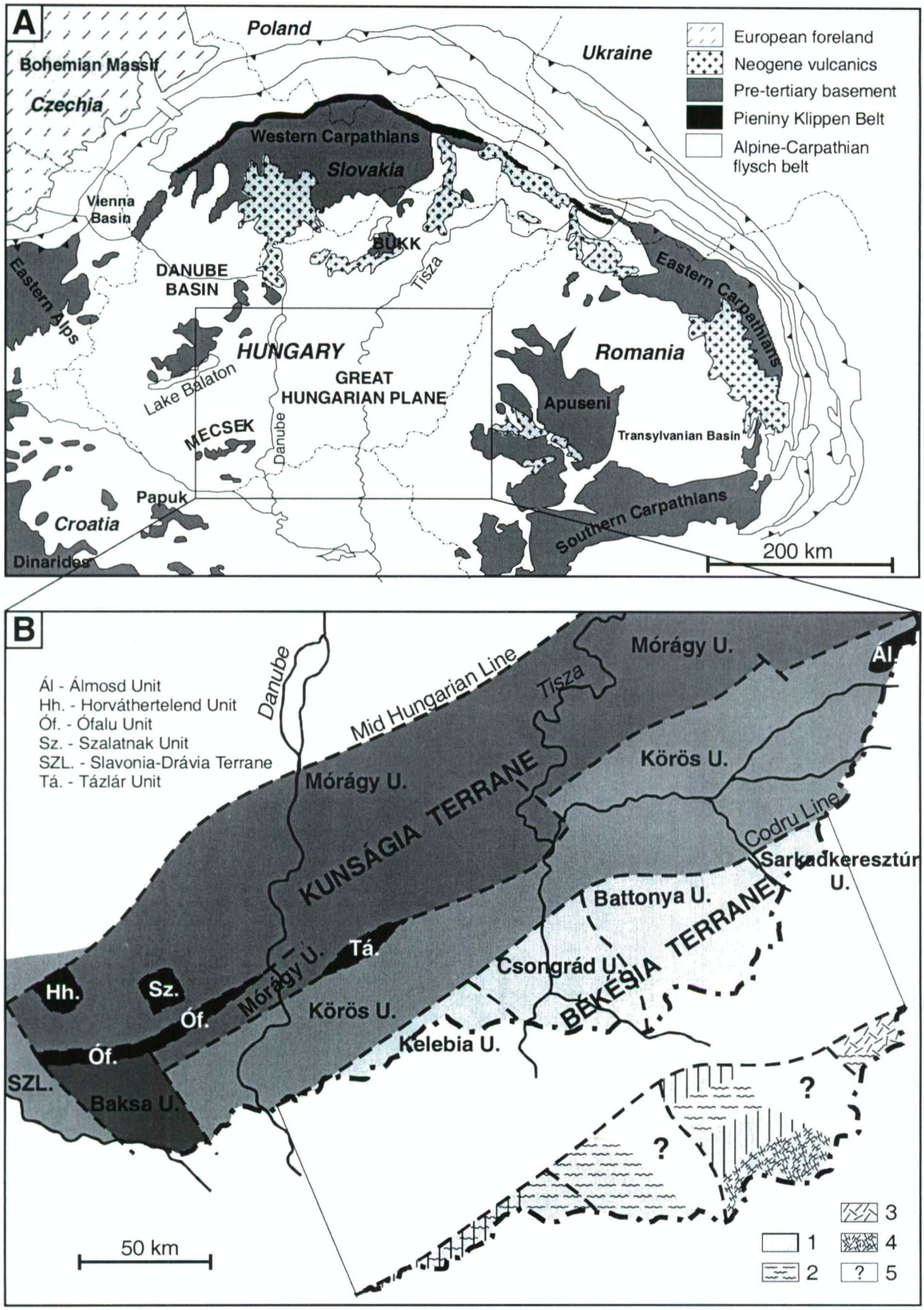

Fig. 1. **(A)** The simplified geological map of the Alpine-Carpathian-Pannonian region. **(B)** Pre-Tertiary regional geology of the Tisia Composite Terrane (SE part of the Pannonian Basin); Békésia Terrane highlighted (modified after Kovács et al., 2000). Legend: 1. Alpine overstep sequence connected to the northern shelf of the Axios/Vardar and related Neotethyan oceanic basins; 2. Variscan medium-grade metamorphosed complex; 3. Migmatic complex; 4. Granitoids; 5. Unknown.

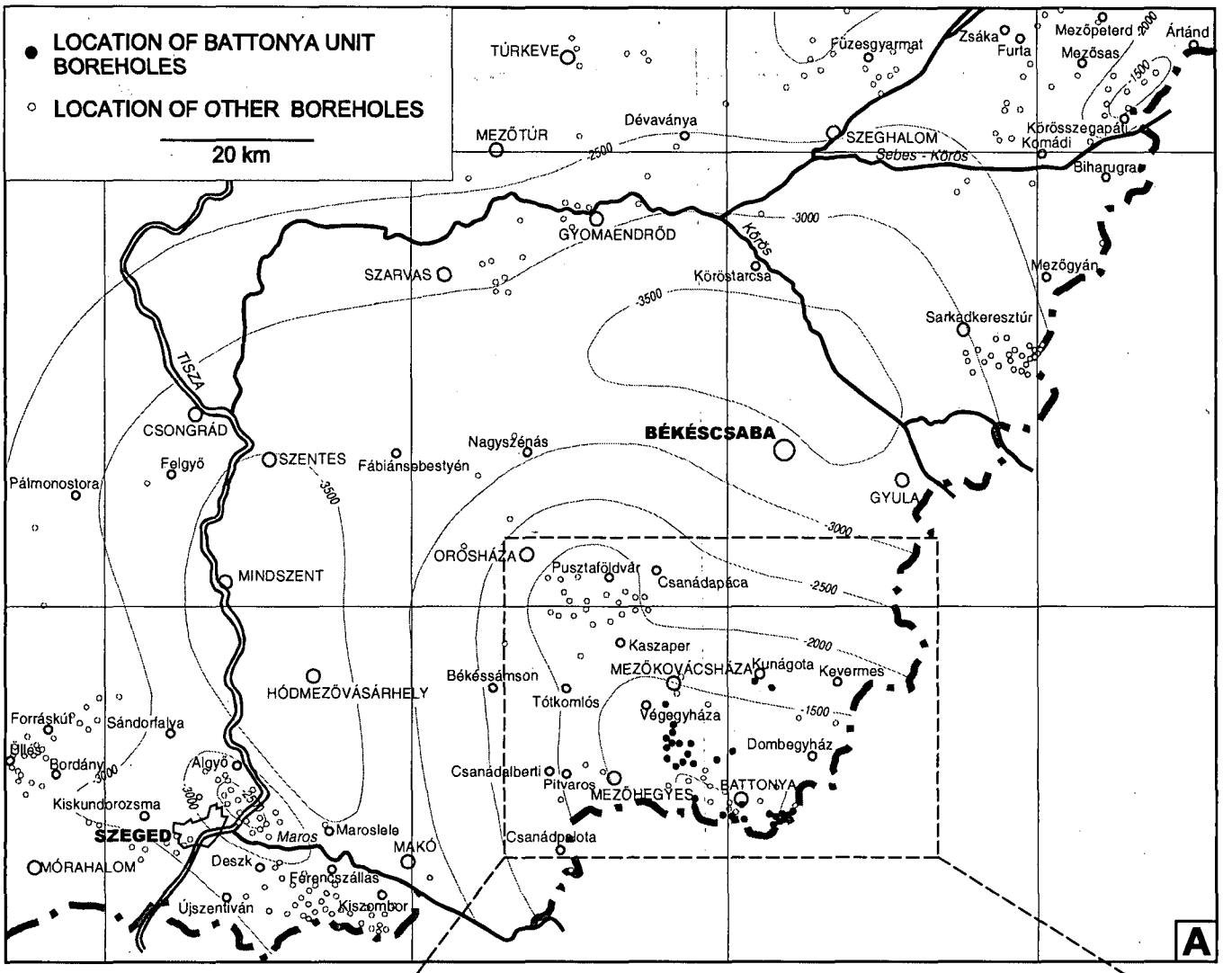

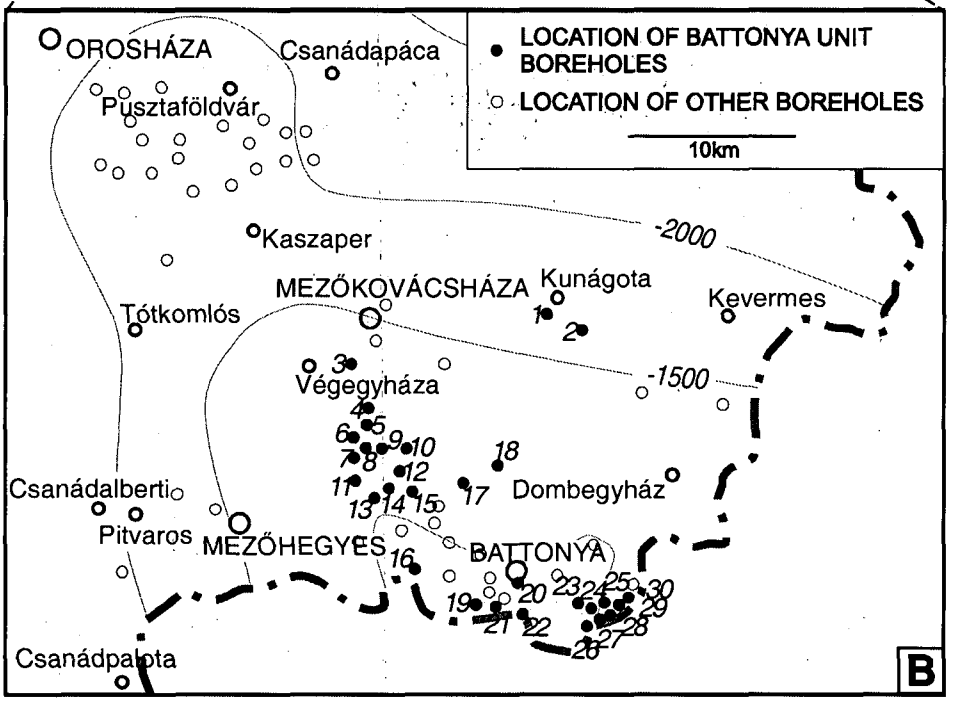

Fig. 2. **(A)** The map of SE Hungary, complemented with the topography of the Pre-Neogene basement and the location of the studied boreholes. **(B)** Precise location of the studied Battonya Unit boreholes. The numbers stand for the following boreholes:
1. Kunágota-2, 2. Kunágota-1, 3. Végegyháza K-1, 4. Végegyháza-2, 5. Mezőhegyes-14, 6. Mezőhegyes-7, 7. Mezőhegyes-5, 8. Mezőhegyes-6, 9. Mezőhegyes-19, 10. Mezőhegyes-11, 11. Mezőhegyes-2, 12. Mezőhegyes-8, 13. Mezőhegyes-1, 14. Mezőhegyes-9, 15. Mezőhegyes-12, 16. Mezőhegyes-20, 17. Dombegyház DNy-2, 18. Dombegyház DNy-1, 19. Battonya-3, 20. Battonya-10, 21. Battonya-64, 22. Battonya-76, 23. Battonya-6, 24. Battonya K-6, 25. Battonya K-9, 26. Battonya K-18, 27. Battonya K-16, 28. Battonya K-11, 29. Battonya K-13, 30. Battonya K-14.

The areas of interest are situated on the Békésia Terrane, which is the part of the Békés-Codru Alpine Zone. The name Békésia Terrane is only applied to the Hungarian part of the basement, since detailed comparative investigations of the Codru Zone in Romania are still missing. The Békésia Terrane can be divided into four units: Kelebia Unit, Csongrád Unit (earlier Tisza Unit (Szederkényi, 1984, 1996)), Battonya Unit (earlier Battonya Complex (Szederkényi, 1984, 1996)) and the Sarkadkeresztúr Unit (Fig. 1B).

The borholes exposing the studied granitoid samples are located in the Battonya Unit (Fig. 2A). The Battonya Unit effectively is a 15-25 km long and 10-15 km wide body with a round-shape layout, forming a flat anticline that is covered by Miocene and Pannonian strata. Its borders are: the front of the South Hungarian Nappe Belt in the north, the Makói Trench in the west, the Békési Basin in the east, and it stretches till the northern front line of the Biharia Nappe in Romania. The average depth of the Hungarian section below the surface is 1000-1500 m (Fig. 2A-B), though, in the surroundings of Pitvaros and Kunágota and in Kevermes it can be detected in a 2000 m depth.

According to Buda (1996), the granitoid rocks have a compound crustal-mantle origin, and formed in a degrading plate boundary environment, therefore, the S-type origin is mixed with a certain degree I-type granitoid origin. At Battonya-Mezőhegyes the magma of the abyssical plutonic body was slightly compressed upwards due to an "in situ" melting in the late, kinematic phase of the Variscan Orogenesis. As a result of this, it developed a slight contact zone (Szepesházi, 1969; Szederkényi, 1984; Kovách et al., 1985).

Sampling and analytical methods

During our research we examined samples that are stored in the rock collection of the Department of Mineralogy, Geochemistry and Petrology, University of Szeged. The following boreholes were examined: Battonya-3, 6, 10, 36, 37, 41, 43, 44, 47, 48, 49, 63, 64, 71, 72, 75, 76; Battonya-K-4, 6, 9, 10, 11, 13, 14, 15, 16, 17, 18; Dombegyháza-DNY-1, 2; Kunágota-1, 2; Mezőhegyes-1, 2, 5, 6, 7, 8, 9, 11, 12, 13, 14, 15, 16, 17, 18, 19, 20; Mezőhegyes-K-1; Végegyháza-2; Végegyháza-K-1 (Fig. 2B). The samples are drill-cores, and both their number and quantity are very limited. The stratigraphical columns of the most relevant Battonya High (Fig. 2A-B) boreholes, that provided the studied granitoid samples, can be seen on Fig. 3. As a part of the geological investigations in this area more than 150 modal analyses and 18 chemical analyses were performed on the studied rocks. The major element composition of samples representing the main rock types was determined with an atomic emission spectrometer (ICP-AES) at the University of Stockholm. The excitation source of the instrument is an inductively coupled plasma (ICP). 50 fixed spectral lines are installed in the spectrometer, thus their simultaneous use (polychromator) makes the multi-element analysis very fast. Besides, it is also equipped with a scanning monochromator. The instrument, named "Spectroflame Modula", was manufactured in Germany by Spectro Analytical Instruments.

Petrography

The samples are mainly of light grey, greenish grey colour. Most of them have a holocrystalline, inequigranular texture, some samples are of equigranular texture. The macroscopic components of the studied granites are quartz, potassium feldspar, plagioclase feldspar, mica (the later can be ±biotite or ±muscovite). The usual size of the main rock forming grains falls between 1-3 mm, therefore, the studied rocks can be considered medium-granular. Subordinately, the rocks can be of bimodal composition, i.e., in a fine-grained matrix phenocrysts are placed, which probably developed due to tectonic effects. In case of some samples, based on the ordered setting of mica, features of textural orientation can be observed, too.

Primarily, the samples are solid and compact rocks, however, this state can be modified by weathering and tectonical effects. As a result of weathering the feldspars form fine dust, while the biotite is chloriticised. Carbonate and limonitic veins penetrate the rocks. As a result of tectonical wearing the texture of the rocks is broken up and gets fragmented, the rock-forming minerals are deformed.

Textural features of the studied samples

During the microscopic analyses the most important textural characteristics and the volumetric percentage were examined in terms of all the main rock forming minerals, accessory and secondary minerals. On the basis of their textures, the studied rocks can be classified in the following four groups:

a., rocks of medium-grained, inequigranular, hypidiomorphic-granular texture;

b., rocks of coarse-grained, hypidiomorphic-granular texture;

c., rocks of medium-grained, equigranular, hypidiomorphic-granular texture;

d., rocks with textural orientation.

Concerning the mineral composition and texture of the rocks, significant differences cannot be detected. On the basis of their composition, the rocks can be considered of similar character. The main rock forming minerals of the studied samples are: quartz ± orthoclase + microcline + plagioclase feldspar (albite-oligoclase) ± biotite + muscovite.

The textural features of the main mineral components are as follows:

quartz: xenomorphous, undulating absence (Fig. 4A), average grain-size is 2-3 mm. In case of several samples as a result of recrystallisation larger grains transform into subgrains (Fig. 4B). As an inclusion and secondary component it occurs in microcline and plagioclase feldspars. At the contact of microcline and plagioclase it appears in the form of myrmekite in the plagioclase (Fig. 4C).

orthoclase: hypidiomorphous, an average 1,5-3 mm size, tabular appearance. Bifold twinning is common, at some places it is perthitic.

microcline: a component of hypidiomorphous, xenomorphous, perthitic, tabular character (Fig. 4D). Its average size is 2-4 mm, however, porphyroblasts of 2-3 cm are not rare either. It contains inclusions of quartz, plagioclase feldspar, mica and zircon. More common than orthoclase, and it is present in a higher volumetric percentage.

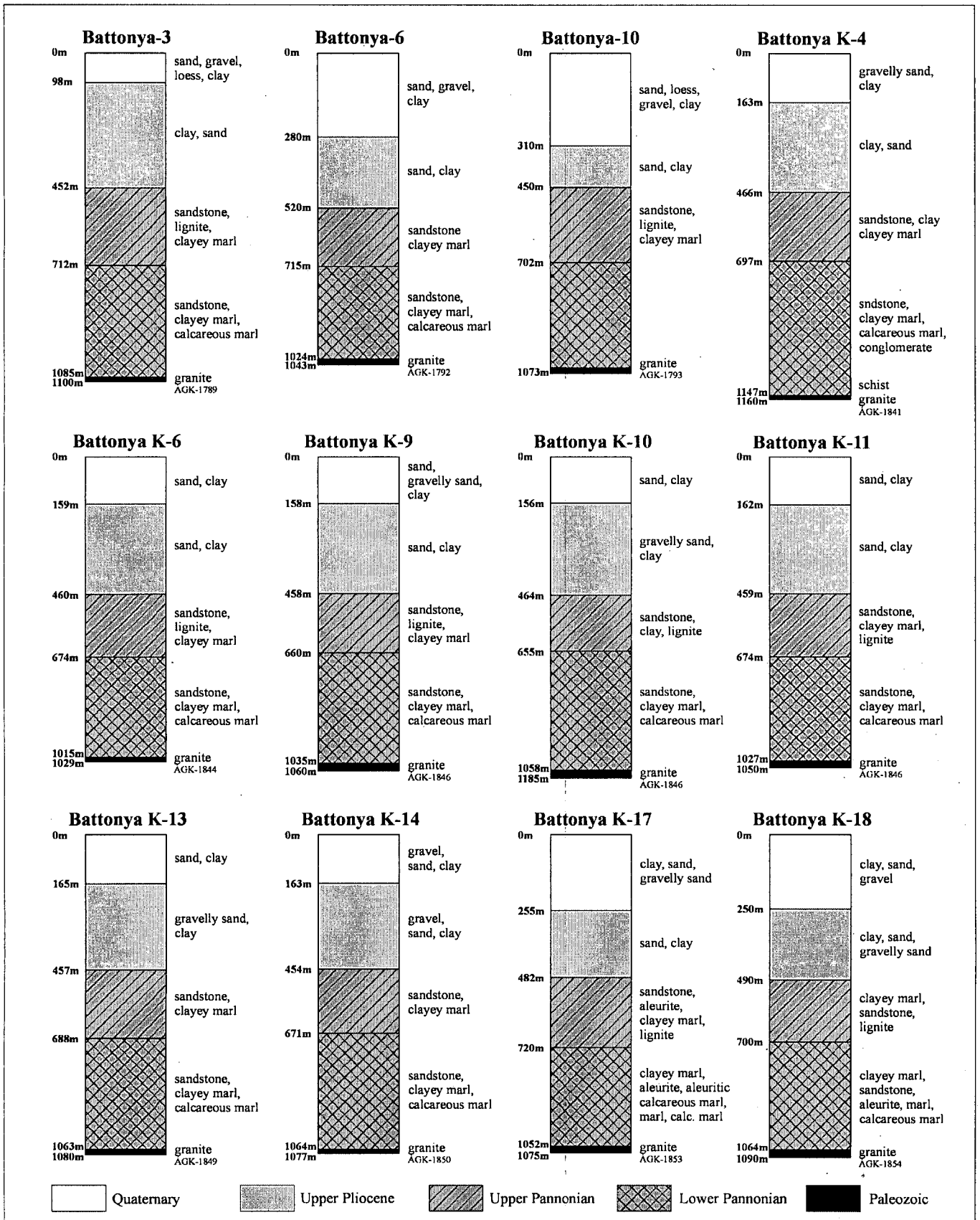

Fig. 3. The stratigraphical columns of the most relevant Battonya Unit boreholes.

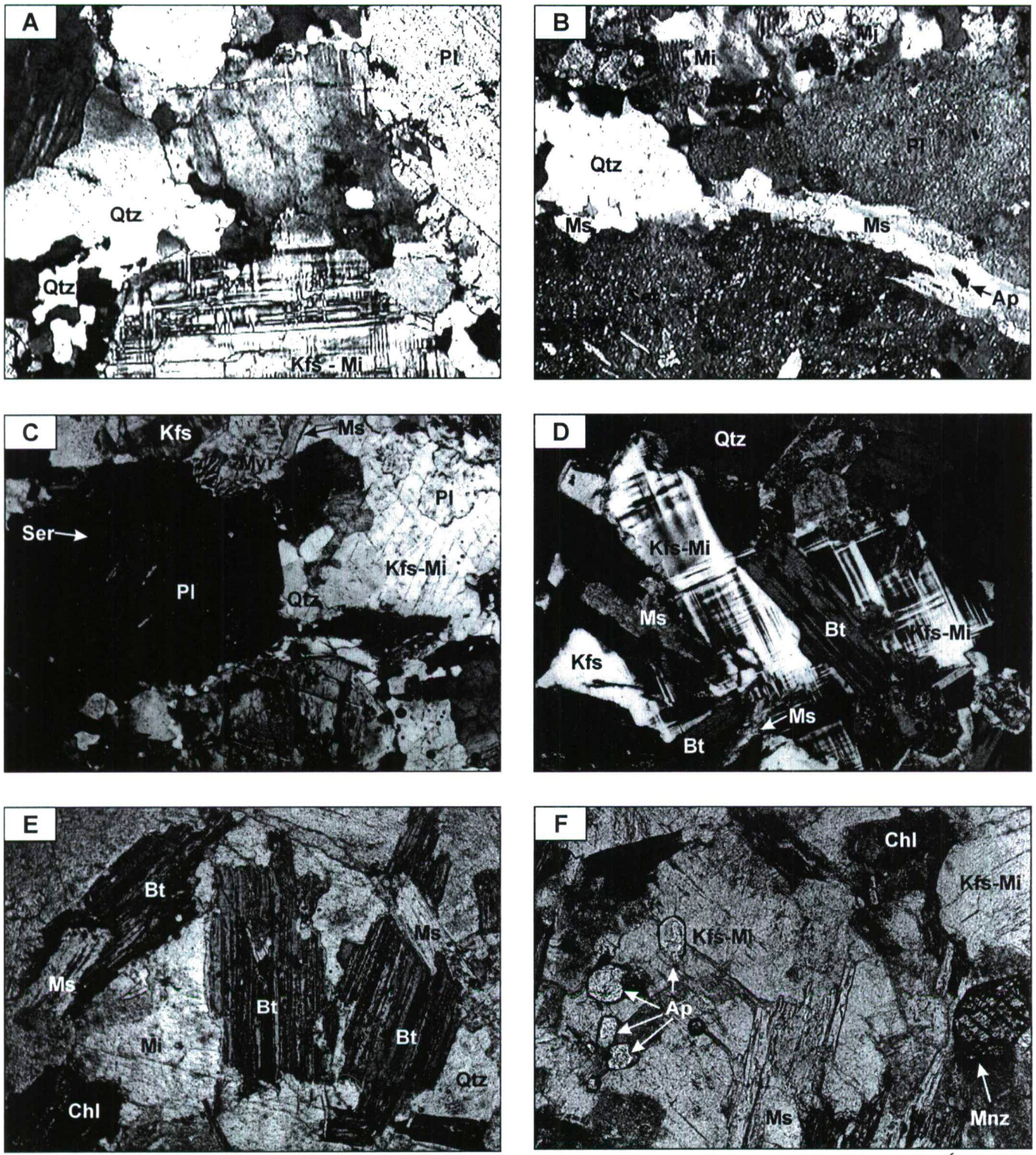

Fig. 4. Photomicrographs showing the mineral composition and texture of the studied granitoids. **(A)** sample ÁGK-1789 (Battonya-3), monzogranite, (+N, x50); **(B)** sample ÁGK-1807/1 (Battonya-36), syenogranite, (+N, x50); **(C)** sample ÁGK-1314 (Dombegyháza Dny-1), (+N, x50); **(D)** sample ÁGK-1841 (Battony K-4), syenogranite, (+N, x50); **(E)** sample ÁGK-1813 (Battonya-41), monzogranite, (1N, x50); **(F)** sample ÁGK-1848 (Battonya K-11), syenogranite, (1N, x100). Abbreviations: Ap – apatite, Bt – biotite, Chl – chlorite, Kfs – K-feldspar, Mi – microcline, Mnz – monazite, Ms – muscovite, Pl – plagioclase, Qtz – quartz, Ser – sericite.

plagioclase feldspar: hypidiomorphous, tabular, often zoned. Its average size is 1-3 mm. Often it is highly seriticised (Fig. 4B-C), less frequently carbonate and epidote grains occur in it as secondary minerals.

biotite: hypidiomorphous, an average size of 1-3 mm. Its pleochlorism is brownish yellow – brownish green (Fig. 4E). Due to the transformation, often only its chlorite pseudomorph is present (Fig. 4F). It occures in plagioclase

feldspar and microcline as an inclusion. Accessory minerals are apatite and zircon. Secondary components are: chlorite rutile, leucoxene, opaque minerals, sericite, carbonate, limonite and epidote.

muscovite: hypidiomorphous grains of an average 1-3 mm size. It occurs either with biotite or alone (Fig. 4E). Some places it forms kink bands (Fig. 4B). Along the cleavages secondary carbonate precipitates.

Accessory components in the studied rocks are apatite, monacite (Fig. 4F), zircone and less frequently titanite.

The rocks mentioned above has been modified to a smaller or larger extent (chloritisation, sericitisation, or rarely saussiritisation). As a result of these transformations the following secondary components appeared: chlorite, sericite, carbonate, epidote, titanite, limonite and opaque components.

Affected by deformations, the main rock forming minerals change, as it was experienced in case of the rocks of textural group d.

On the basis of modal measurements in the Q-A-P diagram (Le Maitre, 1989), the studied rocks plot to three different fields (Fig. 5): syenogranite, monzogranite, and granodiorite

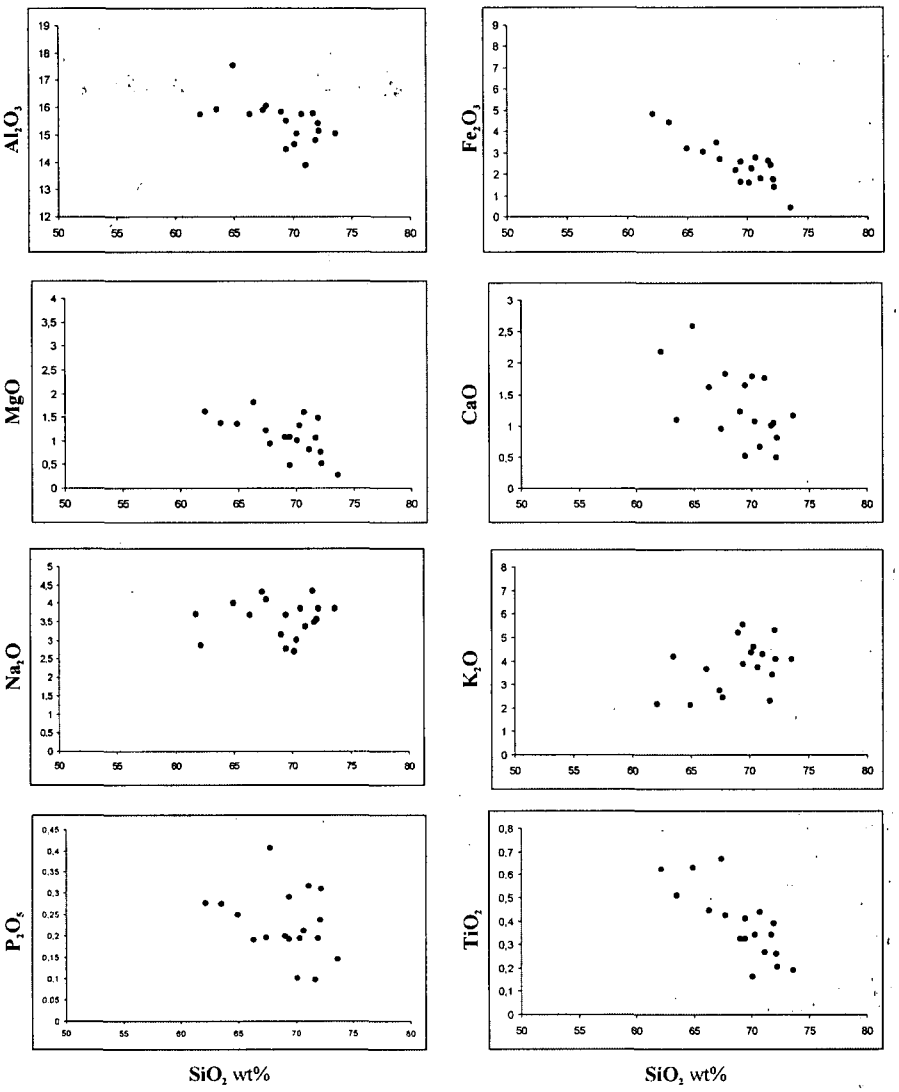

Fig. 6. Harker diagrams for major elements.

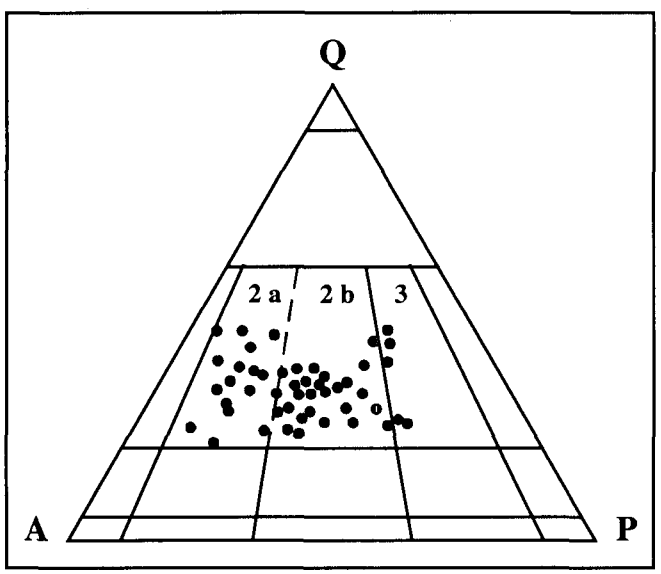

Fig. 5. Modal classification according to the IUGS (Le Maitre, 1989). 2a - syenogranite, 2b - monzogranite, 3 – granodiorite.

MAJOR ELEMENT GEOCHEMISTRY

Eighteen samples were analysed with respect to their major element composition (Table 1).

The SiO_2 content varies between 62.10 and 73.60 wt% (mean value: 69.07 wt%). The alkali content is high: K_2O is between 2.12 and 5.54 wt% (mean value: 3.76 wt%), Na_2O is between 1.68 and 4.01 wt% (mean value: 3.42 wt%). Calcium and magnesium contents are low to moderate; 0.50-2.58 wt% CaO and 0.28-1.81 wt% MgO. However, iron content is relatively high: 0.44-4.82 wt% (mean value: 2.80) $Fe_2O_3^*$ (total Fe). The $Fe_2O_3^*/(Fe_2O_3^*+MgO)$ ratio varies between 0.59 and 0.77.

The normative corundum content of the studied granitoid samples proved to be higher than 2.50 wt% in all cases, the average normative corundum content is 3.99 wt%.

Harker variation diagrams for major elements are shown in Fig. 6. Al_2O_3, $Fe_2O_3^*$, MgO, CaO, P_2O_5, and TiO_2 all decrease with increasing silica content, nevertheless, K_2O increases with increasing silica content and Na_2O content is more or less constant.

The studied rocks were classified on the basis of a total alkalis *vs.* silica diagram (Cox et al., 1979, adapted by Wilson, 1989). The samples plotted to the granite and granodiorite fields (Fig. 7).

When applying the geochemical system of De la Roche et al. (1980) the rocks proved to be syenogranites, monzogranites and granodiorites (Fig. 8).

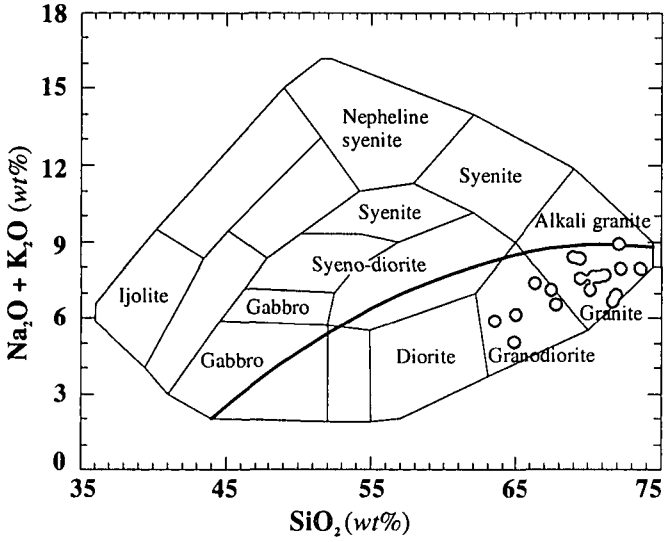

Fig. 7. The chemical classification and nomenclature of plutonic rocks using the total alkalis versus silica (TAS) diagram of Cox et al. (1979) adapted by Wilson (1989) for plutonic rocks. The curved solid line subdivides the alkali from subalkali rocks.

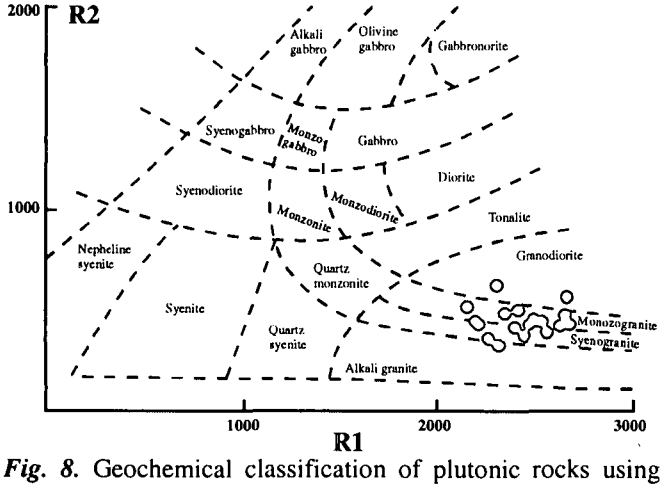

Fig. 8. Geochemical classification of plutonic rocks using parameters R1 and R2 (after De la Roche et al., 1980), calculated from milication proportions. R1 = 4Si-11(Na+K)-2(Fe+Ti); R2 = 6Ca+2Mg+Al

Based on Irvine, Baragar (1971), the rocks are subalkaline (Fig. 9), while according to Peacock's alkali-lime index (Peacock, 1931) they are calcic (Fig. 10).

The granites are peraluminous after Shand's index in the modified Maniar, Piccoli (1989) diagram (Fig. 11).

Concerning the tectonical environment, granitoid rocks can be orogenic or anorogenic. The orogenic class comprises

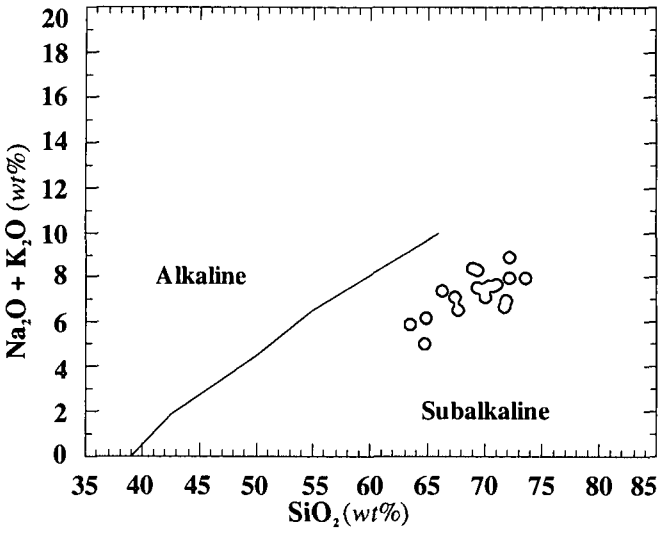

Fig. 9. SiO_2 *vs.* Na_2O+K_2O diagram according to Irvine, Baragar (1971).

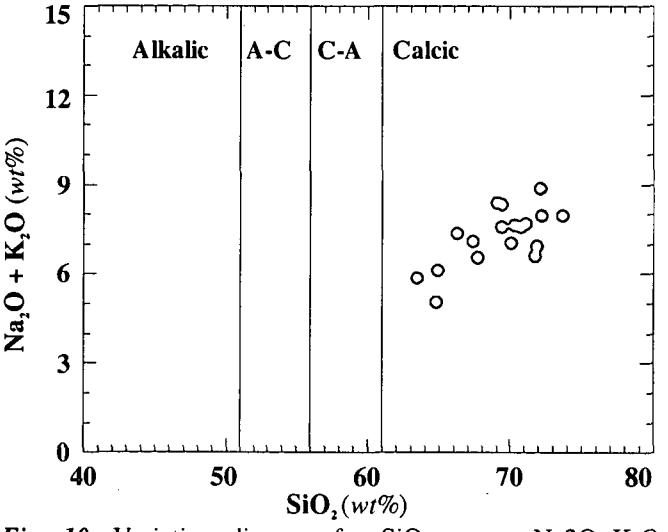

Fig. 10. Variation diagram for SiO_2 versus $Na2O+K_2O$ (Peacock, 1931).

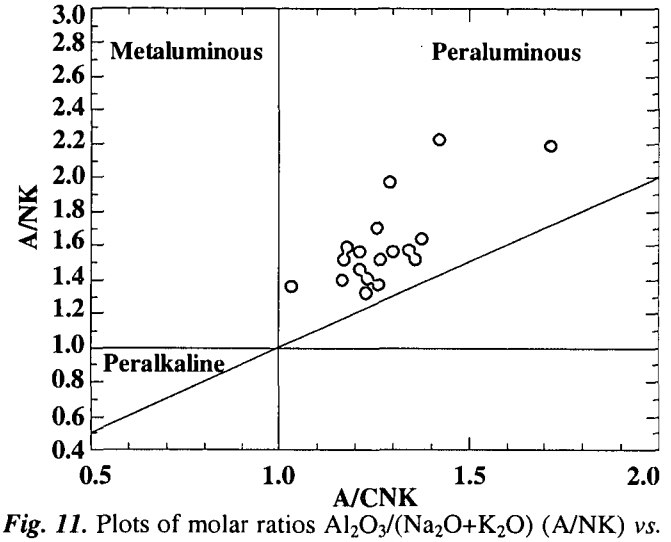

Fig. 11. Plots of molar ratios $Al_2O_3/(Na_2O+K_2O)$ (A/NK) *vs.* molar ratios $Al_2O_3/(CaO+Na_2O+K_2O)$ (A/CNK) (Maniar et al., 1989).

island arc granitoids (IAG), continental arc granitoids (CAG), continental collision granitoids (CCG), and post-orogenic granitoids (POG). Members of the anorogenic class are rift-related granitoids (RRG), continental epirogenic uplift granitoids (CEUG) and oceanic plagiogranites (OP) (Maniar et al., 1989). On the basis of the SiO_2 *vs.* K_2O system (Fig. 12A) the OP group can unambiguously be excludeded (Maniar et al., 1989). According to the SiO_2 *vs.* $FeO^t/(FeO^t+MgO)$ (Fig. 12B), and the SiO_2 *vs.* Al_2O_3 (Fig. 12C) diagarms (Maniar et al., 1989) our studied rocks are orogenic granitoids (IAG+CAG+CCG). In case of CCG the A/CNK ratio (Fig. 11) cannot be lower than 1.05, in the meantime the A/CNK ratio of the IAG+CAG group cannot be higher than 1.15. Since, in our case the A/CNK ratio, with one exception (Mezőhegyes-13-ÁGK1603; A/CNK=1.036), is always higher than 1.15 (A/CNK=1.168-1.716), the studied samples are CCG.

If we consider the R1 vs. R2 system of Batchelor, Bowden (1985) (Fig. 13), which predicts well the tectonic environment of granitoid formation, the analysed rocks can be interpreted as syn-collisional type granitoids.

Chappell, White (1974) designated granites extracted from a sedimentary protholith as S-type granites, while granites from an igneous protholith as I-type granites. White (1979) isolated also an A-type alkali granite, that occurs on continental plates. S-type granitoids are related mainly to compressional tectonic movements at the collision belt of two continental plates, and develop in the ultrametamorphous zone of the sediment-rich continental crust. The ASI $[Al_2O_3/(CaO+K_2O+Na_2O)]$ value of S-type granitoids is > 1.15, the CIPW norm yields > 1% corundum, and they are characterised by a relatively low Na/K ratio, which is a basic criterion (Zen, 1988). Usually, they are two-mica granites, mostly with monazite content. The syn-tectonic Battonya Unit granites are peraluminous, contain muscovite and biotite, and exhibit most of the features associated with S-type granites. On the basis of the major element analysis, the normative corundum content of the studied granites is higher than 1 wt% (mean value: 3,99 wt%), and the Na/K ratio is relatively low. More accurate classification is possible in the future on the basis of trace element content.

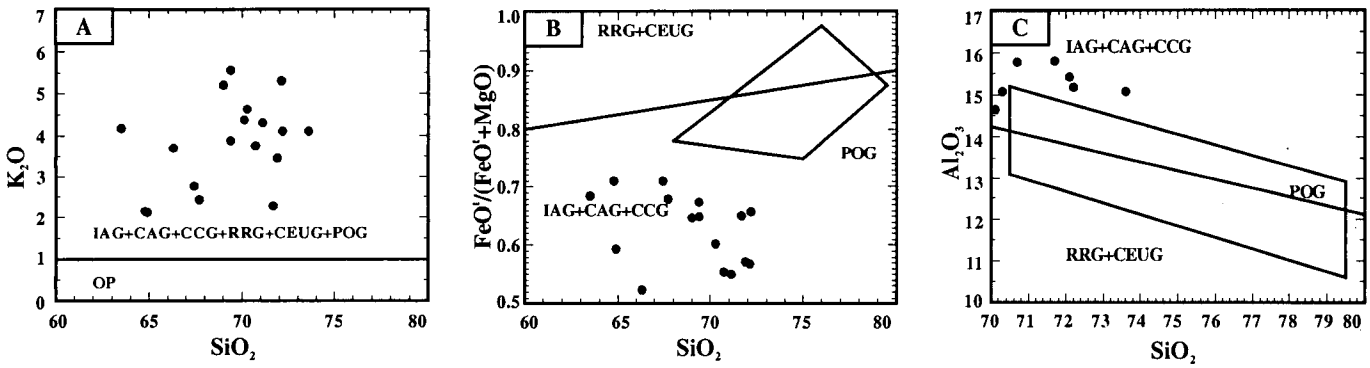

Fig. 12. A selection of diagrams after Maniar et al. (1989). **A.** SiO_2 *vs.* K_2O; **B.** SiO_2 *vs.* $FeO^t/(FeO^t + MgO)$; **C.** SiO_2 *vs.* Al_2O_3. Abbreviations: IAG = island arc granitoids, CAG = continental arc granitoids, CCG = continental collision granitoids, POG = post-orogenic granitoids, RRG = rift-related granitoids, CEUG = continental epirogenic uplift granitoids, OP = oceanic plagiogranites.

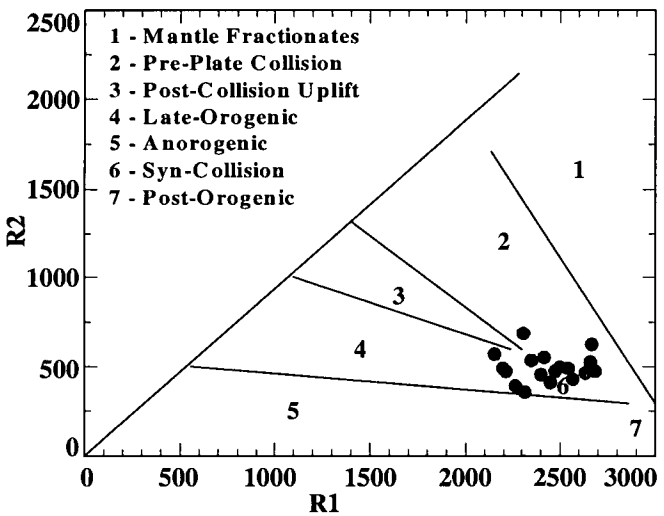

Fig. 13. Tectonical discrimination plots of Batchelor, Bowden (1985). $R_1 = 4Si - 11(Na+K) - 2(Fe+Ti)$; $R_2 = 6Ca + 2Mg + Al$.

Conclusions

(1) On the basis of their composition, the granitoid rocks of the available Battonya Unit boreholes can be considered of similar character. The main rock forming minerals of the studied samples are: quartz ± orthoclase + microcline + plagioclase feldspar (albite-oligoclase) ± biotite + muscovite. Accessory components are apatite, zircone, monacite and less frequently titanite. Their modal composition refers to that of syenogranites, monzogranites and granodiorites.

(2) On the basis of their chemical composition the studied rocks are subalkaline and calcic syenogranites, monzogranites and granodiorites with a peraluminous character.

(3) From a tectonical aspect the studied rocks are of orogenous, syn-collisional, continental collisional origin (CCG).

(4) Most of the characteristics featuring the Battonya Unit granitoids indicate that they are S-type granitoids.

Table 1. Major element data for Battonya Unit granitoids.

wt %	Battonya-48 ÁGK-1816 1174-1176 m	Battonya-63 ÁGK-1835 1029-1034 m	Battonya-72 ÁGK-1837 1136-1137 m	Battonya K-9 ÁGK-1846 1058-1060 m	Battonya K-11 ÁGK-1848 1046-1050 m	Battonya K-13 ÁGK-1849 1069-1071 m	Battonya K-14 ÁGK-1850 1075-1077 m	Battonya K-17 ÁGK-1853 1052-1075 m
SiO_2	72.1	73.6	72.2	70.3	70.7	66.3	69.4	71.9
Al_2O_3	15.41	15.07	15.16	15.05	15.77	15.76	15.53	14.8
TiO_2	0.263	0.193	0.207	0.343	0.441	0.447	0.411	0.392
$Fe_2O_3^*$	1.761	0.441	1.43	2.299	2.799	3.075	2.599	2.452
MnO	0.041	0.021	0.038	0.056	0.056	0.068	0.054	0.053
CaO	0.5	1.164	0.816	1.071	0.669	1.618	1.654	1.045
MgO	0.763	0.2805	0.517	1.321	1.615	1.814	1.081	1.493
K_2O	5.3	4.092	4.089	4.617	3.727	3.683	3.87	3.439
Na_2O	3.582	3.866	3.873	3.011	3.87	3.695	3.687	3.494
P_2O_5	0.238	0.147	0.309	0.194	0.212	0.191	0.193	0.195

Table 1 (continued)

wt %	Battonya K-18 ÁGK-1854 1079-1082 m	Mezőhegyes-13 ÁGK-1603 1184.5-1190 m	Mezőhegyes-15 ÁGK-1605 1194-1198 m	Mezőhegyes-18 ÁGK-1609 1220-1220.8 m	Mezőhegyes-19 ÁGK-1610 1180-1182.5 m	Mezőhegyes-20 ÁGK-1612 1184-1186 m	Mezőhegyes K-1 ÁGK-1613 1328-1330 m
SiO_2	69	71.1	62.1	67.4	64.9	69.4	71.7
Al_2O_3	15.84	13.88	15.76	15.92	17.57	14.49	15.79
TiO_2	0.323	0.268	0.624	0.671	0.632	0.325	0.341
$Fe_2O_3^*$	2.22	1.789	4.829	3.504	3.217	1.632	2.65
MnO	0.050	0.039	0.062	0.034	0.045	0.013	0.048
CaO	1.232	1.773	2.189	0.956	2.589	0.52	1.011
MgO	1.09	0.818	1.63	1.231	1.368	0.482	1.073
K_2O	5.2	4.285	2.167	2.769	2.126	5.54	2.291
Na_2O	3.166	3.388	2.885	4.334	4.017	2.769	4.349
P_2O_5	0.200	0.318	0.277	0.198	0.251	0.292	0.099

Table 1 (continued)

wt %	Dombegyház DNY-2 ÁGK-1315 1350-1352 m	Kunágota-1 ÁGK-1318 1797-1804 m	Kunágota-2 ÁGK-1317 1908-1911 m
SiO_2	67.7	70.1	63.5
Al_2O_3	16.06	14.65	15.93
TiO_2	0.428	0.163	0.511
$Fe_2O_3^*$	2.719	1.599	4.439
MnO	0.055	0.017	0.047
CaO	1.84	1.79	1.097
MgO	0.941	1.019	1.378
K_2O	2.439	4.366	4.175
Na_2O	4.115	2.707	1.682
P_2O_5	0.409	0.102	0.276

(*given as total iron content)

ACKNOWLEDGEMENTS

The financial background of this work was ensured by the Hungarian National Science Found (OTKA) (Grant No. F/029061), the János Bolyai Research Grant and the Swedish Institute.

REFERENCES

ALBU, I., PÁPA, A. (1992): Application of high-resolution seismic is studying reservoir characteristics of hydrocarbon deposits in Hungary. Geophysics, **57**, 1068-1088.

BATCHELOR, R. A., BOWDEN, P. (1985): Petrogenetic interpretation of granitoid rock series using multicationic parameters. Chemical Geology, **48**, 43-55.

BUDA, GY. (1996): Correlation of Variscan granitoids occuring in Central Europe. Acta-Mineralogica Petrographica, Szeged, **37**, Supplement, 24 pp.

CHAPPEL, B. W., WHITE, A. J. R. (1974): Two contrasting granite types. Pacific Geology, **8**, 173-174.

COX, K. G., BELL, J. D., PANKHURST, R. J. (1979): The interpretation of igneous rocks. George, Allen and Unwin, London.

CSONTOS, L. NAGYMAROSI, A. (1999): Late Miocene inversion versus extension in the Pannonian Basin. Tübinger Geowissenschaftliche Arbeiten, Series A, **52**, 132.

DE LA ROCHE, H., LETERRIER, J., GRANDCLAUDE, P., MARCHAL, M. (1980): A classification of volcanic and plutonic rocks using R1-R2 diagrams and major element analyses – its relationship with current nomenclature. Chemical Geology, **29**, 183-210.

IRVINE, T. N., BARAGAR, W. R. A. (1971): A guide to the chemical classification of the common volcanic rocks. Canadian Journal of Earth Sciences, **8**, 523-548.

KOVÁCH, Á., SVINGOR, É., SZEDERKÉNYI, T. (1985): Rb-Sr dating of basement rocks from the southern foreland of the Mecsek Mountains, Southeastern Transdanubia, Hungary. Acta Mineralogica-Petrographica, Szeged, **27**, 51-56.

KOVÁCS, S., HASS, J., BUDA, GY., NAGYMAROSY, A., SZEDERKÉNYI, T., ÁRKAI, P., CSÁSZÁR, G. (2000): Tectonostratigraphic terranes in the pre-Neogene basement of the Hungarian part of the Pannonian area. Acta Geologica Hungarica, Vol. **43/3**, 225-328.

LE MAITRE, R. E. (ed.) (1989): A classification of the igneous rocks and glossary of geological terms. Blackwell.

MANIAR, P. D., PICCOLI, P. M. (1989): Tectomic discrimination of granitoids. Geological Society of America Bulletin, **101**, 635-643.

PEACOCK, M. A. (1931): Classification of igneous rock series. Journal of Geology, **39**, 7-65.

SZEDERKÉNYI, T. (1984): Az alföld kristályos aljzata és földtani kapcsolati (Crystalline basement and geological relations of the Great Plain). D.Sc. Thesis. MTA Library, Budapest, (in Hungarian).

SZEDERKÉNYI, T. (1996): Metamorphic formations and theircorrelation in the Hungarian part of the Tisza Megaunit (Tisa Composite Terrane). Acta Mineralogica-Petrographica Szeged, **37**, 143-160.

SZEPESHÁZY K. (1969): Petrographische Angaben zur Kentniss des Battonyaer Granits. Magyar Állami Földtani Intézet Évi Jelentése 1967, 227-266. Budapest, (in Hung., with German summ.).

TARI, G., DÖVÉNYI, P., DUNKL, I., HORVÁTH, F., LENKEY, L., STEFANESCU, M., SZAFIÁN, P., TÓTH, T. (1999): Lihospheric structure of Pannonian basin derived from seismic, gravity and geothermal data. In Durand B, Jolivet L, Horváth F,Sérane M (eds): The Mediterranean Basins: Tertiary Extension within the Alpine Orogenesis, Geological Society: London. Special Publication, **156**, 215-250.

WHITE, A.J. R. (1979): Sources of granite magmas. Abstracts with programs, Geological Society of America, Annual General Meeting 1979, 539 pp.

WILSON, M. (1989): Igneous petrogenesis. Unwin Hyman, London.

ZEN, E. (1988): Phase relations of peraluminous granitic rocks and their petrogenetic implications. Ann. Rev. Earth Planet. Sci., **16**, 21-51.

Received: December 12, 2001; accepted: April 28, 2002

2ND "MINERAL SCIENCES IN THE CARPATHIANS" CONFERENCE

6-7 March, 2003
Miskolc, Hungary
http://www.uni-miskolc.hu/~asvany

SCOPE:

The first regional mineral science conference in Miskolc, 2000 ("*Minerals of the Carpathians*"), was well appreciated by the participants. That conference included 10 plenary lectures and 111 poster presentations of 143 specialists from all countries of the Carpathian-Pannonian Region and from some other countries of Europe.

Our aim has not changed since 2000: to arrange a stable and suitable meeting point for specialists in mineral sciences (mineralogy, petrology, geochemistry and their applications) of this region. We also welcome mineralogists from outside of the Carpathian-Pannonian Region, promoting the more wide-ranged scientific collaboration between different regions of Europe.

We firmly believe that this 2nd, 2003 MC conference, just like the previous one, will initiate new joint research projects and new educational co-operations in the close future.

DATE AND PLACE

The meeting will be held in Miskolc, Hungary on March 6–7, 2003. The scientific activities will be placed at the University of Miskolc.

SCIENTIFIC PROGRAMME

The scientific programme is planned to cover mineralogy, crystallography, petrology, geochemistry, mineral deposits and their applications in the Carpathians (in broad sense). An Open Session will also be organised depending on demand. Contributions will be presented in (limited) oral and in (extensive) poster sessions.

Plenary lectures on special topics will be presented at the conference, the subject of which will be communicated in the Second Circular.

Scientific board of the meeting
M. Chovan (Slovakia), A. Gawęda (Poland), F. Koller (Austria), V. Kvasnytsya (Ukraine), M. Novák (Czech Republic), G. Papp (Hungary), Gh. Udubasa (Romania)

Conference Language
The official language of the meeting will be English.

Abstracts
You are invited to submit papers in the field of the scientific programme. The abstracts are to be published in a special volume of ***"Acta Mineralogica-Petrographica, Szeged"***.

Important dates

Deadline for returning the First Circular	**September 30, 2002**
Second Circular	**October, 2002**
Deadline for abstracts	**January 10, 2003**

ORGANISERS
Herman Ottó Museum
University of Miskolc

CO-ORGANISERS
Austrian Mineralogical Society
Hungarian Geological Society
Mineralogical Society of Poland
Mineralogical Society of Romania
Slovak Geological Society
Ukrainian Mineralogical Society
CBGA Commission on Mineralogy and Geochemistry

ADDRESS FOR CORRESPONDENCE AND INFORMATION
2nd "Mineral Sciences in the Carpathians" Conference
c/o Department of Mineralogy
Herman Ottó Museum
Kossuth u. 13
H-3525 Miskolc (Hungary)
Phone: +36-46-505098
Fax: +36-46-555397

CONTACT PERSONS OF LOCAL ORGANISING COMMITTEE:
Sándor Szakáll and Béla Fehér:
e-mail: homin@axelero.hu

Acta Mineralogica-Petrographica, Szeged 2001, Vol. 42, pp. 33-37

ACTA
Mineralogica
Petrographica

MYRMEKITE-BEARING GNEISS FROM THE SZEGHALOM DOME (PANNONIAN BASIN, SE HUNGARY). PART I.: MYRMEKITE FORMATION THEORIES

JUDIT ZACHAR[1], TIVADAR M TÓTH[1]

[1] Department of Mineralogy, Geochemistry and Petrology, University of Szeged
H-6701 Szeged, P. O. Box 651, Hungary
e-mail: zachar@geo.u-szeged.hu

ABSTRACT
Myrmekite is a common textural feature in many magmatic and metamorphic rock types. Nevertheless, there are several theories concerning its genesis; myrmekite may form by igneous crystallization, solid state exsolution, progressive or retrograde metamorphism, metasomatism or even as a result of complicated deformation mechanisms. In this paper a brief compilation of these models is given and classified by myrmekite forming processes instead of rock types or minerals involved.
Key words: myrmekite, orthogneiss, Pannonian Basin

INTRODUCTION

Similarly to most metamorphic complexes, the crystalline basement of the Pannonian Basin consists essentially of different varieties of gneiss and amphibolite. Most of these gneisses are of medium metamorphic grade and contain rather consistent mineralogy; quartz, two feldspars and mica with some additional phases. This reason makes obvious characterization of certain gneiss types difficult, and spatial correlation among neighbouring gneiss terrains almost impossible. In order to be able to recognize gneiss types of different kinds of protolith and/or metamorphic evolution, one has to concentrate on accessory minerals and particular textural information.

In this paper we focus on occurrences of myrmekite in different metamorphic rocks. Myrmekite has been reported from several places of different rock types all around the world. Presence of myrmekite was published from granites (Shelley 1964; Collins 1997a, 1998; Phillips and Carr, 1973) basic igneous rocks (Shelley, 1967; Dymek, Schiffries, 1987; Pavlov, Karskiy, 1949) and from different metamorphic rocks (gneisses, mica schists, mylonites) (Phillips, Ransom, 1970; Phillips and Carr, 1973; Shelley, 1967, 1973; Siddhanta, Akella, 1966; Phillips et al., 1972; Nold, 1984; Simpson, Wintsch, 1989; Hippertt, Valarelli, 1998). It can develop through diverse processes; subsolidus exsolution, metasomatism, deformation, silica infiltration or even due to progressive and retrograde metamorphism.

Several authors reported presence of myrmekite from the metamorphic basement of the Pannonian Basin (e.g. Szalay, 1977; Balázs et al., 1986) too. In order to be able to better understand the origin of these myrmekitic feldspars, in the first part of our two end-to-end papers we briefly compile the diverse explanations one can find in the literature concerning myrmekite definition and genesis.

DEFINITION OF MYRMEKITE

A generally accepted, proper definition for myrmekite is still missing; almost every author has his own definition depending on the type of occurrence and related minerals..

Phillips (1974) among others assigned myrmekite as an intergrowth of quartz and plagioclase. He said the presence of K-feldspar is implicit adjacent to the intergrowth, while its absence is explained as the result of cut of thin section. According to Shelley (1973), myrmekite is a poikiloblastic intergrowth of quartz and plagioclase, Simpson, Wintsch (1989) defined symplectitic intergrowth of oligoclase and quartz as myrmekite. Augusthitis (1973) doesn't put a premium on the presence of K-feldspar and says myrmekitic quartz may occur in micas and epidote too as they represent intracrystalline solutions (Augusthitis, 1973, 1990). Dymek, Schiffries (1987) define labradorite – bytownite intergrowth as myrmekite too, while Koller, Kloetzli (1995), in concert with Augusthitis (1973), determinate symplectitic intergrowth of quartz and biotite as myrmekite as well.

Shelley (1993) gives a common definition of myrmekite: "*...myrmekite is an intergrowth of branching rods of quartz set in a single crystal of plagioclase, neighbouring quartz rods have the same lattice orientation and extinguish together. It is almost ubiquitous in granites and granitic gneisses and most commonly occurs at grain boundaries of K-rich feldspar. Myrmekites appear to have grown inwards from grain boundaries, invading and replacing K-feldspar. The quartz rods branch in that direction and the plagioclase may be euhedral or bulbous representing a minimum surface area to volume configuration for the plagioclase.*" As Shelley wrote this is the most common occurrence of myrmekite and this is a widely accepted definition but it cannot be generalized. In the highest sense of the word myrmekite always is associated with feldspars and quartz,

so intergrowths of other minerals are better to call symplectites. Several models have been matured on myrmekite genesis over more than a hundred years, but a generally accepted model have not yet been published since the first description of Michel-Lévy (1875). According to its wide spread in different rock types beyond granites, Shelley (1964), Phillips (1972), Phillips, Ransom, Vernon (1972) agree that myrmekite may be polygenetic.

GENESIS OF MYRMEKITE

Here we give a short description of the most common models on myrmekite formation. Although, most approaches take into account effects of several processes, we classify the models in order to facilitate reader to look over them. In addition to the three classical ideas on myrmekite genesis (igneous crystallization; solid state exsolution; metasomatic replacement) also more up-to-date models, which appeared in the last decades are presented.

1. Igneous crystallization models

The theory of myrmekite genesis by igneous crystallization suggests that myrmekite forms as a result of a late stage simultaneous crystallization of plagioclase and quartz from a melt or solution. The textures, however, are more indicative of simultaneous crystallization are graphic or granophyric, which have no necessary relationship with myrmekitic textures. According to Shul'Diner (1972) myrmekitic plagioclase grain nucleates on the surface of another plagioclase grain and advances toward the adjacent K-feldspar. Myrmekitic plagioclase grows in optical continuity with the original plagioclase grain. But the available literature does not mention any suture in contact of the old grain, which is common on overgrowth structures (Hippertt, Valarelli, 1998). Hibbard (1987) regards myrmekite in orthogneiss as recrystallization at a late stage of deformation of an incompletely crystallized magma in the presence of water saturated melt.

2. Solid state exsolulion models

In Schwantke's (1909) solid-state exsolution model, the presence of a "high silica" $CaAl_2Si_6O_{16}$ molecule in high temperature K-feldspar is assumed. Through unmixing *An* produces releasing four molecules of silica. The existence of this "Schwantke molecule" has, however, not been proven yet.

3. Progressive metamorphic reaction models

"Progressive myrmekite" develops at the transition between greenschist and amphibolite facies in pelitic schist in quartz rich segregation layers, when albite changes to Ca-oligoclase (Shelley, 1973) in the following reaction (Ashworth, 1986):

$$(1+x)NaAlSi_3O_8 + xCa^{2+} = Na_{1-x}\,Ca_xAl_{1+x}Si_{3-x}O8 + 4xSiO_2 + 2xNa^+$$

He suggests that it will be preserved only if it formed at the thermal climax of metamorphism.

For biotite oligoclase gneisses of the Adirondack Massif, Collins (1997b) showed that the rock gained K and Si and lost Ca, Fe, Mg and Al during progressive thermal metamorphism. Following Engel, Engel (1958) in such a rock plagioclase is progressively replaced by microcline. Carl (1988) suggests that K was originated from breakdown of nearby biotite and muscovite. They all suppose myrmekite formation in connection with formation of microcline.

4. Retrograde metamorphic reaction models

Siddhanta, Akella (1966) examined three types of myrmekite in Pre-Cambrian sphene and epidote bearing hornblende plagioclase gneisses. Type I. is a myrmekite in association with microcline or orthoclase without any contact with non-myrmekitized plagioclase; type II. is a myrmekite in association with plagioclase; and type III. is a myrmekite, which forms between plagioclase and K-feldspar grains. During the retrograde evolution, K-metasomatism took place as it is inferred by presence of postkinematic biotite with no pre-existing potassium phase in the rock. They found a tight correlation between the amounts of sphene + epidote and myrmekite, respectively. It was explained by a series of consecutive reactions between hornblende, K-feldspar, anorthite, sphene and ilmenite, which may result in myrmekite formation of different occurrences. The main myrmekite producing reactions are the followings:

$$3\,Ca_2(Mg,Fe)\,4\,Al(Si_7AlO_{22})(OH)_2 + 4\,KAlSi_3O_8 + H_2O =$$
(common hornblende) (potassium feldspar)
$$= 4\,K(Mg,Fe)_3(Si_3AlO_{10})(OH)_2 + 3\,CaAl_2Si_2O_8 + 3\,CaO + 15\,SiO_2$$
(biotite) (anorthite) + (quartz)

$$3Ca_2(Mg,Fe)\,4Al(Si_7AlO_{22})(OH)_2 + 4KAlSi_3O_8 + 3TiO_2 + H_2O =$$
(common hornblende) (potassiun feldspar) (rutile)
$$= 4\,K(Mg,Fe)_3(Si_3AlO_{10})(OH)_2 + 3\,CaAl_2Si_2O_8 + 3\,CaTiSiO_5 + 12\,SiO_2$$
(biotite) (anorthite) (sphene) (quartz)

A model for myrmekite formation during a retrogressive metamorphic evolution was given by Phillips (1972) as well. He proposed the following reaction:

$$3KAlSi_3O_8 + H_2O = KAl_2(AlSi_3)O_{10}(OH)_2 + 6SiO_2 + K_2O$$
(potassium feldspar) (muscovite)

Phillips, Ransom, Vernon (1972) point out that retrogressive metamorphism appears to be connected with myrmekite formation and in these cases muscovite is an important accompanying mineral. The reaction may take place as follows:

$$3\,KAlSi_3O_8 \,.\, NaAlSi_3O_8 + CaAl_2Si_2O_8 \,.\, NaAlSi_3O_8 =$$
(alkali feldspar) (calcic plagioclase)
$$= CaAl_2Si_2O_8 \,.\, 2\,NaAlSi_3O_8 + 6\,SiO_2 + KAl_2AlSi_3O_{10}(OH)_2 + K_2O$$
(more sodic plagioclase) (quartz) (muscovite)

$$3\,KAlSi_3O_8 + H_2O = KAl_2AlSi_3O_{10}(OH)_2 + 6\,SiO_2 + K_2O$$
(orthoclase) (muscovite) (quartz)

5. Metasomatic replacement models

The idea of myrmekite as a result of metasomatic replacement was first published by Becke (1908) whereof myrmekite replaces K-feldspar by the following reaction with Na and Ca bearing fluids:

$$1.25\,KAlSi_3O_8 + 0.75\,Na^+ + 0.25\,Ca^{2+} = Na_{075}Ca_{025}Al_{1.25}Si_{2.75}O_8 + 1.25\,K^+ + SiO_2$$
(137 cc/mol) *(100 cc/mol)* (23 cc/mol)

Drescher-Kaden (1948) suggests that myrmekite forms during a reaction in which K-feldspar metasomatically replaces plagioclase. He showed that at some cases myrmekite is older than K-feldspar. The origin of excess silica, which is needed for this replacement reaction, was explained by Bhattacharyya (1972) and Phillips (1972). In their opinion silica can be introduced from solutions or by dry ionic diffusion, and they stated there is no direct relationship between the amount of myrmekitic quartz and

the basicity of plagioclase. Pavlov, Karskiy (1949) made investigations on the origin of myrmekite in basic rocks where K-feldspar was absent. They recommend a reaction between quartz and plagioclase as follows:

$$3(CaAl_2Si_2O_8 \,.\, NaAlSi_3O_8) + CaO = 4\,CaAl_2Si_2O_8 \,.\, 1\,NaAlSi_3O_8 + 3SiO_2 + Na_2SiO_3$$
(plagioclase) (more basic plagioclase) (quartz)

Dymek, Schiffries (1987) examined myrmekite in andesine anorthosites. They stated that non-myrmekitized plagioclase is $An_{40\pm3}$, while myrmekitic grains are An_{80} in composition. In their model sodic plagioclase was replaced by calcic plagioclase accompanied by precipitation of quartz. They calculated the amount of quartz that would have precipitated during the alteration of An_{40} to An_{80} and the result accords well with the observed amount of quartz in thin section. In their opinion these calcic myrmekites are products of interaction between plagioclase crystals and a magmatically derived aqueous fluid.

In conception of Collins (1997b) myrmekite in deformed granodiorites may form during progressive replacement of fresh normal zoned plagioclase by inversely zoned plagioclase. During the replacement process, deformed plagioclase crystals have ample openings for fluids and elements to move inside or outside. Primarily Ca and Al subtract and Na is left over, while K infiltrates and begins to grow inside the plagioclase grain. While K replaces Ca and Al, the volume of the plagioclase grain increases inducing pressure at the adjacent grains. Displaced Na atoms infiltrate to less altered plagioclase grains to cause them recrystallize as a more sodic plagioclase. According to the zoning of the original plagioclase in the diorite the core is $An_{37\text{-}39}$ while the rim is $An_{17\text{-}20}$ in composition. The recrystallized plagioclase is an $An_{12\text{-}15}$ oligoclase with albite twinning. Myrmekite forms at places where Ca, Al, Na and Si remain in a wrong proportion to recrystallize only as plagioclase. Replacement of Na and Ca with K however is never perfect, relic islands may remain that later separate to form albitic perthite lamellae. The shape and thickness of quartz vermicules depend on the composition of the original plagioclase.

Another hypothesis by Collins (1997a) is based on processes he observed in clinopyroxene granites. Here Na^+ and Ca^{2+} bearing fluids as follows metasomatize perthitic K-feldspar:

$$KAlSi_3O_8 + Na^+ = NaAlSi_3O_8 + K^+$$
$$2\,KAlSi_3O_8 + Ca^{2+} = CaAl_2Si_2O_8 + 4\,SiO_2 + 2K^+$$
(myrmekite)

Collins (1997a) observed that the K-feldspar part of perthite is replaced by An_{20} plagioclase, while relic plagioclase lamellae remain untouched and no myrmekite forms. If alteration took place by mass-to-mass mode, quartz vermicules would appear in the plagioclase so the alteration must happen by volume-to-volume way. Because of the larger density of the secondary plagioclase, silica is consumed in the process and no excess quartz appears.

Following Koller (1995 in Collins 1997c) myrmekite formed by exsolution shows perthitic appearance with Ba-zoning, while myrmekite formed by K-metasomatism appears at the edges of perthitic microcline lacking Ba-zonation. Ghost myrmekite is the characteristic of the later too, which may appear strongly depending on thin section orientation Passchier, Trouw (1996).

6. Deformation models

The significant modification of the stability field of minerals under high strain conditions was first suggested by Harker (1932); Wintsch, Knipe (1983) showed that deformation also might result in replacement reactions. In the last decades the relationship between deformation and myrmekite formation at grain boundaries came into prominence. (e.g. Hanmer 1982, Tullis 1983, Simpson 1983, Hibbard 1987, Simpson, Wintsch, 1989).

Shelley (1964, 1993) interprets myrmekite as a special kind of poikiloblastic texture without any proportional relationship between the amount of quartz in myrmekite and basicity of plagioclase. In his model albite in solid-state exsolves from high-T feldspar, which also encloses quartz inclusions. Following a cataclastic event these quartz grains recrystallize and form vermicules in myrmekite. However in many granites with well developed myrmekite there is no evidence for presence of strained quartz. Further this hypothesis does not explain myrmekite around plagioclase inclusions in alkali feldspar megacrysts (Hippertt, Valarelli, 1998).

Hanmer (1982) studied deformed granites from Newfoundland and showed that myrmekite must be of post-deformational origin, since the soft vermicular texture would have been destroyed during deformation. Simpson (1985) has observed progressive intergrowth of myrmekite in millimetre scale shear zones in mylonitic granodiorites from East-California that provides evidence for syn-deformation myrmekite emplacement.

Simpson, Wintsch (1989) made examinations on deformation-induced myrmekites in amphibolite facies mylonites derived from granitoid protolith. The samples were muscovite poor S-C mylonites and foliated mylonitic gneisses. In that instance Simpson and Wintsch (1989) defined symplectitic intergrowth of oligoclase and quartz as myrmekite that developed on both edges facing the incremental shortening direction of strained K-feldspar grains. Myrmekite does not occur on the edges of the incremental stretching direction. Replacement of K-feldspar by plagioclase and quartz results in decreasing volume that favours high strain surrounding the grain. Although P, T and the chemical conditions govern the replacement reaction, because of additive shear it concentrates along the edges facing incremental shortening direction of the K-feldspar. The role of stress and shear energy in replacement reactions has not yet been clarified.

In the Collins (1997a) model existence of original high-T ternary feldspar is assumed; a K-feldspar (orthoclase) containing dissolved Ca and Na. On lower T under stress conditions orthoclase alters into microcline, Na and Ca in turn dissolute from the K-feldspar to form myrmekite at the edges of the grain. Plagioclase with more anorthite component requires less amount of silica than K-feldspar or Na-feldspar thus the amount of myrmekite is determined by the composition (An component) of the plagioclase:

$$\begin{matrix} KAlSi_3O_8 \\ NAlSi_3O_8 \\ Ca(AlSi_3O_8)_2 \\ \text{H-T K-feldspar} \end{matrix} \quad = \quad \begin{matrix} KAlSi_3O_8 + NaAlSi_3O_8 + SiO_2 \\ CaAl_2Si_2O_8 \\ \\ \text{K-feldspar, myrmekite} \end{matrix}$$

Several myrmekite generating models among the numerous deformation-induced approaches assume silica infiltration following deformation, first of which was suggested by Michel-Lévy (1875).

Hippertt, Valarelli (1998) examined K-feldspar porphyroblast-bearing high grade (720-750 °C, 3-6 kbar) mylonitic augen gneisses. They observed two types of myrmekite occurences: 1. a lobe shaped myrmekite on the edge of K-feldspar megacryst, 2. bulbous myrmekite inclusion in K-feldspar megacryst. They found that K-feldspar replaces myrmekite in both cases. Silica needed to form myrmekite can be served by pressure solution of the matrix quartz. This process also is necessary to compensate the volume growth of the growing K-feldspar. The fact that myrmekite is not present in rocks lacking quartz suggests that silica necessary for myrmekite formation must originate from internal sources. The brittle deformation structure of the plagioclase grains may be the result of local stress, which is caused by the volume increase during plagioclase replacement by K-feldspar. Microcracks serve suitable pathways for silica infiltration. K-feldspar apophyses grow into the quartz vermicules indicate that K follows Si in infiltration. Myrmekitic plagioclase usually is richer in Ca than the recrystallized grains, but its *Ab/An* ratio is identical to the non-recrystallized plagioclase relics in the matrix. This observation suggests that myrmekitic plagioclase is the original phase that hosted subsequently developing quartz vermicules. Si infiltration is evidenced by occurrence of undeformed quartz vermicules or rods in deformed plagioclase grains. The source of Si and the factors of transportation are still not known.

Conclusions

Far the most frequent rock types in the metamorphic basement of the Pannonian Basin are different kinds of gneiss. As they are of close to identical chemical composition and metamorphic evolution, their mineralogy and textural features are rather similar as well. The aim of this paper was to introduce how informative myrmekitic feldspar grains of different origin may be in discriminating and correlating gneiss localities in a terrane of complex metamorphic evolution.

Abundant literature on myrmekite genesis shows that myrmekite can form due to diverse igneous, metamorphic and other processes. Despite, however, intensive investigations, important questions concerning the origin of this texture are still under debate. There regularly appear new rock types with myrmekitic grains, which do not fit to any of the models listed above. A cautious study of microscopic features and mineral chemical data is needed to be able to interpret myrmekitic texture correctly and so to utilize myrmekite for characterization of certain gneiss types.

We aimed to collect mineral systems, reactions as well as possible processes, which may develop myrmekite, just as to offer a brief survey of dozens of theories about myrmekite formation. There are several ways how to organize these ideas to serve a well-arranged system. In this paper an arbitrary classification scheme is presented, in which models are listed by myrmekite forming processes instead of rock types or minerals involved.

In the second part of our papers we attempt to interpret origin of myrmekitic feldspar grains found in a small area of the metamorphic basement of the Pannonian Basin (Szeghalom dome, Fig. 2. in M Tóth, Zachar, 2002). Here myrmekite occurs in intensely deformed polymetamorphic gneiss samples. Granite-related fluids also metasomatically altered the terrane.

Acknowledgement

Lelkes-Felvári Gy. is thanked for her comments on the early version of the manuscript. The project was financially supported by the Hungarian Research Found (grant no. OTKA F32792), the Hungarian Ministry of Culture (grant no. FKFP 0139/2001) and the János Bolyai Research Grant.

References

Ashworth, J. R. (1986): Myrmekite replacing albite in prograde metamorphism. American Mineralogist, **71**, 895-899.

Augustithis, A. A. (1973): Atlas of the textural patterns of granites, gneisses and associated rock types. Elsevier, Amsterdam.

Augustithis, S. S. (1990): Atlas Of Metamorphic-Metasomatic Textures And Processes. Elsevier, Amsterdam.

Balázs, E., Cserepes-Meszéna, B., Nusszer, A., Szili-Gyémánt, P. (1986): An attempt to correlate the metamorphic formations of the Great Hungarian Plain and the Transylvanian Central Mountains (Muntii Apuseni). Acta Geologica Hungarica **29/3-4**, 317-320.

Becke, F. (1908): Über myrmekit. Mineralogie und Petrographie Mitteilungen, **27**, 377-390.

Bhattacharyya, C. (1972): Myrmekite from the charnockitic rocks of the Eastern Ghats, India – a discussion. Geological Magazine **109**, 372.

Carl, J. D. (1988): Popple Hill gneiss as dacite volcanics: a geochemical study of leucosome and mesosome, Northwest Adirondacks, New York. Geological Society of America Bulletin, **100**, 841-849.

Collins, L. G. (1997a): Origin of myrmekite and metasomatic granite: Myrmekite, ISSN 1526- 5757, electronic Internet publication, no. 1, http://www.csun.edu/~vcgeo005/revised1.htm.

Collins, L. G. (1997b): Replacement of primary plagioclase by secondary K-feldspar and myrmekite: Myrmekite, ISSN 1526-5757, electronic Internet publication, no. 2, http://www.csun.edu/~vcgeo005/revised2.htm.

Collins, L. G. (1997c): Myrmekite formed by exsolution?: Myrmekite, ISSN 1526-5757, electronic Internet publication, no. 5, http://www.csun.edu/~vcgeo005/revised5.htm.

Drescher-Kaden, F. (1948): Die Feldspar-Quartz-Reaktionsgefuege der Granite und Gneise. Berlin-Springer, 259 p.

Dymek, R. F., and Schiffries, C. M. (1987): Calcic myrmekite: possible evidence for the involvement of water during the evolution of andesine anorthosite form St. Urbain, Quebec: Canadian Mineralogist, **25**, 291-319.

Engel, E. J., Engel, C. G. (1958): Progressive metamorphism and granitization of the major paragneiss, Northwest Adirondack Mountains, New York, Part I, Total rock. Geological Society of American Bulletin, **69**, 1369-1414.

Hanmer, S. K. (1982): Microstructure and geochemistry of plagioclase and microcline in naturally deformed granite. Journal of Structural Geology, **4**, 197-214.

Harker, A. (1932): Metamorphism. Methuen, London.

Hibbard, M. J. (1979): Myrmekite as a marker between preaqueous and postaqueous phase saturation in granitic systems. Geological Society of American Bulletin, **90**, 1047-1062.

HIBBARD, M. J. (1987): Deformation of incompletely crystallized magma systems, granitic gneisses and their tectonic implications. Journal of Geology, **95**, 543-561.

HIPPERTT, J. F., VALARELLI, J. V. (1998): Myrmekite constraints on the available models and a new hypothesis for its formation: European Journal of Mineralogy, **10**, nr. 2, 317-331.

KOLLER, F. AND KLOETZLI, U. S. (1995): Remnants of lower crustal mineral assemblages in granitoid rocks: Examples from the South Bohemian pluton, Austria; in The Origin of Granites and Related Rocks, III. Hutton Symposium, Abstracts, U.S. Geological Survey Circular **1129**, 82-83.

MICHEL-LÉVY, A. M. (1875): Structure microscopique des roches acides anciennes. Société Francaise de Mineralogie et de Crystallographie, Bulletin, **3**, 201-222.

NOLD, J. L. (1984): Myrmekite in Belt Supergroup metasedimentary rocks – northeast border zone of the Idaho Batholith. American Mineralogist, **69**, 1050-1052.

PASSCHIER, C. W., TROUW, R. A. J. (1996): Microtectonics. Springer

PAVLOV, N. V., KARSKIY, B. E. (1949): Myrmekite in basic rocks: Ivestiya Akademii Nauk SSSR Seriya Geologischeskaya, **5**, 128.

PHILLIPS, E. R., AND RANSOM, D. M. (1970): Myrmekitic and non-myrmekitic plagioclase compositions in gneisses from Broken Hill, New South Wales. Mineralogical Magazine, **37**, 729-732.

PHILLIPS, E. R., RANSOM, D. M., AND VERNON, R. H. (1972): Myrmekite and muscovite developed by retrograde metamorphism at Broken Hill, New South Wales. Mineralogical Magazine, **38**, 570-578.

PHILLIPS, E. R. (1972): Myrmekites of exsolution and replacement origins: a discussion. Geological Magazine, **110**, 74-77.

PHILLIPS, E. R., CARR, G. R. (1973): Myrmekite associated with alkali feldspar megacrysts in felsic rocks from New South Wales: Lithos, **6**, 245-260.

PHILLIPS, E. R. (1974): Myrmekite - one hundred years later: Lithos, **7**, 181-194.

SCHWANTKE, A. (1909): Die Beimischung von Ca in Kalifeldspat und die Myrmekitbildung. Zentralblatt für Mineralogie, 311-316.

SHELLEY, D. (1964): On myrmekite: American Mineralogist, **49**, 41-52.

SHELLEY, D. (1967): Myrmekite and myrmekite-like intergrowths: Mineralogical Magazine, **36**, 491-503.

SHELLEY, D. (1973): Myrmekites from the Haast schists, New Zealand: American Mineralogist, **58**, 332-338.

SHELLEY, D. (1993): Igneous and Metamorphic Rocks under the microscope, Chapman & Hall, London

SHUL'DINER, V. I. (1972): The problem of myrmekites: International Geology Review, **14**, 354-358.

SIDDHANTA, S. K., AKELLA, J. (1966): The origin of myrmekites in hornblende-plagioclase gneisses and in the associated pegmatites: Acta Geologica Hungarica, **10**, 31-52.

SIMPSON, C. (1983): Strain and shape fabric variations associated with ductile shear zones. Journal of Structural Geology, **5**, 61-72.

SIMPSON, C. (1985): Deformation of granitic rocks across the brittle-ductile transition. Journal of Structural Geology, **7**, 503-511.

SIMPSON, C., WINTSCH, R. P. (1989): Evidence for deformation-induced K-feldspar replacement by myrmekite: Journal of Metamorphic Geology, **7**, 261-275.

SZALAY, Á. (1977): Metamorphic-granitogenic rocks of the basement complex of the Great Hungarian Plain, Eastern Hungary. Acta Mineralogica-Petrographica Szeged **XXIII/1**, 49-69.

TULLIS, J. A. (1983): Deformation of feldspars. In Feldspar Mineralogy (ed.by Ribbe, P.H.), Mineralogical Society of America short course notes, **2**, 297-323.

WINTSCH, R. P., KNIPE, R. J. (1983): Growth of a zoned plagioclase porphyroblast in a mylonite. Geology, **11**, 360-363.

Received: December 4, 2001; accepted: July 3, 2002

Acta Mineralogica-Petrographica, Szeged 2001, Vol. 42, pp. 39-43

ACTA
Mineralogica
Petrographica

MYRMEKITE-BEARING GNEISS FROM THE SZEGHALOM DOME (PANNONIAN BASIN, SE HUNGARY). PART II.: ORIGIN AND SPATIAL RELATIONSHIPS

JUDIT ZACHAR[1], TIVADAR M TÓTH[1]

[1] Department of Mineralogy, Geochemistry and Petrology, University of Szeged
H-6701 Szeged, P. O. Box 651, Hungary
e-mail: zachar@geo.u-szeged.hu

ABSTRACT

The metamorphic basement of the Pannonian Basin consists essentially of diverse types of amphibolite and gneiss. Due to the rather complicated structural evolution since the Variscan orogeny, the basement is at present a mosaic of crystalline blocks of incompatible evolution. That is why an exact identification of each rock type is crucial for being able to correlate wells spatially. Myrmekitic feldspar is an important constituent of one gneiss type, which is inferred to be of igneous origin. The orthogneiss zone seems to be an extensive part of the basement.

Key words: myrmekite, orthogneiss, Pannonian Basin

INTRODUCTION

Myrmekitic feldspar is a very common phase in diverse igneous and metamorphic rocks. To explain its origin and development, dozens of theories were constructed in the last century. In the first part of our end-to-end papers (Zachar, M Tóth, 2002) we attempted to compile a close to entire conclusion about these models in order to create the right conditions for understanding the role of myrmekitized feldspar in the metamorphic rocks of the basement of the Pannonian Basin.

Several authors reported presence of myrmekite from diverse rock types in this crystalline basement (e.g. Szalay, 1977; Balázs et al., 1986). Although they describe the textural details of the myrmekite occurrences, they do not pay much attention to the genetic relationship. Zachar (2000) found myrmekitized feldspar an essential constituent in gneiss samples from the northern flank of the Szeghalom crystalline high. In what follows we study whether myrmekite can be relevant in specifying certain stages of the metamorphic evolution in this area of the metamorphic basement.

GEOLOGICAL SETTING

Due to the complex Neogene evolution of the Pannonian Basin (for details see Tari et al, 1999 and references therein), in its basement several deep sub-basins formed with elevated crystalline highs among them. One of the deepest and largest sub-basins is Békés-basin surrounded by a series of highs from the north (Fig. 1). Although, Szeghalom dome (SzD) is not the largest one among them because of the boring activity of the hydrocarbon industry in the last three decades several dozens of wells penetrated the metamorphic basement making a detailed petrological study possible. For this reason Szeghalom dome is a good candidate for being a reference area throughout the geological examination of the basement.

Previous studies about the evolution and structure of the SzD inferred co-existence of rocks of significantly different history. These rock types define at least four homogeneous blocks, which got juxtaposed due to the subsequent tectonic events of the Pannonian Basin (M Tóth et al., 2000). Following this model, there are three blocks in the central and southern part of the SzD, while the northern flank of the high consists of one single block. In addition to amphibolite, different gneiss varieties and granite are essential constituents in all blocks. They differ both in protolith and metamorphic evolution. While Szederkényi (1984) suggests a uniform protolith of sedimentary origin for them, Szepesházy (1973) assumes the presence of an orthogneiss belt from the Jánoshalma high in the SW towards the SzD. Based on the geochemical discrimination method of Bhatia (1983), paragneiss represents active continental margin sediments (Zachar, 2000, M Tóth et al. 2000).

Concerning mineralogy, gneiss in the central and the southern part of the SzD usually contains sillimanite, while there in the northern flank sillimanite is missing, and in several samples also amphibole occurs. Most gneiss samples in the north contain myrmekitized feldspar grains. Feldspars in gneisses of the SzD can be divided into two basic categories; strongly altered sericitic and fresh feldspars, respectively. Typical examples of the latter are chessboard and polysynthetic twinning, myrmekitic plagioclase and perthitic K-feldspar. In the paleosome part of metatexite (biotite plagioclase gneiss), Szalay (1977) observed two generations of plagioclase. The first is An_{15-20} in composition; the second is lower in *An* and replaces the original grains. Quartz that crystallized after plagioclase is xenomorphic and emplaced in the space between the feldspar grains. Its recrystallization resulted in replacement reactions. Three generations of myrmekitic plagioclase in granodioritic diatexites were observed in the metamorphic basement of the SE part of the Pannonian Basin. The first generation is sericitic and kaolinic An_{15-20} oligoclase. Resorption occurs generally on the edge of the crystals where fresh albite (second generation) can be observed. The fresh or slightly sericitic plagioclase crystals of the third generation are An_{17} in composition. Myrmekite is abundant on all three

generations. The latest generation can be observed in contact with microcline.

Here, myrmekite-bearing gneiss samples from the northern flank of the SzD are examined (e.g. wells Sz-4, 6, 7, 15, 16 and 50). Samples studied are epidote and chlorite bearing biotite, amphibole two-feldspar gneisses. Several specimens also contain relics of a previous HT event, which is thought to have been igneous based on preserved poligonal textures as well as idiomorphic accessory phases, like zircon, turmaline and allanite. Based on thermobarometric calculations and modelling (DOMINO/THERIAK, de Capitani, 1994), the stable paragenesis of the gneiss suggests an upper greenschist, lower amphibolite facies metamorphism (well Szeghalom-15; T~550 °C, P<6 kbar) (M Tóth et al., 2000). Following the peak metamorphism, the metamorphic basement was intruded by a postkinematic granite body and crosscut by several granitoid dykes and sills.

METHODS

Microprobe measurements were carried out at the Johannes Gutenberg University at Mainz on a Camecabax microbeam machine at 15 kV acceleration voltage and 12 nA using natural standards.

PETROGRAPHY

In the gneiss samples studied there are different textural positions where myrmekite occurs. At some places myrmekite can be observed on the common edge of matrix plagioclase and K-feldspar grains (Fig. 2a), while the most common myrmekite type forms sericitic inclusions in fresh K-feldspar grains (Fig. 2b). At these places apophyses of the fresh host mineral (microcline) are advancing into the sericitic myrmekite (Fig. 2c) separating relics of the 'old' myrmekitic feldspar, which are of the same lattice orientation (Fig. 2d). Quartz blebs can be found in fresh K-feldspar only close to the myrmekitic islands (Fig. 2e). Myrmekitic inclusions generally are xenomorphic in shape, but in many instances they also may be hipidiomorphic with well-developed straight grain boundaries (Fig. 2f).

In the rock studied myrmekitic and non-myrmekitic grains are situated adjacent to each other. The grain boundaries usually are wiggly and the latter often surround myrmekitic grains without any definite grain boundary between myrmekite and K-feldspar (Fig. 2g). The arrangement of myrmekite in the samples studied does not indicate any orientation. Several feldspar grains are perthitic with lamellae oriented subparallel to the bitoite and amphibole defined foliation.

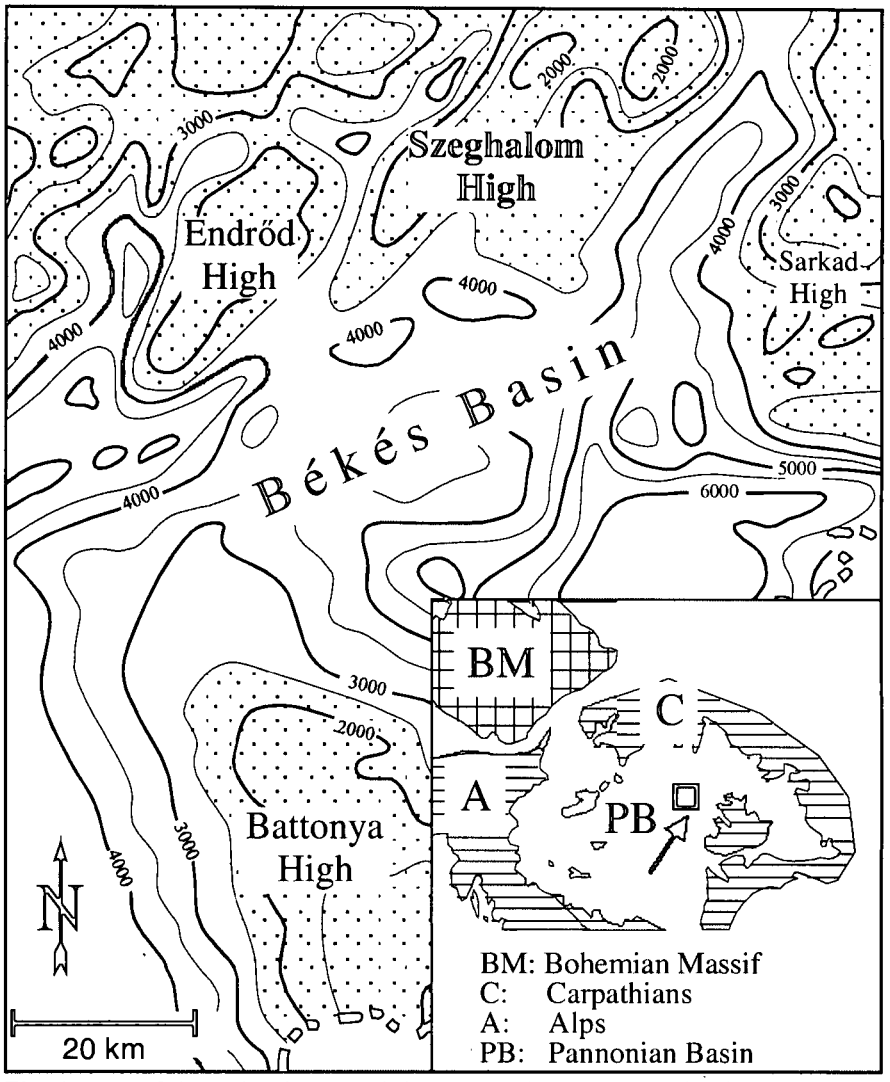

Fig. 1. Map of the Békés basin and the surrounding metamorphic highs. Present-day depth of the pre-Neogene basement is shown. Inset: Location of the Pannonian Basin in the Alpine-Carpathian-Pannonian system.

MINERAL CHEMISTRY

Compositions of several myrmekitic feldspar grains were measured form the northern SzD orthogneiss samples. Each grain measured exhibits similar structure with myrmekitic plagioclase inclusions of around An_{22} and a pure K-feldspar host mineral. At the contact between the relic plagioclase and the microcline a thin zone of pure albite (An_1) occurs. Some grains are also zoned with increasing K towards the rim. Representative data are given in Table 1.

Table 1. Representative compositions of myrmekitic plagioclase grains (Pl1), albitic rim (Ab) and microcline host mineral (Kfp) of the well Sz-15.

	Plmx1	Plmx1	P11	P12	P13	Ab1	Kfp1	Kfp2
SiO_2	63.67	60.56	65.73	65.38	64.97	71.09	66.11	66.26
Al_2O_3	22.71	23.06	21.42	19.46	20.74	18.93	17.01	17.57
CaO	3.5	3.98	4.61	3.91	4.21	0.23	0.00	0.00
Na_2O	7.59	8.58	8.53	8.05	7.94	9.82	0.64	0.23
K_2O	0.4	0.23	0.17	0.33	0.22	0.29	15.34	16.02
Total	97.87	96.41	100.51	97.22	98.21	100.49	99.20	100.14
An	20	20	23	21	22	1	0	0
Ab	78	78	76	77	77	97	6	2
Or	3	1	0	2	1	2	94	98

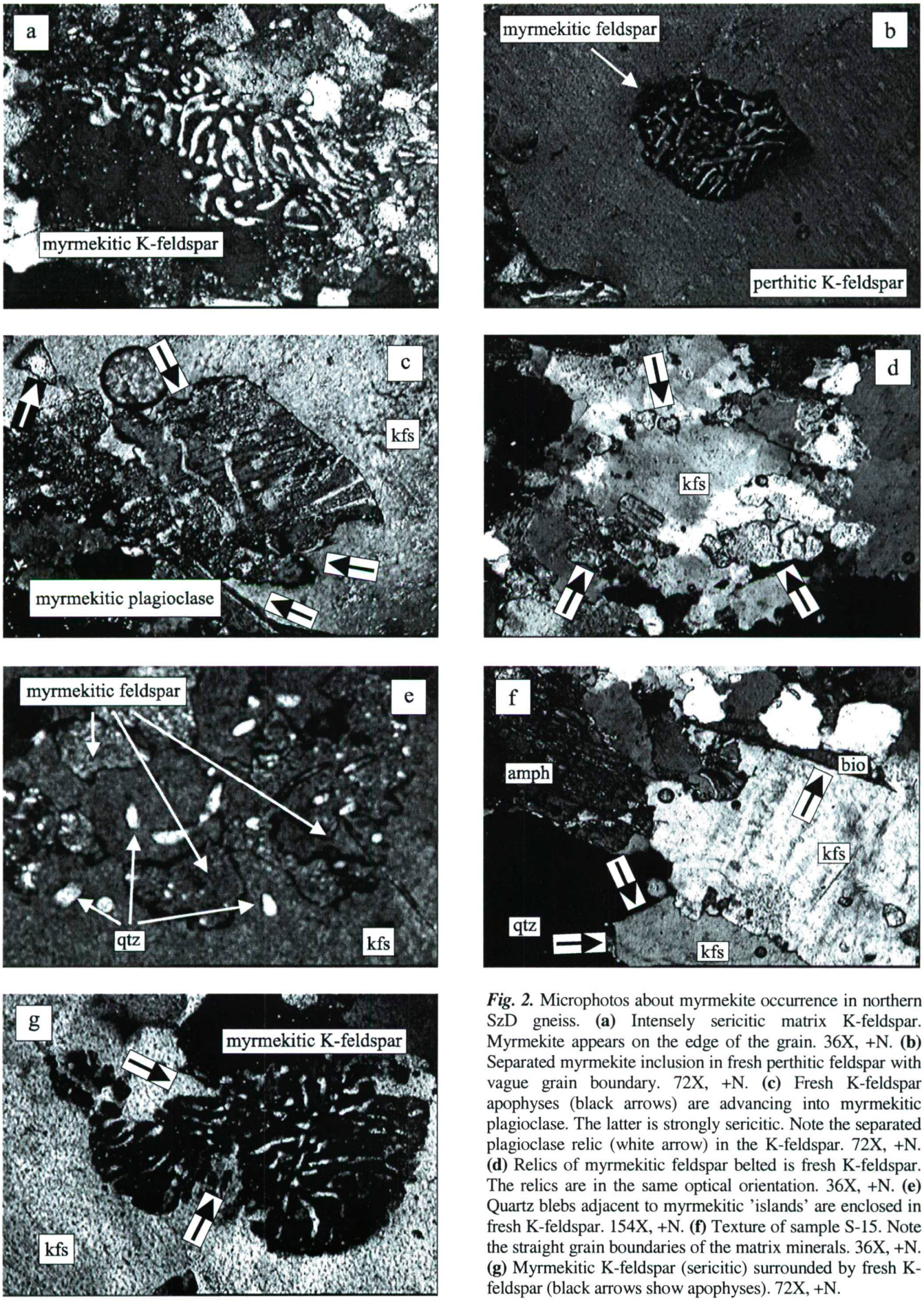

Fig. 2. Microphotos about myrmekite occurrence in northern SzD gneiss. **(a)** Intensely sericitic matrix K-feldspar. Myrmekite appears on the edge of the grain. 36X, +N. **(b)** Separated myrmekite inclusion in fresh perthitic feldspar with vague grain boundary. 72X, +N. **(c)** Fresh K-feldspar apophyses (black arrows) are advancing into myrmekitic plagioclase. The latter is strongly sericitic. Note the separated plagioclase relic (white arrow) in the K-feldspar. 72X, +N. **(d)** Relics of myrmekitic feldspar belted is fresh K-feldspar. The relics are in the same optical orientation. 36X, +N. **(e)** Quartz blebs adjacent to myrmekitic 'islands' are enclosed in fresh K-feldspar. 154X, +N. **(f)** Texture of sample S-15. Note the straight grain boundaries of the matrix minerals. 36X, +N. **(g)** Myrmekitic K-feldspar (sericitic) surrounded by fresh K-feldspar (black arrows show apophyses). 72X, +N.

Discussion: Origin of the myrmekite in the SzD gneiss

Comparing our observations with those made by diverse authors concerning myrmekite formation, we attempt to delimit genetic circumstances of the myrmekite of the SzD gneiss samples. Textural data suggest the presence of strongly sericitized myrmekitic feldspar inclusions in fresh K-feldspar, usually microcline. Such a relationship indicates the replacement of myrmekite by a secondary K-feldspar and infers that myrmekite must have formed earlier. Approving the results of the previous calculations concerning metamorphic history of the SzD, one can state that gneiss of the northern flank reached peak conditions at around 550 °C. Myrmekitic texture is usually unstable above greenschist facies because at slightly elevated temperature the feldspar system tends to achieve equilibrium by static recrystallization. In the present case myrmekite grains formed either during the low-temperature stage of the progressive metamorphism and started to consume afterwards, or they are relics of an even older process. Keeping also the composition of the inclusions (An_{22}) to be similar to the matrix plagioclase grains (Table 1), as well as their altered appearance within a fresh host mineral into account, formation of the myrmekitic feldspar due to the last progressive metamorphic event can be excluded.

Although intensely deformed gneiss is rather common in the study area, these mylonitized samples generally miss undeformed myrmekite grains. Present studies (Schubert, M Tóth, 2002) suggest, that the ductile event followed the peak metamorphism and developed mylonite along the retrograde pathway. It also coincided with significant gain in Si, Al and K in the most sheared zones; metasomatism, however, resulted in crystallization of mica instead of feldspar. Because there is no indication of any orientation in the myrmekite studied, we exclude deformation-induced origin. Formation due to silica infiltration also is improbable because there is no clear evidence for deformation in myrmekitic plagioclase.

Several post-kinematic granitoid dykes and sills crosscut the gneiss terrane in question, which may be a potential source for post-metamorphic metasomatic fluids. The presence of myrmekite and sericitic feldspar remnants in fresh microcline seems to corroborate the hypothesis of Collins (1998) that plagioclase can be replaced by microcline, and myrmekite produces during the metasomatic alteration. Drescher-Kaden (1948) also suggests that myrmekite forms during the reaction, in which K-feldspar metasomatically replaces plagioclase. The fact that relic quartz blebs of an old myrmekite are present in the fresh, replacing feldspar contradicts both theories as myrmekite does not grow but consumes in the observed reaction. Granite-related fluids, on the other hand, may be responsible for carrying extra K and Si to form secondary microcline.

Where myrmekitic plagioclase recrystallizes, the quartz lobes of the myrmekite are consumed in the K-feldspar producing reaction, or a more sodic plagioclase forms lacking polysynthetic twinning. Where myrmekitic K-feldspar recrystallizes, quartz lobes cannot consume in the reaction, and one can recognize separated quartz lobes in the fresh feldspar grains adjacent to the replacement front. These grains are in the same lattice orientation forming myrmekite-like intergrowth. In this case we cannot speak about myrmekite, because quartz lobes are relics and are not in a genetic connection with the host recrystallized K-feldspar. The fact that in some cases myrmekite is absent can be interpreted with the advanced state of the reaction. Generally 'old' sericitic myrmekite is situated on the edge of the grains. Where the replacement reaction is advanced, the myrmekitic edge of the 'old' grain is consumed in the reaction progress and no myrmekite can be found in the sericitic feldspar grain.

All textural reasons consequently suggest that myrmekite must be older than the last deformation, metamorphic and metasomatic events, and seems to represent a relic phase in the recrystallized feldspar grains. We conclude, that it formed in the pre-metamorphic igneous protolith either due to igneous crystallization or by subsolidus exsolution. Replacement of myrmekitic plagioclase and K-feldspar by non-myrmekitic fresh feldspar grains can be interpreted as metamorphic recrystallization under lower amphibolite facies conditions with or without utilization of granite-related K-, and Si-bearing fluids.

Either the external or an internal K-source also can be responsible for perthite formation in the SzD feldspar. One can assume the presence of a HT ternary myrmekitic feldspar characteristic of the original magmatic rocks. Consuming free K and Si from the quartz blebs of the myrmekite, magmatic feldspar recrystallizes as LT, pure K-feldspar. The Ca and Na content remains in the newly formed grain and may form perthitic lamellae.

Conclusions

The aim of this study was to investigate the connection between myrmekite formation and metamorphic evolution of gneiss in the northern flank of the SzD. Using textural and mineral chemical data and comparing our observations to the most commonly accepted myrmekite models we concluded that myrmekite did not form due to metamorphic, deformation and metasomatic processes. We appointed that myrmekite is a relic phase, which represents the original igneous protolith and so developed due to magmatic crystallization. Thus the studied type of myrmekite is not appropriate in determining the metamorphic evolution, but it can be of great significance in recognizing the magmatic origin of the protolith.

Analysis of the myrmekite-bearing feldspar suggests an evolution analogous to that deduced for the northern SzD gneiss previously (M Tóth et al., 2000). After intrusion the igneous protolith cooled down and altered significantly, the originally myrmekitic plagioclase partially altered to sericite. Metamorphic overprint produced orthogneiss under lower amphibolite facies conditions that caused recrystallizaton of unstable feldspar to microcline. Whether during this reaction also an external K-source was needed and the intrusion of the post-kinematic granite bodies coincided to this event or not, needs further chemical consideration.

Putting back the study area to a more regional context, we can conclude, that the northern flank of the SzD should be a part of the orthogneiss zone, first mentioned by Szepesházy (1973). In recognizing this rock type throughout the metamorphic basement of the Pannonian Basin, the presence of myrmekite we discussed in the present paper may be of basic importance.

ACKNOWLEDGEMENT

R. Oberhansli (Johannes Gutenberg Uniersity, Mainz, Germany) as well as L. W. Diamond (Montanuniversitat, Leoben, Austria) are acknowledged for making electron microprope analyses possible. The project was financially supported by the Hungarian Research Found (grant no. OTKA F32792), and the Hungarian Ministry of Culture (grant no. FKFP 0139/2001) and the János Bolyai Research Grant.

REFERENCES

BALÁZS, E., CSEREPES-MESZÉNA, B., NUSSZER, A., SZILI-GYÉMÁNT, P. (1986): An attempt to correlate the metamorphic formations of the Great Hungarian Plain and the Transylvanian Central Mountains (Muntii Apuseni). Acta Geologica Hungariae **29/3-4**, 317-320.

BHATIA, M. R. (1983): Plate tectonics and geochemical composition of sandstones. Journal of Geology **91/6**, 611-627.

COLLINS, L. G. (1998) Primary microcline and myrmekite formed during progressive metamorphism and K-metasomatism of the Popple Hill gneiss, Grenville Lowlands, northwest New York, USA: Myrmekite, ISSN 1526-5757, electronic Internet publication, no. 28, http://www.csun.edu/~vcgeo005/popple.htm

DE CAPITANI, C. (1994): Gleichgewichts-Phasendiagramme: Theorie und Software. Beihefte zum European Journal of Mineralogy, 72. Jahrestagung der Deutschen Mineralogischen Gesellschaft **6**, 48 p.

DRESCHER-KADEN, F. (1948): Die Feldspar-Quartz-Reaktionsgefuege der Granite und Gneise. Berlin-Springer, 259 p.

M TÓTH, T., SCHUBERT, F., ZACHAR, J. (2000): Neogene exhumation of the Variscan Szeghalom dome, Pannonian Basin, E. Hungary. Geological Journal **35**, 265-284

SCHUBERT, F., M TÓTH, T. (2002): Structural evolution of mylonitized gneiss zone from the northern flank of the Szeghalom Dome (Pannonian Basin, SE Hungary). Acta Mineralogica-Petrographica, this volume

SZALAY, Á. (1977): Metamorphic-granitogenic rocks of the basement complex of the Great Hungarian Plain, Eastern Hungary. Acta Mineralogica-Petrographica Szeged **XXIII/1**, 49-69.

SZEDERKÉNYI, T. (1984): Az Alföld kristályos aljzata és földtani kapcsolatai. (The crystalline basement of the Great Hungarian Plain and its geological connections.) (In Hungarian) Academic doctor theses, Hungarian Academy of Sciences, Budapest

SZEPESHÁZY, K. (1973): A Duna Tisza Köze déli részének metamorf kőzetei. MÁFI évi jelentése az 1973. évről, 147-166

TARI, G., DÖVÉNYI, P., DUNKL, I., HORVÁTH, F., LENKEY, L., STEFANESCU, M., SZAFIÁN, P., TÓTH, T. (1999): Lithospheric structure of the Pannonian basin derived from seismic, gravity and geothermal data. In: Durand, B., Jolivet, L., Horváth, F., Séranne, M. (eds) The Mediterranean Basins: Tertiary Extension within the Alpine Orogen. Geological Society, London, Special Publications, **156**, 215-250.

ZACHAR, J., M TÓTH, T. (2002): Myrmekite-bearing gneiss from the Szeghalom Dome (Pannonian Basin, SE Hungary). Part I.: myrmekite formation theories. Acta Mineralogica-Petrographica, this volume

ZACHAR, J. (2000): Szeghalmi polimetamorf gneiszek PT modellezése. Thesis in Hungarian.

Received: December 4, 2001; accepted: July 3, 2002

EUROPEAN CURRENT RESEARCH ON FLUID INCLUSIONS CONFERENCE

4-9 June, 2003
Budapest, Hungary
http://ecrofi17.geology.elte.hu

The conference provides an international forum for the exchange of research and new ideas of geoscientists from East to West focusing on studies of

FLUID AND SILICATE MELT INCLUSIONS.

SECTIONS

Analytical techniques and experimental results and theoretical models
Hydrothermal systems and ore deposits
Metamorphic fluids
Fluid flow and deformation, and fracturing
Sedimentary systems and application to environmental geology
Silicate melt inclusions

THREE POST-MEETING FIELD TRIPS WILL BE ORGANIZED

3 days to Tokaj Mountains
1 day to Balaton Highland
1 day to Eger region

CONTACT PERSON: CSABA SZABÓ, PH.D.

Department of Petrology and Geochemistry
Department of Mineralogy
Department of Geophysics
Eötvös University, Budapest

Pázmány Péter sétány 1/c
H-1117 Hungary

Phone: (36) 1 209 0555 ext. 8338
Fax: (36) 1 381 2108
E-mail: ecrofi17@geology.elte.hu

Acta Mineralogica-Petrographica, Szeged 2001, Vol. 42, pp. 45-50

ACTA Mineralogica Petrographica

SEQUENCE OF CHROMITE CRYSTALLIZATION AT BOULA - NAUSAHI IGNEOUS COMPLEX, ORISSA, INDIA

J. K. MOHANTY[1], A. K. PAUL[2], R. K. SAHOO[3]

[1]Regional Research Laboratory, Bhubaneswar, Orissa- 751 013.
[2]Deptartment of Geology, Utkal University, Bhubaneswar.
[3](Retd. Scientist), Regional Research Laboratory, Bhubaneswar.

ABSTRACT

The chromite deposit at Boula-Nausahi Igneous Complex is of stratiform type where chromite occurs as layers in ultramafic rocks. The chromites in this complex can be ascribed to early and late stage crystallization based on differences in their physical, chemical and beneficiation characteristics. The early stage chromites are characterised by their association with serpentinite, coarser grain size, nonmagnetic nature, high Cr content, high Cr/Cr+Al ratio, average chemical composition (Cr_2O_3-51.9%, FeO-26.9%, MgO-10.3%, Al_2O_3-10.2%, TiO_2-0.45%, V_2O_3-.2%, Cr/Fe-1.74) and amenability to simple beneficiation techniques. On the contrary, the late stage chromites are characterised by their association with fine grained fibrous and magnetic silicates, fine grain size, magnetic behaviour, low Cr content, low Cr/Cr+Al ratio, average chemical composition (Cr_2O_3-27%, FeO-53.7%, MgO-6%, Al_2O_3-10.5%, TiO_2-2.5, V_2O_3-0.4% and Cr/Fe-0.45) and difficult to beneficiation.

Key words: chromite, crystallization, Boula-Nausahi igneous complex, Orissa.

INTRODUCTION

Chromite deposits of Pre Cambrian (Iron Ore Group and Eastern Ghats) and Tertiary age are distributed in shield and tectonically mobile areas in India. Out of the 11 major chromite deposits distributed in 9 states of India, Orissa hosts the largest chromite reserve of the country and also produces the lion share of total Indian production. In Orissa, the two major deposits i. e. Sukinda Ultramafic Belt and Boula Nausahi Igneous Complex hold around 98% of the total Indian reserve. Boula-Nausahi Igneous complex (21°18'-21°15' N; 86°18'-86°20'E) consists of three rock units i e., the ultramafic rocks, mafic rocks and the felsic rocks. The ultramafic body, which hosts four chromite lodes, occurs as a dyke like pluton of 3 km long and 0.6 km width at the central part. Besides chromite, the ultramafic-mafic rocks host PGE mineralisation along with sulphides (Cu-Ni-Fe-Ag). Mining activity in this area is going on since 1942 for chromite. Though most of the workers are in favour of a magmatic origin for the chromite and the associated rock types in this complex, opinions are divided on the stage(s) of chromite crystallization as to whether they are early magmatic (Barooah, 1948; Ghosh, Prasad Rao, 1952; Mukherjee, 1962) or late magmatic (Chakraborty, 1958).

An attempt has been made in this paper to find out the stages of chromite crystallization based on the physical, mineralogical, chemical and beneficiation characteristics of chromites.

GEOLOGY

The mafic-ultramafic suit with chromite and Ti-V magnetite of early Proterozoic age is well exposed in the southeastern periphery of the Singhbhum Granitic batholith. Many plutons are emplaced into the cratonic nucleus comprising Singhbhum Granite, Iron Ore Group and the Early Proterozoic supracrustal rocks. Boula-Nausahi complex is situated on the girdle of Sukinda-Nilgiri shear zone that extends discontinuously from Nilgiri in the east through Boula-Nausahi upto Sukinda in the west. The chromiferous ultramafic rocks have been emplaced within the interbanded sequence of quartzite, chert, quartz-mica schist of Iron Ore Group (Fig. 1). Age of emplacement of this complex is between 2000 – 2100 Ma (Saha, 1994). The ultramafic rocks occur as elongated pluton with tapered ends and extends in a NNW-SSE direction with moderate dip towards east. They host 4 layers of chromitite ore bodies of varying thickness. They are Durga, Laxmi, Sankar and Ganga arranged from bottom to top in a northerly direction. These four ore bodies alternate with ultramafic (± mafic) rocks exhibit layering typical of stratiform igneous complexes.

PETROGRAPHY

The ultramafic rocks are represented by dunite-peridotite, websterite, lherzolite and enstatitite. Olivine is the major mineral followed by orthopyroxene. Detail mineralogical and chemical studies of the rock types and the associated chromite ore bodies have been carried out by Mohanty (1994). The salient features are as follows:

The chromiferous ultramafic rocks exhibit magmato-sedimentary structures/ textures such as cumulus, rhythmic and cryptic layering, graded bedding (grain size variation), current bedding and cusp etc. The chromitites exhibit primary (cumulus, chain syneusis, clot, exsolution, foam), deformational (brecciation, mylonitisation, pull-apart) and alteration (zoning) textures. The four layers exhibit size grading from coarse at bottom to fine at top. A log normal straight line size distribution indicates uninterrupted

chromite crystallization. Unimodal size distribution of chromite and predominance of coarse grains of chromite in layers from bottom to top indicate continuous crystallization in quiet - plutonic condition from a single source. Gravity settling of the chromite crystals under steady state condition is responsible for the formation of chromitite layers. The rocks and the ore bodies are co-magmatic in nature. They are derived from a low K-tholeiitic magma in a decreasing temperature and increasing oxygen fugacity condition.

CHROMITE

Chromite mostly consists of chromite with subordinate amounts of ferritchromit, magnetite, ilmenite and secondary silicates like serpentine, talc, tremolite, uvarovite and kammererite. Though the chromite grains are predominantly euhedral in nature, they exhibit two fold variations in physical, mineralogical and chemical characters which can be correlated with their formation at different stages during crystallization process. In this complex, chromites have crystallized in two stages. The chromites from two stages differ in these following aspects.

Mineralogical and physical characters

The chromites of two stages exhibit variations in physical properties, optical characters and mineralogy.

The chromite grains exhibit a variation in reflectivity from 12.5 to 16.2%. The reflectivity measurement data indicates two clusters around 13% and 16%. The chromites which exhibit reflectivity around 16 may represent late stage crystallization. The low reflectivity cluster indicates early stage chromite crystallization. Chromites with higher reflectivity may be due to higher trivalent iron content (Eales, 1980).

The chromite grains contain inclusions of various shape, size and composition. The inclusions in early stage chromites are mostly olivine and enstatite (now altered to serpentine) and in late stages they are mostly diopside, amphibole, muscovite etc.

The two stage chromites have different magnetic character. The early stage chromites are non-magnetic with a very low magnetic susceptibility (3.4 X 10^{-5} emu/gm.Oe) compared to the late stage ores which are highly

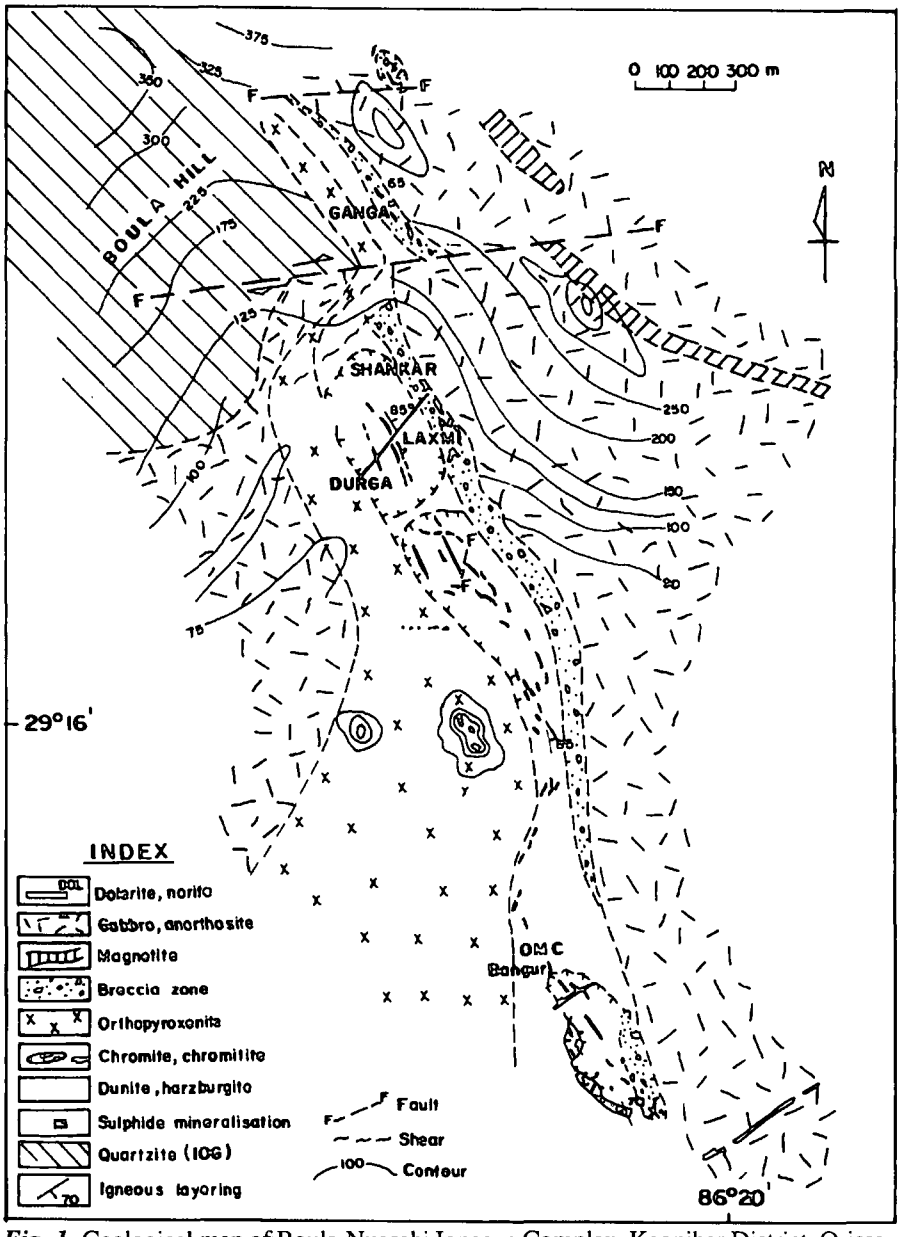

Fig. 1. Geological map of Boula-Nuasahi Igneous Complex, Keonjhar District, Orissa.

magnetic with high magnetic susceptibility (0.11 emu/gm. Oe). Mossbauer study of the chromite samples indicates that the early and late stage chromites exhibit spectral differences. While the early stage chromites exhibit normal spinel spectra, the late stage chromites exhibit two magnetically split narrow sextets. They also exhibit superposition of magnetically ordered, paramagnetic and super paramagnetic components.

Besides magnetic behaviour, the chromites also exhibit variation in their cell dimension. The early formed chromites have cell dimension around 8.28A° where as the late formed chromites almost approach the cell dimension of magnetite (8.37A°). The variation in magnetic character and cell dimension of chromites may be due to increase in trivalent iron content.

The alteration characters of the two types also vary in a sense that the early formed chromites which are generally associated with olivine alter to magnetite along with the silicate mostly altered to serpentine. The late stage chromites which are associated with pyroxene alter to ferritchromit + magnetite association with associated silicates mostly altering to talc and sometimes to chlorite.

The late stage chromites contain ilmenite granules and exsolution lamellae where as the early formed chromites are devoid of it. Presence of ilmenite in late stage chromites indicates their crystallization from Fe-Ti rich Cr poor magma.

Sulphide minerals are ubiquitous in ultramafics. In this complex both primary and secondary sulphide minerals are present through out the ultramafic belt. The late formed chromites contain primary sulphide minerals (pentlandite, chalcopyrite, pyrrhotite etc.) as inclusions where as the early formed chromites devoid of any primary sulphide minerals. However secondary sulphide minerals are present in both early and late stage chromites.

Broadly speaking the mineralogical assemblage of the two stages of chromite mineralisation can be expressed as chromite (+magnetite) + sulphide (secondary) + serpentine for the early stage and chromite (+ ferritchromite + magnetite) + Sulphide (primary + secondary)+ ilmenite + talc + tremolite + chlorite for the late stage chromites.

Chemical characters

To know the compositional variations in the chromites of two stages, massive fresh chromite samples were collected from the four ore bodies and the concentrates were analysed by wet chemical methods. The data are presented in Table 1. From the Table 1, it is observed that the early chrome spinels are rich in Cr_2O_3 content which varies from 41% to 59.5%. Cr/Fe ratio varies between 2.7 to 1. Al_2O_3 content varies from 5 to 14%. The variations of FeO(t), MgO, TiO_2 and V_2O_3 are 22% to 39%, 6.7% to 12.5%, 0.26 to 0.76% and 0.1 to 0.3% respectively. Comparatively late chromites are characterised by low Cr_2O_3 (21.5 to 36%), high FeO (48 to 58%), high TiO_2 (1.8-2.7%) and low Cr/Fe ratio (<1). When the composition data are plotted in Stevens' classification diagram (1944), the chromites belong to aluminian field with a minor distribution in chromian magnetite and ferrian chromite fields (Fig. 2). The chromites also exhibit compositional variation from Cr corner towards (Fe + 2Ti) corner in Cr-Al- (Fe+2Ti) diagram of Eales (1980). From the distribution of chromite in these diagrams two stages of chromite crystallization is clearly revealed. The two stages of crystallization seems to be a continuous one and the stages are assigned early stage giving rise to normal chromite spinel and late stage

Table 1. Chemical analysis of chromites from different ore bodies of Boula Nausahi igneous complex (wt%)

Sl.No	Ore body	Cr_2O_3	FeO	MgO	Al_2O_3	TiO_2	V_2O_3	Total
1	DURGA	59.48	22.01	12.56	5.27	0.37	0.1	99.79
2		57.72	22.61	12	6.65	0.53	0.12	99.63
3		54.91	23.71	11.64	9.82	0.27	0.1	100.45
4		55.21	23.24	12	9.24	0.3	0.11	100.1
5		55.32	23.4	11.84	9.12	0.26	0.1	100.04
6	LAXMI	54.21	24.53	10.34	9.37	0.38	0.16	99.01
7		53.42	26	9.8	10.2	0.38	0.2	100
8		52.64	26.72	9.26	10.78	0.45	0.22	100.07
9		52.81	25.65	10.5	9.8	0.3	0.1	99.16
10		52.65	25.80	10.34	9.95	0.28	0.2	99.22
11		52.55	26	10.2	10	0.33	0.21	99.28
12		52.12	28.04	9.43	9.84	0.35	0.21	100.08
13		51.32	25.36	8.95	11.87	0.53	0.24	98.27
14		52.26	25.84	9.62	11.35	0.57	0.25	99.89
15		51.45	28.56	9.65	8.75	0.45	0.21	99.07
16		51.63	27.15	10.33	9.25	0.6	0.22	99.18
17		52.38	27.18	10.83	9.84	0.35	0.19	100.77
18		51.63	25.59	10.34	11.44	0.27	0.18	99.45
19		51.54	26.52	10.85	10.15	0.42	0.22	99.7
20		49.96	28.46	10.54	10.21	0.56	0.21	99.94
21	SHANKAR	49.48	26.08	8.89	14.4	0.62	0.25	99.72
22		49.91	27	8.65	13.86	0.74	0.30	100.46
23		47.32	32.06	6.85	12.9	0.76	0.34	100.23
24		44.65	35.75	9.18	10.2	0.41	0.15	100.34
25		40.78	39.02	8.78	11.23	0.73	0.11	100.65
26	GANGA	35.83	48.02	7.83	6.48	1.77	0.3	100.23
27		29.05	50.52	6	11.57	2.67	0.33	100.14
28		25.51	54.91	5.8	11.36	2.63	0.42	100.63
29		23.07	57	5.3	10.78	2.63	0.41	99.19
30		21.57	57.81	5.12	12.35	2.73	0.35	99.63

(Sl.No. 1-25: Early stage chromite; Sl.No. 26-30: Late stage chromite)

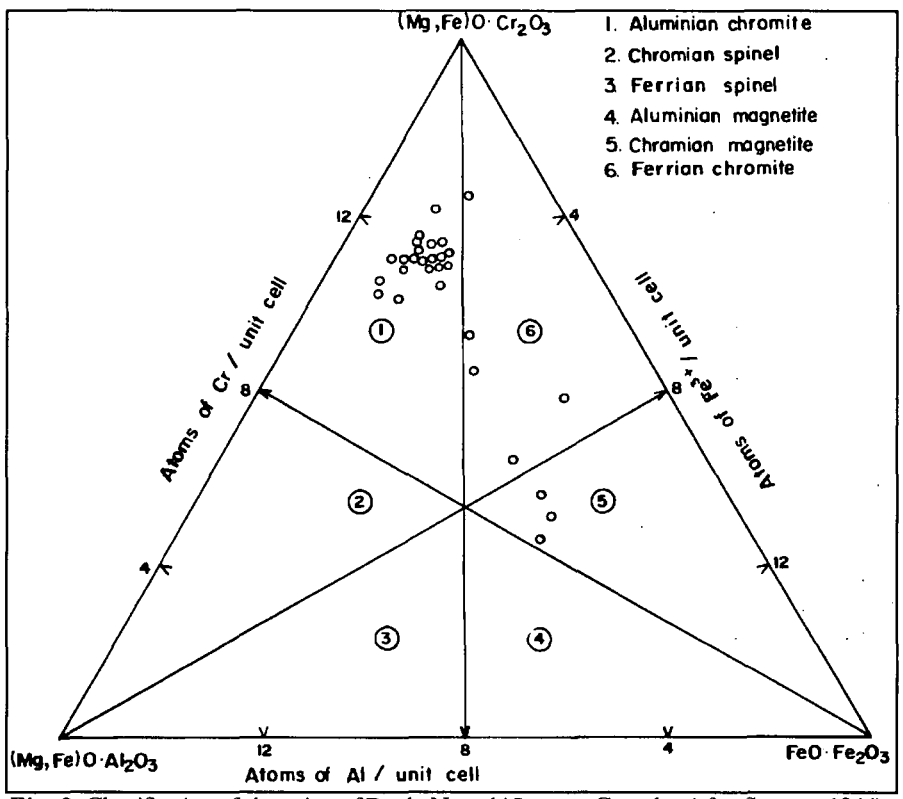

Fig. 2. Classification of chromites of Boula-Nuasahi Igneous Complex (after Stevens, 1944).

giving rise to iron rich chromite spinel. The two types of chromites show distinct chemical differences averages of which are clearly reflected in Table 1. The compositional variation in entire gamut of chromites of this complex is graphically represented in Fig. 3.

Depending upon the composition of the parent magma, concentration of Cr, temperature and oxygen fugacity, chromite crystallizes independently or in association with olivine or orthopyroxene. In this complex, chromite is predominantly associated with olivine and orthopyroxene. However the late stage chromites are associated with orthopyroxene and clinopyroxene which are now altered to talc, tremolite. Depending upon the temperature of crystallization and concentration of different elements, cationic substitution takes place in the chromite structure and it is reflected in the chemical composition of the chromites. The chemical composition of clean chromites indicates that Cr content in the unit cell decreases from 12.44 in the early formed chromite to 4.6 in the late formed chromites. Likewise other cations also exhibit similar variation in the chromites. Typical cationic distribution in chromites from two stages is given below;

$12.44Cr + 1.64\ Al + 1.82\ Fe^{3+} \rightarrow$
$4.6\ Cr + 3.8\ Al + 6.8\ Fe^{3+}$
(Early stage → Late stage)

This cation distribution indicates that Cr content of the early stage chromites are being substituted by both Al and Fe^{3+} in the late stage chromites. Similarly Mg is substituted by Fe^{2+} at the tetrahedral site in the late stage chromites (Fig. 4).

When these chromites are plotted in Y_{Cr} and Y_{Fe3+} vs. MMF diagram, two stages of chromite crystallization is clearly observed. Chromites with higher Y_{Cr}, Cr/Cr+Al and Cr/Fe ratio represent the early stage whereas the chromites with high Y_{Fe3+} and low Cr/Fe ratio indicate late stage of crystallization. The early formed chromites have high Y_{Cr}, Cr cation >10 and Cr/Cr+ Al ratio whereas the late stage chromites are low in Y_{Cr}, Cr cation <10 and low Cr/Cr+ Al. Higher Cr/Cr+ Al ratio of the early formed chromites indicate a higher temperature of crystallization (Irvine, 1967).

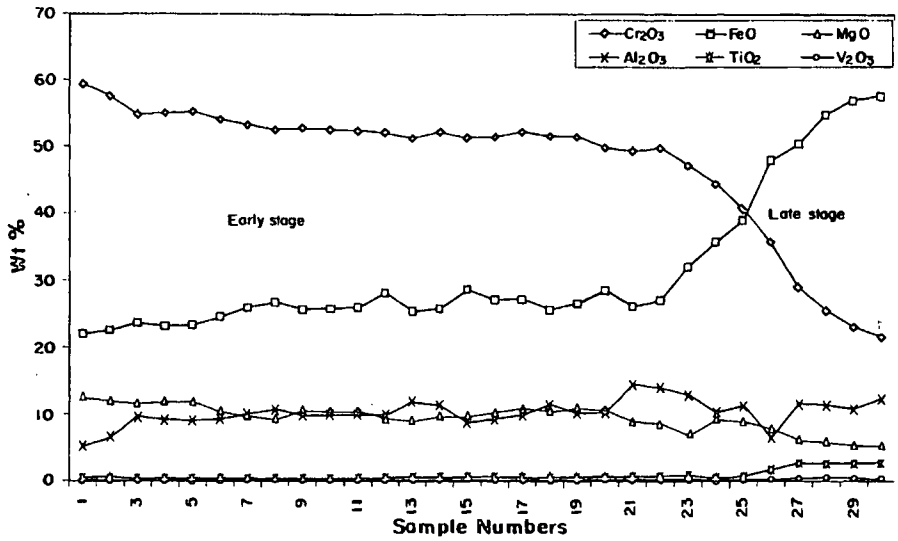

Fig. 3. Compositional variations in chromites of Boula-Nuasahi Igneous Complex.

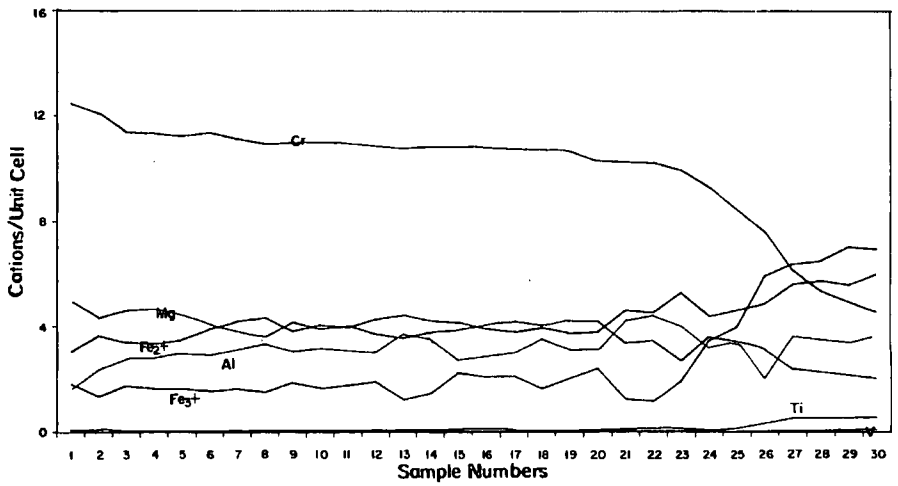

Fig. 4. Cation distribution in chromites of Boula-Nuasahi Igneous Complex.

Olivine associated with early chromite is Mg rich. From the trivalent iron content in the chromites it is observed that the early stage chromites are formed at a lower f_{O2} than the late stage chromites (Murck, Campbell, 1986). Owing to a relative increase in the iron content during late stage, some of Fe^{2+} were oxidised to Fe^{3+} and entered into the octahedral site substituting Cr. It is worthwhile to note that chromites are in co-existence with olivine and pyroxene; minerals deficient in Al. It is also noted that plagioclase is almost negligible in the ultramafics which host chromite. Since Al scavenging minerals did not precede chromite crystallization, the Al remained in the residual magma and along with Fe^{3+} substituted Cr during the late stage of chromite crystallization.

Individual grains from the different ore bodies were also analysed by EPMA to exhibit compositional variation between the two stages of chromite crystallization (Table 2).

Table 2. EPMA data of chromites from different lodes.

Oxides	Durga	Laxmi	Shankar	Ganga
Cr_2O_3	62.47	62.342	62.232	25.963
FeO	11.30	11.475	11.842	57.212
MgO	16.77	16.623	15.805	0.613
Al_2O_3	8.14	8.467	8.608	8.822
TiO_2	0.134	0.142	0.146	0.824
V_2O_3	0.003	0.003	0.003	0.007
NiO	0.105	0.100	0.099	0.255
Total	98.923	99.152	98.735	93.696

From the Table 2, it is observed that late stage chromite from Ganga ore body is rich iron and titanium compared to the early stage chromite from other three ore bodies.

Due to a combined effect of temperature, oxygen fugacity and relative concentration of cations during the whole course of chromite crystallization, the early and late stage chromites show significant differences in chemical composition reflecting their trivalent and divalent cations content at both octahedral and tetrahedral sites respectively (Table 3).

Table 3. Cation distribution in chromites from Boula-Nausahi Igneous omplex

Sl.No.	Cr	Al	Fe^{3+}	Ti	V	Mg	Fe^{2+}
1	12.44	1.64	1.824	0.08	0.016	4.96	3.04
2	12.1	2.39	1.37	0.112	0.032	4.35	3.65
3	11.408	2.808	1.768	0.048	0.016	4.608	3.392
4	11.36	2.832	1.656	0.048	0.016	4.664	3.336
5	11.272	3.008	1.656	0.048	0.016	4.496	3.504
6	11.392	2.936	1.56	0.072	0.04	4.096	3.904
7	11.136	3.168	1.64	0.08	0.048	3.816	4.184
8	1096	3.36	1.536	0.096	0.048	3.64	4.36
9	11.024	3.096	1.856	0.064	0.032	4.16	3.84
10	11.032	3.2	1.672	0.064	0.032	3.936	4.064
11	11.016	3.08	1.792	0.064	0.04	4.024	3.976
12	10912	3.064	1.912	0.064	0.048	3.72	4.28
13	10.856	3.744	1.24	0.112	0.048	3.568	4.432
14	10.864	3.52	1.456	0.112	0.048	3.776	4.224
15	10.872	2.752	2.232	0.096	0.048	3.848	4.152
16	10.832	2.896	2.096	0.128	0.048	4.08	3.92
17	10.768	3.008	2.12	0.064	0.048	4.2	3.8
18	10.712	3.544	1.664	0.048	0.032	4.048	3.952
19	10.68	3.136	2.048	0.08	0.048	4.24	3.76
20	10.296	3.136	2.4	0.112	0.048	4.208	3.792
21	10.28	4.264	1.256	0.144	0.064	3.376	4.624
22	10.224	4.44	1.168	0.12	0.048	3.464	4.536
23	9.936	4.032	1.924	0.144	0.064	2.708	5.296
24	9.272	3.192	3.464	0.08	0.032	3.6	4.4
25	8.42	3.46	3.95	0.144	0.016	3.42	4.58
26	7.6	2.056	5.92	0.352	0.064	3.136	4.864
27	6.12	3.64	6.36	0.528	0.064	2.392	5.608
28	5.344	3.552	6.496	0.512	0.096	2.296	5.704
29	4.928	3.424	7.012	0.528	0.096	2.144	5.586
30	4.55	3.66	6.94	0.544	0.08	2.03	5.97

Beneficiation Characters

Besides exhibiting physical and chemical differences, the chromites belonging to early and late stages also show variations in their beneficiation characteristics. The early stage chromites are easy to beneficiate because they are associated with serpentine; altered product of olivine. Serpentine is a hydrous magnesium silicate and possesses contrasting physical properties. It is nonmagnetic and has lower specific gravity contrary to the high specific gravity of chromite. These chromites are easy for beneficiation by gravity and heavy media separation methods. By this process a good concentrate with high Cr:Fe ratio and Cr_2O_3 can be obtained. The mineralogical study indicates that the late stage chromites are mostly associated with talc, tremolite and chlorite. The silicate gangues are fibrous and very fine grained. It is very difficult to separate the fine gangue from the chromite. Besides chlorite, which is associated with chromite; exhibits magnetic behaviour similar to the associated chromite. So beneficiating the late stage chromites by gravity, heavy media and magnetic methods are not fully successful. In order to get a pure concentrate, a combination of methods such as heavy media, gravity, magnetic and acid treatment is required. So from the laboratory beneficiation tests, it is observed that early stage chromites are easy to beneficiate compared to the late stage chromites.

CONCLUSIONS

In Boula - Nausahi igneous complex, chromite layers are confined to ultramafic rocks (now altered to serpentinite, talc, tremolite, chlorite assemblage). The grain size distribution indicates a continuous crystallization process. However the chemical characters reveal two stages of chromite crystallization. Besides the chemical differences, the chromites representing two stages also exhibit differences in their average grain size, reflectivity, associated silicate mineralogy, their composition, cell dimension, magnetic behaviour and beneficiation characteristics. The early chromites are generally coarse grained and associated with olivine. Their cell dimensions vary from 8.27 to 8.29 A° and they are nonmagnetic. On the contrary, the late stage chromites are fine grained, associated with pyroxene. They are magnetic and have cell dimension around 8.39A°. The chemical data indicate that early stage chromites have formed at a higher temperature and low oxygen fugacity conditions than the late stage chromites. Lower temperature and oxidising conditions prevailing during the late stage crystallization facilitated significant cationic substitution both at tetrahedral and octahedral sites in the late stage chromites. The early stage chromites are easy to beneficiate compared to the late stage ones which require complex beneficiation operations.

ACKNOWLEGEMENTS

The authors are grateful to the Director for his kind permission to publish this work. Sincere thanks are due to the Mines managers of FACOR, IMFA and OMC Ltd. at Boula for their help in sample collection and other field assistance.

REFERENCES

BAROOAH, S. K. (1948): The chromite deposits of Nausahi, Keonjhar state, Eastern state Agency, India. Trans. Min. Met. Inst. India, **44**, 79-89.

CHAKRABORTY, K. L. (1958): Chromite ores associated with the ultramafic rocks of Nausahi, Keonjhar district, Orissa, India-Their mineragraphy and genesis. Proc. Nat.Inst.Sci. India, **24A**, 78-88.

EALES, H.V. (1980): The application of reflectivity measurements to the study of chromiferous spinels. Can. Minerl., **18**, 17-24.

GHOSH, A. M. N., PRASAD RAO, G. H. S. V. (1952): Some observations on the chromite occurrences of Nausahi, Keonjhar district, Orissa. Rec.G.S.I., **LXXXII**, Pt.2, 281-299.

IRVINE, T. N. (1967): Chromian spinel as a petrogenetic indicator. Part II. Can.J. Earth Sci., **2**, 648-672.

MOHANTY, J. K. (1994): Geology, mineralogy and geochemistry of the igneous complex around Boula, Keonjhar district, Orissa with particular reference to the associated economic minerals. Unpublished Ph.D. Thesis, Utkal University, Orissa, India.

MUKHERJEE, S. (1962): Geology, mineralogy and geochemistry of the chromite deposits of Nausahi, Keonjhar district, Orissa. Quart. J. Geol. Min. Met. Soc. India, **34**, 29-45.

MURCK, B. W., CAMPBELL, I. H. (1986): The effects of temperature, oxygen fugacity and melt composition on the behaviour of chromium in basic and ultrabasic melts. Geochim. Cosmochim. Acta, **50**, 1871-1887.

SAHA, A. K. (1963): Crustal evolution of Singhbhum, N. Orissa, India. Mem. Geol. Soc. India, **27**, 1-34.

STEVENS, R. E. (1944): Composition of some chromites of the West Hemisphere. Am. Miner., **29**, 1-34.

Received:October 24, 2001; accepted: August 13, 2002

Acta Mineralogica-Petrographica, Szeged 2001, Vol. 42, pp. 51-58

ACTA Mineralogica Petrographica

PETROLOGICAL CHARACTERISTICS OF ALGYŐ-FERENCSZÁLLÁS-MAKÓ AREA GRANITOIDS (SE HUNGARY)

ELEMÉR PÁL-MOLNÁR[1], GÁBOR KOVÁCS[1], ANIKÓ BATKI[1]

[1] Department of Mineralogy, Geochemistry and Petrology, University of Szeged
H-6701 Szeged, P. O. Box 651, Hungary
e-mai: palm@geo.u-szeged.hu

ABSTRACT

Boreholes located in the axis zone of the uplifted Algyő High (Csongrád Unit, Békésia Terrane, Tisia Composite Terrane, Pannonian Basin) reached granitoid rocks in the Variscan crystalline basement at a depth of 2250-2550 m. On the basis of their textures, these granitoids can be classified in the following two groups: granites of medium-grained, inequigranular, hypidiomorphic-granular texture and meta-granitoid rocks of medium-grained, inequigranular texture with preferred orientation. However, concerning the mineral composition and the texture of the rocks, significant differences cannot be recorded, they are of similar character. The main rock forming minerals of the studied samples are: quartz + microcline ± orthoclase + plagioclase feldspar + biotite + muscovite. Accessory components are apatite, zircone and garnet. Based on their modal composition, the rocks are syenogranites. According to their major element geochemistry, they are granite sensu stricto (syenogranite), subalkaline rocks with a peraluminous character. Concerning their tectonic origin the studied rocks are orogenous, syn-collisional, continental collisional granites (CCG). The samples generally display an S-type character with respect to their mineralogy and major element composition.

Key words: granite, geochemistry, crystalline basement, Csongrád Unit, Tisia Composite Terrane, Hungary

INTRODUCTION

The Pre-Alpine crystalline basement of SE Hungary, namely the Tisia Composite Terrane can be divided into three large structural units: the Slavonia-Dravia Terrane; the Kunságia Terrane [earlier "Central Hungarian Autochthon" (Szederkényi, 1984; Szederkényi et al., 1991), then "Paraautochthon Terrane" (Kovács et al., 1996/97;, Szederkényi, 1996]; and the Békésia Terrane [earlier "South Hungarian Nappe Zone" (Szederkényi, 1984; Szederkényi et al., 1991)] (Fig. 1). The Békésia Terrane can be divided further into: Kelebia Unit, Csongrád Unit, Battonya Unit and Sarkadkeresztúr Unit. The crystalline rocks of these units are of Variscan age, and covered by a 2500-6500 m thick Miocene-Pliocene sedimentary complex. Thus, the direct analysis of these rocks is only possible with the help of borehole samples. Although, it is not reinforced, based on the events affecting the Variscan Europe, the occurrence of a Pre-Variscan event on the Hungarian part of the Tisia Composite Terrane is still highly possible. The proven Pre-Mesozoic deformation and metamorphic processes in the Tisia Composite Terrane can only be related to Variscan events. The rocks of the Tisia Composite Terrane during the climax of the Variscan tectogenesis went under a medium pressure and temperature (Barow-type) metamorphosis (Kovács et al. 1996/97, 2000; Szederkényi, 1996). At the same time palingenetic granite belts were formed in the axis zones of the synclinoria. Later, these rocks were affected by a low pressure - high temperature event as well (Kovács et al., 2000).

This paper presents the results of the petrographical and major element geochemical analyses performed on the available granitoid and metagranitoid borehole samples that are originating from the Algyő High uplift (Csongrád Unit, Békésia Terrane) from a depth of approximately 2500-3000 m (Fig. 2B).

GEOLOGICAL SETTING AND LOCATION

The research area is located in the Csongrád Unit (earlier Tisza Complex) (Szederkényi, 1984, 1996), that is a part of the Békésia Terrane (the Pre-Alpine basement of the Alpine Békés-Codru zone) (Fig. 1). The morphology of the Csongrád Unit is dominated by the Algyő High (Fig. 2A-B).

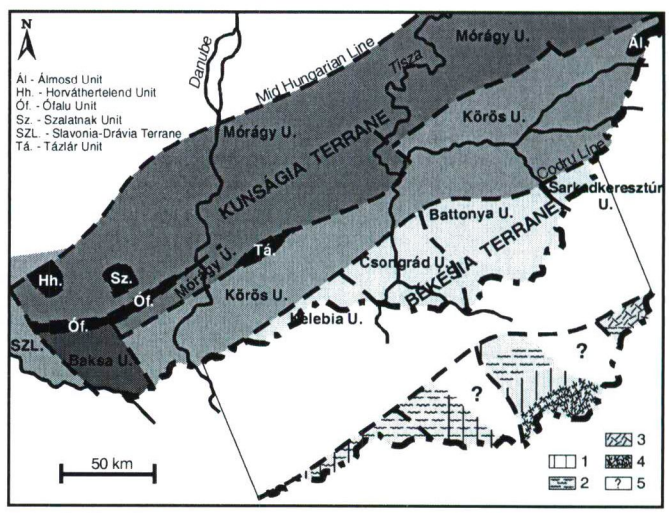

Fig. 1. Pre-Tertiary regional geology of the Tisia Composite Terrane (SE part of the Pannonian Basin); Békésia Terrane highlighted (modified after Kovács et al., 2000).
Legend: 1. Alpine overstep sequence connected to the northern shelf of the Axios/Vardar and related Neotethyan oceanic basins; 2. Variscan medium-grade metamorphosed complex; 3. Migmatic complex; 4. Granitoids; 5. Unknown.

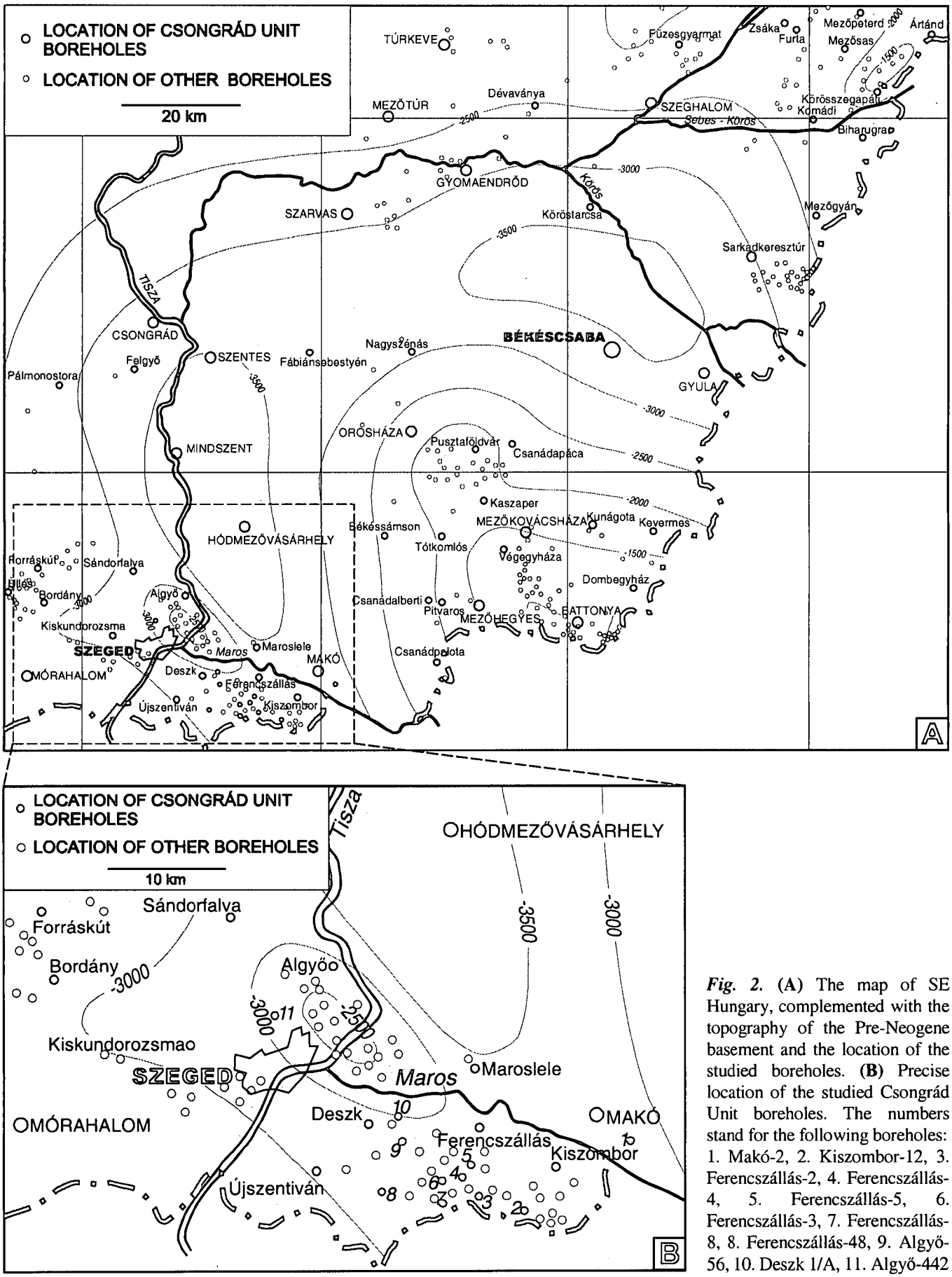

Fig. 2. **(A)** The map of SE Hungary, complemented with the topography of the Pre-Neogene basement and the location of the studied boreholes. **(B)** Precise location of the studied Csongrád Unit boreholes. The numbers stand for the following boreholes: 1. Makó-2, 2. Kiszombor-12, 3. Ferencszállás-2, 4. Ferencszállás-4, 5. Ferencszállás-5, 6. Ferencszállás-3, 7. Ferencszállás-8, 8. Ferencszállás-48, 9. Algyő-56, 10. Deszk 1/A, 11. Algyő-442

The Algyő High is interpreted after Tari et al. (1999) – based on the low-angle normal fault contact separating high-grade metamorphites from unmetamorphosed Mesozoic carbonates; the presence of mylonites; the characteristically retrogade metamorphism within the lower plate (Fülöp, 1994); and fission-track dating – as a subsurface Middle Miocene (Alpine) metamorphic core complex. [The Alpine development of the Tisia Composite Terrane started with the multi stage oceanisation of the Mesozoic Thetys. The first stage of compression can be put to the end of the Lower Cretaceous (Austrian Phase), while the last stage fell to the appearance and formation of the Pannonian Basin (Neogene-Quaternary).]

The borders of the Csongrád Unit are: the northern front of the South Hungarian Nappe Belt in the north, the Ásotthalom-Bordány Depression in the west, the so called Makói Trench in the east, and towards the south it stretches to the Vajdaság, where its border is formed by the northern front of the Biharia Nappe System (Kemeneci et al., 1997). According to Szederkényi (1984), the main phase of the unit's polimetamorphism was a 350-330 Ma Barrow type event with a temperature of 500-570 °C and a pressure of 6-8 Kb. This was followed by a Variscan late kinematic, T = 590-620 °C, P= 2,8-3,9 Kb event 330-270 Ma ago, which resulted in the formation of andalusite in higher grade schists, and the development of small size granite bodies in the migmatite zone, that were significantly homogenised due to a certain upward compression (Deszk, Ferencszállás). This second phase was accompanied by a stronger shear along the cleavage planes, and the formation of blastomilonite in lower grade crystalline schists.

Sampling and analytical methods

The studied samples were obtained from Csongrád Unit boreholes. The rocks were taken from the rock collection of the Department of Mineralogy, Geochemistry and Petrology, University of Szeged. The samples are drill cores, that were brought to the surface uncontinuously during core sampling, therefore the number and quantity of the samples is limited. The Kiszombor-12, Ferencszállás-3, 4, 5, 8, 48, Deszk 1/A, Algyő-56, 442 boreholes were deepened in the axis zone of the Algyő High, that has a NW-SE stretch, while the Makó-2 borehole originates from the NE wing of the dome (Fig. 3).

The major element analyses were made with an atomic emission spectrometer (ICP-AES) at the University of Stockholm.

Mineralogical and geochemical characteristics of the studied granitoid rocks

Macroscopic description

The colour of the studied samples is mainly light grey, subordinately pale rose-colour. Their texture is mostly holocrystalline, medium-grained inequigranular and equigranular. Based on the situation of mica, in some places the studied rocks are characterised by a preferred orientation in their texture. The major rock forming minerals are quartz, potassium feldspar, plagioclase feldspar and mica (biotite, muscovite).

Textural features of the studied granite samples

During the microscopic analyses both the modal proportion and the most important textural characteristics were examined in terms of the main rock forming, accessory and secondary minerals. On the basis of their textures, the studied rocks can be classified in the following two groups:

a. rocks of medium-grained, inequigranular, hypidiomorphic-granular texture (Fig. 4A),

b. meta-granitoid rocks of medium-grained, inequigranular texture with preferred orientation (Fig. 4B).

Concerning the mineral composition and the texture of the rocks, significant differences cannot be recorded. On the basis of their composition, the rocks can be considered of similar character. The main rock forming minerals of the studied samples are: quartz + microcline ± orthoclase + plagioclase feldspar + biotite + muscovite.

The textural character of the main mineral components are as follows:

quartz: xenomorphous grains of 1-2 mm average size. As a result of tectonic deformation it is always of undulating absence (Fig. 4C) and it is frequently recrystallised (Fig. 4B), what lead to the decrease of grain size and the development of subgrains. It appears both in microcline and plagioclase feldspars as a rounded grain. Rarely, it forms myrmekite in plagioclase feldspars.

orthoclase: hypidiomorphous, tabular appearance (Fig. 4C) with an average 1-3 mm size. Bifold twinning is common, in some places it is perthitic. It is subordinate compared to microcline.

microcline: a component of hypidiomorphous, xenomorphous, perthitic, tabular character. Its average size is 1-4 mm. Poikiloblastic appearance is common, it contains quartz, plagioclase feldspar, mica and zircon minerals (Fig. 4A). Sometimes, round-shape quartz grains appear in it.

plagioclase feldspar: hypidiomorphous, tabular, often zoned (Figs. 4A, 4C). Its average size is 1-3 mm. Many times it is highly seriticised, moreover, it occurs sometimes that only its sericitic pseudomorph can be found in the rock. Sometimes, there are carbonatised cores in the zoned crystals. Similarly to microcline, it also contains round-shape quartz grains and zircon in the form of inclusions. Due to the deformation it is characterised by bent twin lamellae. It is common in gneiss.

biotite: hypidiomorphous, 0,5-1 mm in average. Its pleochlorism is brownish yellow – greenish. Due to the transformation, often only its pseudomorph, built up of chlorite, opaque minerals and/or rutile needles can be detected (Fig. 4C). It occurs as a secondary component in plagioclase feldspar, in microcline as an inclusion, too. It contains apatite and zircon inclusions. In some places in mica-rich zones it has a preferred orientation. It may turn into muscovite, as well. In textures of preferred orientation it developed after biotite, by intersecting the foliation, marked by the later.

muscovite: hypidiomorphous grains of an average 0,5-1,5 mm size; it can form kink bands (Figs. 4B, 4D). Often it occurs in intercrescense of biotite, in some cases it grows through the biotite.

Accessory components are apatite, zircone and garnet (Fig. 4D). These can be found in any of the rock forming minerals.

The studied rocks went under certain transformational processes too, such as chloritisation, sericitisation, carbonatisation.

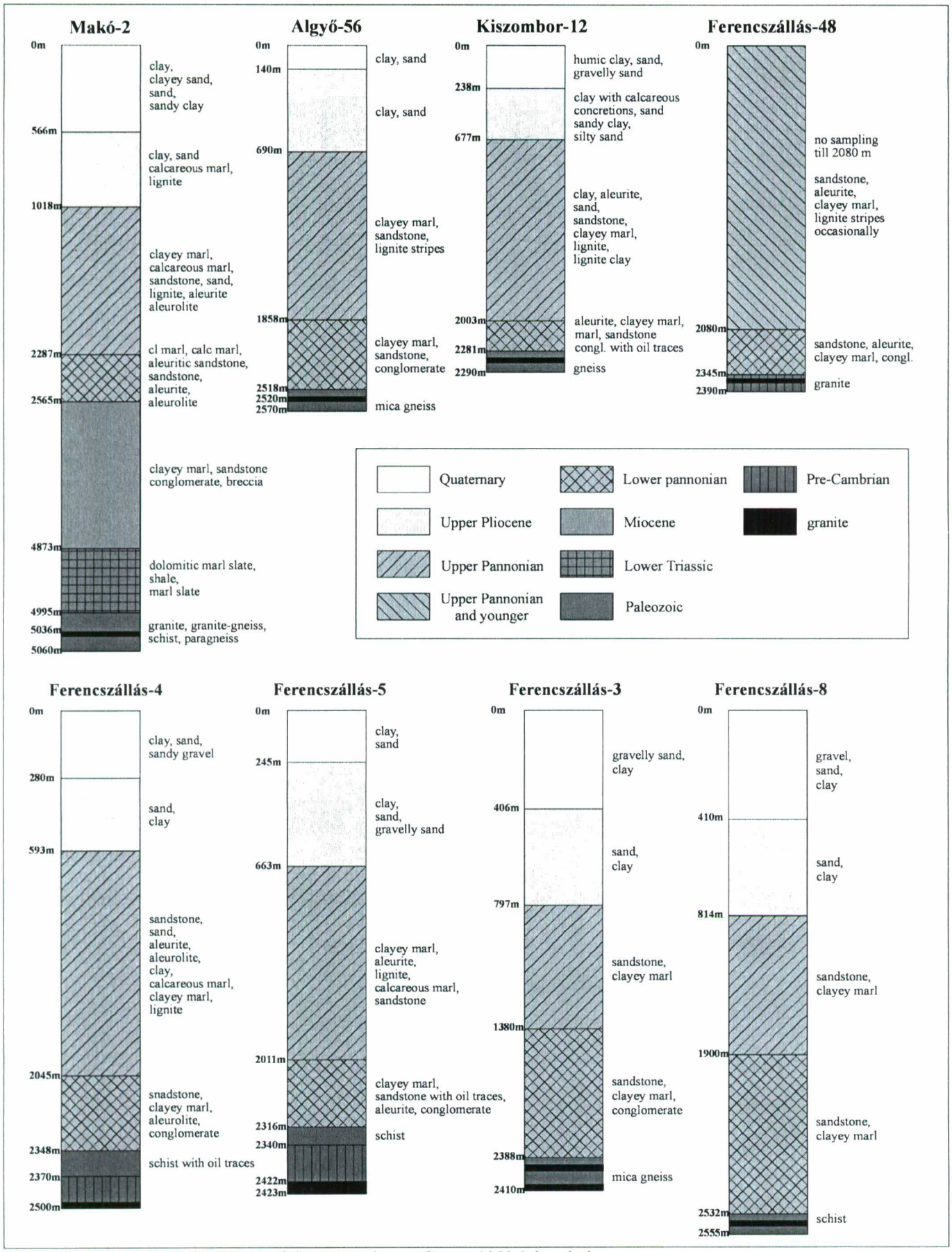

Fig. 3. The stratigraphical columns of the most relevant Csongrád Unit boreholes.

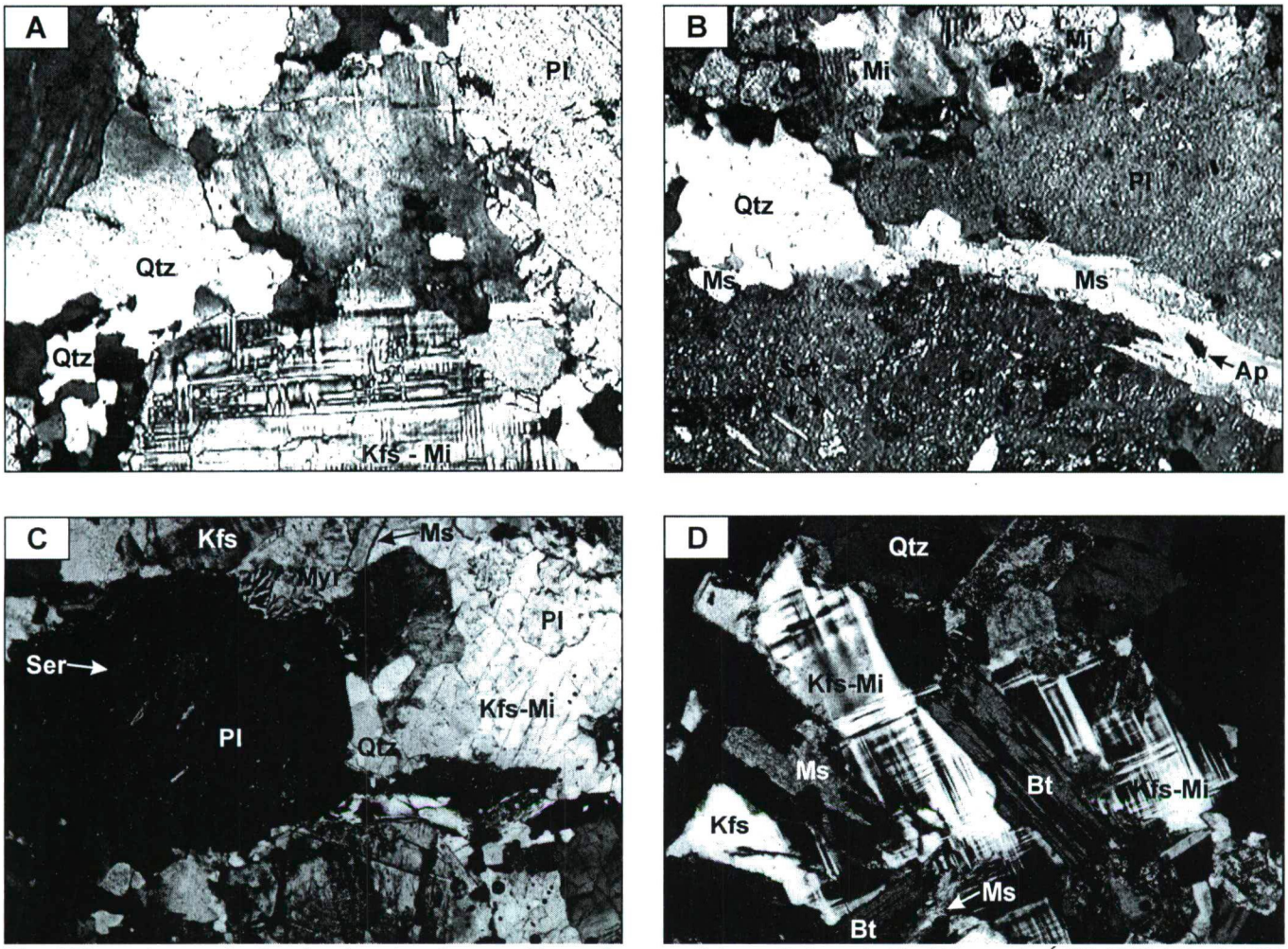

Fig. 4. Photomicrographs showing the mineral composition and texture of the studied granitoids. **(A)** sample ÁGK-1782 (Algyő-442), syenogranite (+N, x50); **(B)** sample ÁGK-1659 (Ferencszállás-8), syenogranite (+N, x50); **(C)** sample ÁGK-1782 (Algyő-442), syenogranite (+N, x50); **(D)** sample ÁGK-1241 (Deszk 1/A), syenogranite (+N, x100). Abbreviations: Ap – apatite, Bt – biotite, Chl – chlorite, Kfs – K-feldspar, Mi – microcline, Mnz – monazite, Ms – muscovite, Pl – plagioclase, Qtz – quartz, Ser – sericite.

Table 1. Representative major element data for the Algyő-Ferencszállás-Makó area granites

Sample	Ferencsz.-5 ÁGK-1657	Ferencsz.-8 ÁGK-1659	Makó-2 ÁGK-1209	Ferencsz.-3 ÁGK-1214	Kiszom.-12 ÁGK-1219	Deszk-1/A ÁGK-1241
SiO_2	75.7	75	68.3	72.3	84	73
TiO_2	0.176	0.103	0.378	0.143	0.294	0.206
Al_2O_3	14.9	14.14	14.91	13.81	8.6	14.92
$Fe_2O_3^*$	1.391	0.995	2.821	1.39	1.483	1.643
MnO	0.029	0.013	0.028	0.026	0.013	0.02
MgO	0.316	0.31	1.441	0.389	0.461	0.449
CaO	0.608	0.617	0.886	0.825	0.134	0.735
Na_2O	3.07	3.297	2.387	3.176	1.703	3.158
K_2O	5.56	4.676	4.801	4.494	2.582	5.06
P_2O_5	0.176	0.231	0.36	0.239	0.047	0.295

(*given as total iron content)

Concerning their modal composition (450 points/sample were counted) the rocks plot to the syenogranite field in the Q-A-P diagram of Le Maitre et al. (1989) (the field is not shown).

Some representative results of the major element analyses are listed in Table 1.

The granites are fractioned from a moderate to high extent. The SiO_2 content varies between 68.3 and 84.00 wt% (mean value: 74.71 wt%). The alkali content is high: K_2O is between 2.58 and 5.56 wt% (mean value: 4.51 wt%), Na_2O is between 1.70 and 3.29 wt% (mean value: 2.79 wt%). The K_2O/Na_2O-ratios range between 1.41 and 2.01. Calcium and magnesium contents are low; 0.13-0.88 wt% CaO and 0.31-1.44 wt% MgO. The iron

content is 0.99-2.82 wt% $Fe_2O_3^*$ (total Fe). The $Fe_2O_3^*/(Fe_2O_3^*+MgO)$ ratio varies between 0.66 and 0.81.

Based on the chemical analyses, the studied samples represent granites in the alkalis *vs.* silica diagram [Cox et al. (1979) adapted by Wilson (1989)] (Fig. 5). When applying the geochemical system of De la Roche et al. (1980) the rocks prove to be syenogranites (Fig. 6). This is in absolute correspondence with the modal Q-A-P classification.The granites are subalkaline (Fig. 5), calc-alkaline (after Irvine et al., 1971 – not shown). Considering the distribution of molar ratios $Al_2O_3/(Na_2O+K_2O)$ (A/NK) *vs.* molar ratios $Al_2O_3/(CaO+ Na_2O+K_2O)$ (A/CNK) (Shand's index, modified by Maniar et al., 1989) the granites are of peraluminous character (Fig. 7).

The chemical characteristics of granitoid rocks from different tectonic environments can be summarised in the following classes (1) island arc granitoids (IAG); (2) continental arc granitoids (CAG); (3) continental collision granitoids (CCG); (4) post-orogenic granitoids (POG); (5) rift-related granitoids (RRG); (6) continental epirogenic uplift granitoids (CEUG); (7) oceanic plagiogranites (OP) (Maniar et al., 1989). After discriminating OP from the rest of the granitoid classes (Maniar et al., 1989) (Fig. 8A), and considering the richness of the studied rocks in potassium feldspars it is obvious that the samples are not OP. The discrimination between the IAG+CAG+CCG group and the RRG+CEUG group can be seen on the MgO *vs.* $Fe_2O_3^*$ (total Fe) and the CaO *vs.* $Fe_2O_3^*$ +MgO diagrams (Fig. 8A-B) (Maniar et al., 1989). Hence, the studied samples are orogenic granitoids, i.e. plot to the IAG+CAG+CCG group. The discrimination of CCG from IAG+CAG can be made on the basis of the A/CNK molar ratio (Fig. 7), the Na_2O/CaO wt% ratio, the Na_2O/K_2O wt% ratio, the $MgO/Fe_2O_3^*$ wt% ratio and the MgO/MnO wt% ratio. The value of the A/CNK ratio in the samples is higher than 1.05 (A/CNK = 1.19-1.47); the mean value of Na_2O/CaO = 5.74; the mean value of Na_2O/K_2O = 0.59; the mean value of $MgO/Fe_2O_3^*$ = 0.3; the mean value of MgO/MnO = 34.25. In the end, this means that the studied rocks are CCG (Maniar et al., 1989) granitods, what is reinforced by the biotite, muscovite ± garnet mineral composition, as well.

When considering Batchelor, Bowden's (1985) R1 vs. R2 system (Fig. 9), that gives a good estimation on the tectonic environments during granitoid formation, the analysed granitoids turn to be of Syn-Collisional type.

The ASI $[Al_2O_3/(CaO+K_2O+Na_2O)]$ value of the samples is > 1.15, the CIPW norm yields > 1% corundum (mean value: 3.4 %), and the samples are characterised by a relatively low Na/K ratio. These are characteristics of S-type granites(Zen,1988).

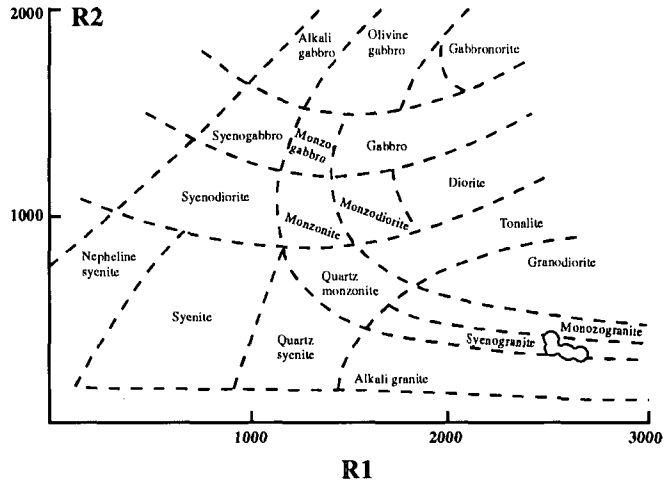

Fig. 6. Geochemical classification of plutonic rocks using parameters R1 and R2 (after De la Roche et al., 1980), calculated from milication proportions. R1 = 4Si-11(Na+K)-2(Fe+Ti); R2 = 6Ca+2Mg+Al

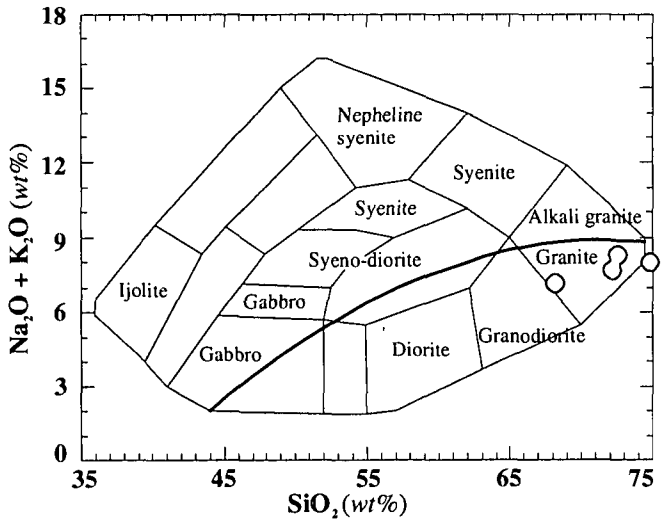

Fig. 5. The chemical classification and nomenclature of plutonic rocks using the total alkalis versus silica (TAS) diagram of Cox et al. (1979) adapted by Wilson (1989) for plutonic rocks. The curved solid line subdivides the alkali from subalkali rocks

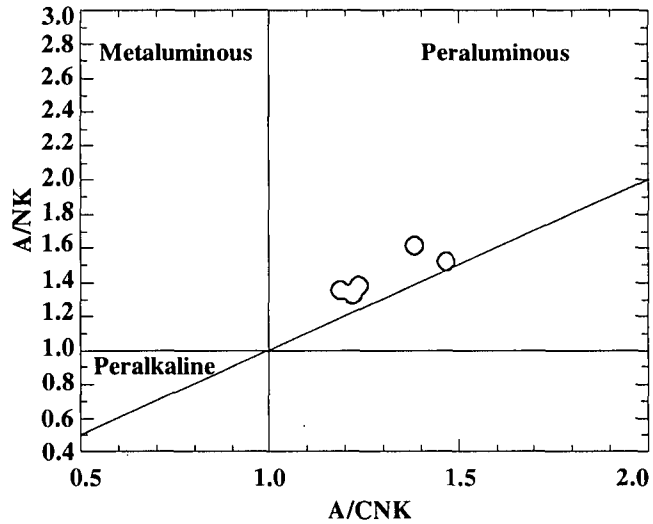

Fig. 7. Plots of molar ratios $Al_2O_3/(Na_2O+K_2O)$ (A/NK) *vs.* molar ratios $Al_2O_3/(CaO+Na_2O+K_2O)$ (A/CNK) (Maniar, et al., 1989).

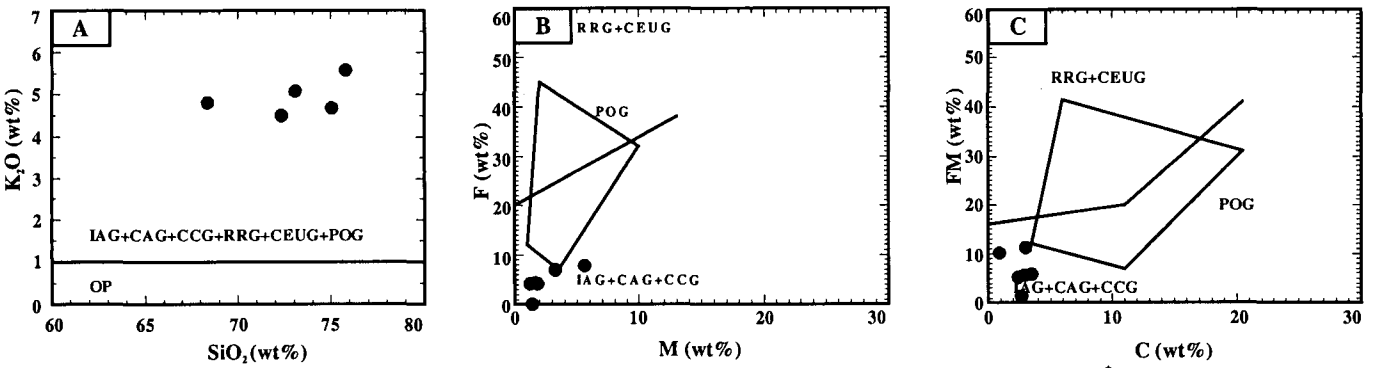

Fig. 8. A selection of diagrams after Maniar et al. (1989). **(A)** SiO_2 *vs.* K_2O; **(B)** MgO (M) *vs.* $Fe_2O_3^*$ (F) (*=total iron); **(C)** CaO vs. ($Fe_2O_3^*$+MgO) (*=total iron).
Abbreviations: IAG = island arc granitoids, CAG = continental arc granitoids, CCG = continental collision granitoids, POG = post-orogenic granitoids, RRG = rift-related granitoids, CEUG = continental epirogenic uplift granitoids, OP = oceanic plagiogranites.

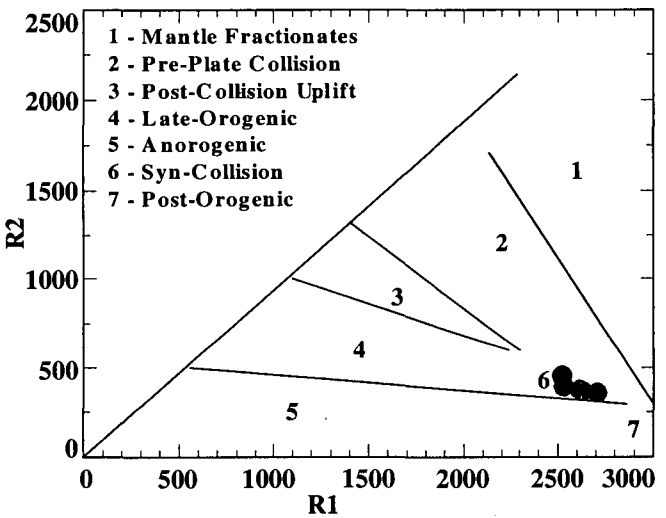

Fig. 9. Tectonical discrimination plots of Batchelor, Bowden (1985). R_1=4Si-11(Na+K)-2(Fe+Ti); R_2=6Ca+2Mg+Al

Conclusions

(1) On the basis of their textures, the studied granites of the Csongrád Unit can be classified in the following two groups:

a. granites of medium-grained, inequigranular, hypidiomorphic-granular texture;

b. meta-granitoid rocks of medium-grained, inequigranular texture with preferred orientation.

Concerning the mineral composition and texture of the rocks, significant differences cannot be recorded. On the basis of their composition, the granites can be considered of similar character. The main rock forming minerals of the studied samples are: quartz + microcline ± orthoclase + plagioclase feldspar + biotite + muscovite. Accessory components are apatite, zircone and garnet. The rocks modal composition refers to that of syenogranites.

(2) According to the major element analyses, the granites of the Csongrád Unit are granite sensu stricto (syenogranite), they are subalkaline with a peraluminous character.

(3) From a tectonical aspect the studied rocks are of orogenous, syn-collisional, continental collisional origin (CCG).

(4) The granites of the Csongrád Unit generally display an S-type character with respect to their mineralogy and major element composition.

Acknowledgements

The financial background of this work was ensured by the János Bolyai Research Grant, the Hungarian National Science Found (OTKA) (Grant No. F/029061), and the Swedish Institute.

References

Batchelor, R. A., Bowden, P. (1985): Petrogenetic interpretation of granitoid rock series using multicationic parameters. Chemical Geology, **48**, 43-55.

Cox, K. G., Bell, J. D., Pankhurst, R. J. (1979): The interpretation of igneous rocks. George, Allen and Unwin, London.

De la Roche, H., LeTerrier, J., Grandclaude, P., Marchal, M. (1980): A classification of volcanic and plutonic rocks using R1-R2 diagrams and major element analyses – its relationship with current nomenclature. Chemical Geology, **29**, 183-210.

Fülöp, J. (1994): Geology of Hungary, Paleozoic II. Akadémiai Kiadó, Budapest (In Hungarian). 447 pp.

Irvine, T. N., Baragar, W. R. A. (1971): A guide to the chemical classification of the common volcanic rocks. Canadian Journal of Earth Sciences, **8**, 523-548.

Kemenci, R., Čanović, M. (1997): Geologic setting of the Pre-Tertiary basement in Vojvodina. Part I: The Tisza Megaunit of North Vojvodina. Acta Geologica Hungarica, **40/1**, 1-36.

Kovács, S., Szederkényi, T., Árkai, P., Buda, Gy., Lelkes-Felvári, Gy., Nagymarosi, A. (1996/97): Explanation to the terrane map Hungary. In Papanikolaou, C. (ed): IGCP Project No. 276 Terrane Maps and Terrane Descriptions. Ann. Géol. Pays Helléniq., **37**, 245-270.

Kovács, S., Hass, J., Buda, Gy., Nagymarosy, A., Szederkényi, T., Árkai, P., Császár, G. (2000): Tectonostratigraphic terranes in the pre-Neogene basement of the Hungarian part of the Pannonian area. Acta Geologica Hungarica, Vol. **43/3**, 225-328.

Le Maitre, R. E. (ed.) (1989): A classification of the igneous rocks and glossary of geological terms. Blackwell.

Maniar, P. D., Piccoli, P. M. (1989): Tectomic discrimination of granitoids. Geological Society of America Bulletin, **101**, 635-643.

Peacock, M. A. (1931): Classification of igneous rock series. Journal of Geology, **39**, 7-65.

Szederkényi, T. (1984): Az alföld kristályos aljzata és földtani kapcsolati (Crystalline basement and geological relations of the Great Plain). D.Sc. Thesis. MTA Library, Budapest, (in Hungarian).

Szederkényi, T. (1996): Metamorphic formations and their correlation in the Hungarian part of the Tisza Megaunit (Tisa Composite Terrane). Acta Miner., Petr. Szeged, **37**, 143-160.

SZEDERKÉNYI, T., ÁRKAI, P., LELKES-FELVÁRI, GY. (1991): Crystalline groundfloor of the Great Hungarian Plain and South Transdanubia, Hungary. Serb. Acad. Sci. Arts, Nat., Math., Sci., **62/4**, 261-272.

TARI, G., DÖVÉNYI, P., DUNKL, I., HORVÁTH, F., LENKEY, L., STEFANESCU, M., SZAFIÁN, P., TÓTH, T. (1999): Lihospheric structure of Pannonian basin derived from seismic, gravity and geothermal data. In Durand B, Jolivet L, Horváth F, Sérane M (eds): The Mediterranean Basins: Tertiary Extension within the Alpine Orogen,. Geological Society: London. Special Publication, **156**, 215-250.

WILSON, M. (1989): Igneous petrogenesis. Unwin Hyman, London.

ZEN, E. (1988): Phase relations of peraluminous granitic rocks and their petrogenetic implications. Ann. Rev. Earth Planet. Sci., **16**, 21-51.

Received: November 10, 2001; accepted: February 6, 2002

Acta Mineralogica-Petrographica, Szeged 2001, Vol. 42, pp. 59-64

ACTA
Mineralogica
Petrographica

STRUCTURAL EVOLUTION OF MYLONITIZED GNEISS ZONE FROM THE NORTHERN FLANK OF THE SZEGHALOM DOME (PANNONIAN BASIN, SE HUNGARY)

FÉLIX SCHUBERT[1], TIVADAR M TÓTH[1]

[1] Department of Mineralogy, Geochemistry and Petrology, University of Szeged
H-6701 Szeged, P. O. Box 651, Hungary
e-mail: schubert@geo.u-szeged.hu

ABSTRACT
Metamorphic basement of the Pannonian Basin consists of blocks of incompatible metamorphic and structural evolution in the area of the Szeghalom high. Here evolution of a large-scale shear zone from the northern flank of the uplifted dome is studied. Textural relics suggest that the original rock type was orthogneiss widespread in the surroundings. Deformation produced a wide (over 200 m) shear zone with well-developed mylonite in the centre. We show, that the deformation followed the last progressive metamorphic event of the basement.
Key words: Pannonian Basin, orthogneiss, shear zone, mylonite

INTRODUCTION

Although metamorphic basement of the Pannonian Basin was regarded substantially impermeable for a long time, more recent works demonstrated that the fractured basement plays a significant role in the present hydraulic system of the Pannonian Basin (Tóth et al., 2001). This highly deformed rock mass not only conducts and stores a huge amount of water, it also contains a significant amount of hydrocarbon, which could migrate to the basement rocks along tectonic zones from the adjacent, deeper sedimentary basins.

One of the most important basement reservoirs in the Pannonian Basin is the Szeghalom Dome (SzD), which is part of the elevated basement highs embracing the deep Békés Basin on the north (Fig. 1). Previous studies suggested a rather complicated structure of the region. Analysing seismic data D. Lőrincz (1996) inferred activity of seven subsequent tectonic events from the Upper Cretaceous up to present for the wide surroundings. SzD itself was subdivided into four blocks of incompatible metamorphic and structural evolution, which got juxtaposed due to Neogene movements (M Tóth et al., 2000). They mention mylonitized gneiss samples from the northern flank of the crystalline high in question, which produce evidence for a considerable ductile shear zone. Unpublished reports of the Hungarian Oil- And Gas Co. regularly mention mylonite in core description based on the disturbed fabric of the rock too.

The aim of this study is to characterise the shear zone of the northern SzD based upon the changing microstructural features along the wide shear zone. Samples were collected from core material of two neighbouring wells, which penetrated the basement from a moderately deformed gneiss zone down to mylonite. Characterisation of this event is of basic importance in case of the fractured oil reservoir, because tectonic zones of different evolution may result in rather distinct migrational properties.

GEOLOGICAL SETTING

Based on geochemical, petrological and age constraints Szeghalom Dome (SzD) can be subdivided into four independent regimes (M Tóth et al, 2000). Three of them form the southern and central parts of the high, while the northern flank consists of a single block dominated by medium grade orthogneiss and post-kinematic granite.

Igneous relics in the gneiss are widespread throughout the area. M Tóth et al. (2002) inferred altered myrmekitic inclusions in fresh K-feldspar grains of magmatic origin that is also confirmed by the frequent appearance of euhedral zircon, apatite and tourmaline crystals. Resorbed garnet

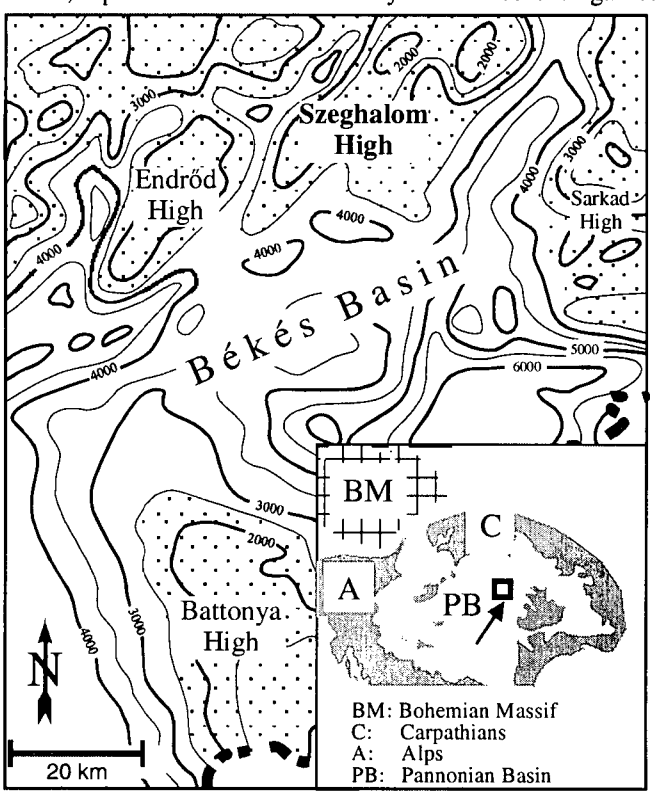

Fig. 1. Map of the Békés Basin and the surrounding metamorphic highs. Present-day depth of the pre-Neogene basement is shown. Inset: Location of the Pannonian Basin in the Alpine-Carpathian-Pannonian system.

indicates the earliest metamorphic event of the area, which was followed by cooling down allowing pseudomorphic replacement of garnet by chlorite. Secondary biotite generally surrounds these chlorite-bearing pseudomorphs suggesting a second progressive event (M Tóth et al., 2000). The peak of this metamorphism did not reach 600 °C.

There is not much presented about the deformation history of the northern SzD orthogneiss terrane. Mylonite samples of the neighbouring Sz-É-2 and -11 wells, nevertheless, clearly suggest the presence of a ductile shear zone.

Methods

18 rock specimens were studied, which represent the two wells with significant hiatuses. The cores are not oriented. Thin sections were made along the plane perpendicular to the foliation and parallel to the lineation.

Results

In order to be able to reconstruct the petrological, microstructural and geochemical constraints of the deformation event observed in several borecores from the northern flank of the SzD, we studied samples from two neighbouring wells, Sz-É-2 and Sz-É-11, respectively. Both wells penetrated the metamorphic basement over a hundred metres and served a sufficient material for a detailed petrological and geochemical study.

Petrography

Petrographically, each sample studied reminds of an analogous starting material, the studied wells penetrated the two-feldspar biotite gneiss terrane typical in the surrounding area. A continuous change in both mineralogical and microstructural properties of the gneiss can be followed along the wells, while maximal strain is reached at the deepest structural level. The most obvious parameters, which appoint to the vertical variation, are the following:

a) matrix biotite is increasingly replaced by chlorite,
b) chlorite is replaced by muscovite,
c) average grain size decreases,
d) number of the garnet pseudomorphs diminishes,
e) quantity of opaque grains parallel to the mean foliation increases,
f) the strongly folded, gneissosity (S1) diminishes and is succeeded by a mylonitic foliation (S2).

Based on these features the rock column was divided into three rough intervals. The uppermost zone is only hardly deformed allowing the original textural features clearly observe. The deepest zone exhibits a pure mylonitic texture, and we also defined a transition zone between the two extremes. Hereafter petrographical characterization of the three zones follows.

Uppermost zone

The rather disturbed and non-contiguity foliation of the gneiss is defined by reddish brown to dark green coloured biotite flakes. At places the foliation is strongly folded, and biotite forms kink-band microstructure. Biotite is partially replaced by chlorite and contains interlayered carbonate grains. Some feldspar clasts exhibit a continuous excitation from the rim to the core and usually are strongly altered to sericite inside. The most frequent accessory phases are apatite, zircon and tourmaline, which show euhedral and subhedral habit. Apatite crystals range in size up to 400 μm. Large, isometric relics were found in all structural levels consisting mainly of chlorite, quartz and an undetermined carbonate phase. In the core of a few of these pseudomorphs also small (300 μm) garnet remnant could survive. Quartz grains usually are aligned in curved (S-shape) (Fig. 2A) rows.

Some feldspar grains contain V-shaped deformation twins, which are tapered to towards the crystal centre and are restricted to certain parts of a crystal (Fig. 2B) (Passchier et al., 1996). Both the growth twins and the deformation twins are often curved.

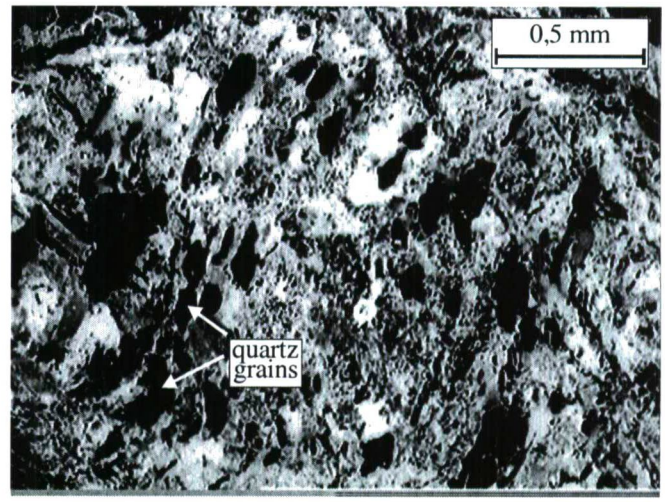

Fig. 2A. Microphoto of garnet pseudomorph with subvertical, curved inclusion trails (invert photo).

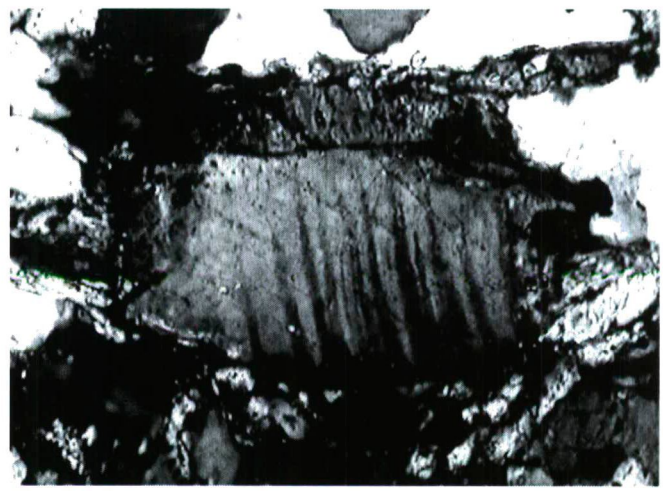

Fig. 2B. Microphoto of V-shaped, slightly curved deformation twins in feldspar.

Transition zone

Rock samples of the transition zone consist essentially of medium-grained feldspar and quartz. Biotite is almost entirely replaced by chlorite. The rock is determined by S2 mylonitic foliation, S1 gneissosity occurs only in relic fragments.

Mineral aggregates of sigmoidal shape are common, in which the core is composed of feldspar and recrystallized quartz forms the wings. Quartz generally develops

recrystallized and strongly elongated lenses or ribbons, which generally are bordered by phyllosilicate packets. Huge quartz grains (ca 10 mm) are boudinaged and oriented sub-parallel to the S2. The neck and fractured parts within the boudins consist of carbonate (Fig. 2C). Also carbonate grains form ribbons along the S2 foliation, which are characterized by sub-microscopic grain size and a dark brown colour.

There are only a few garnet pseudomorphs of the type mentioned above, which are rimmed by an asymmetric (stair stepping) aggregate of fine-grained minerals (Fig. 2D). The rim of the pseudomorph is formed by biotite, while the wings

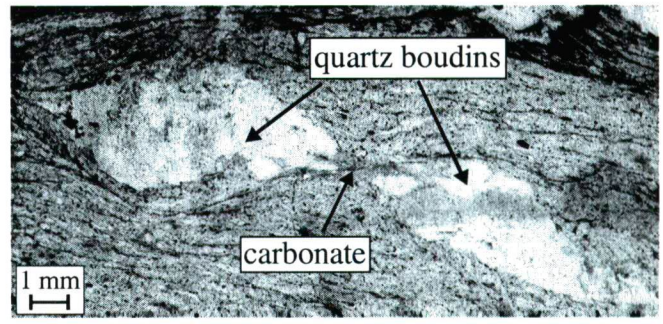

Fig. 2C. Microphoto of quartz boudinage with a neck composed of carbonate.

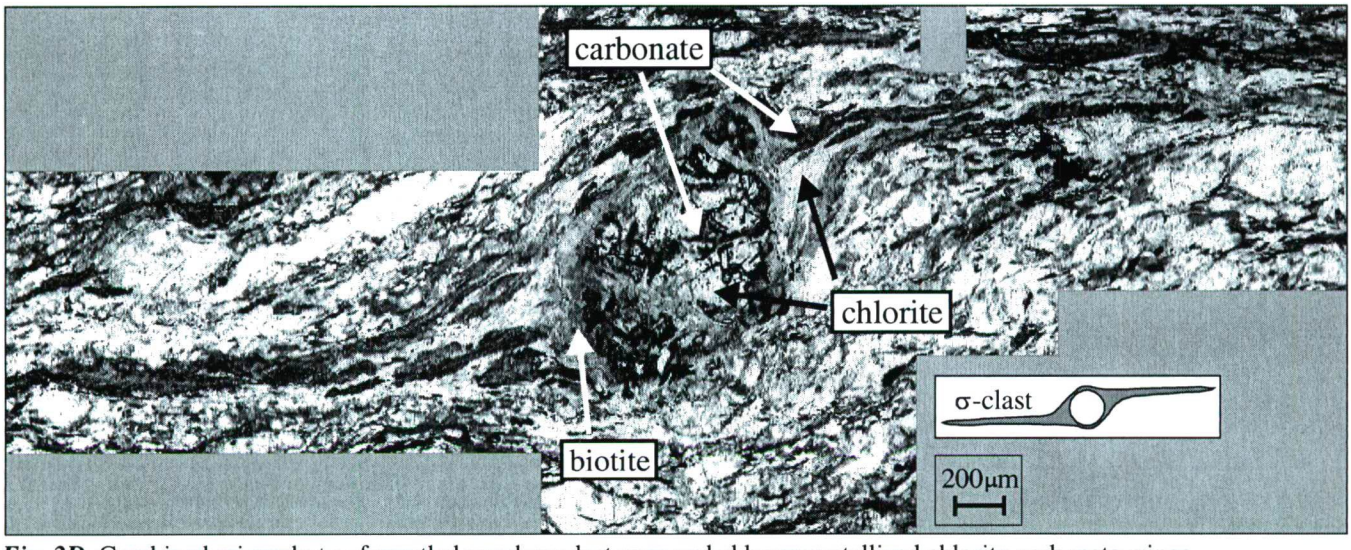

Fig. 2D. Combined microphoto of mantled porphyroclast surrounded by recrystallized chlorite-carbonate wings.

consist of carbonate, and chlorite in the internal core. The accessory minerals mentioned earlier also occur in the transition zone, although apatite crystals are smaller in size and show rounded, fractured habit.

Lowermost zone

The rock samples, which represent the deepest explored part of the shear zone consist mainly of quartz and chlorite. There is no trace of S1 gneissosity in the rock matrix, S2 foliation is defined by high contiguity chlorite bunches. The main foliation is often crosscut by high strain shear bands (S3), which contain fine-grained quartz ± chlorite ± carbonate infill (Fig. 2E). In addition white mica of pale green colour occurs. Its up to 3 mm small flakes generally

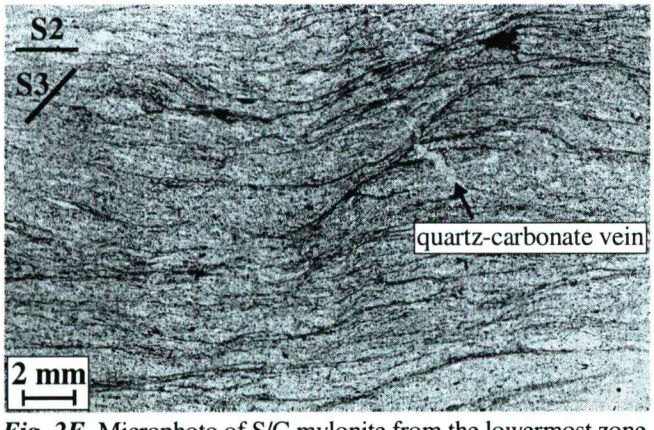

Fig. 2E. Microphoto of S/C mylonite from the lowermost zone.

form mica fishes parallel to the S2 foliation. Along the cleavage plains of the mica flakes, tails of opaque mineral grains appear.

In all structural levels of the shear zone studied microstructural features of a post-mylonitic deformation occur. In some hand specimens fresh mylonite and cohesive breccia are in contact along a sharp boundary. The fine-grained carbonate-cemented breccia encloses fractured pieces of the adjacent mylonite. In several parts fractured quartz grains with a strong undulose extinction form chocolate tablet microstructure. The reconstructed shape of the fragments, which are sitting in a very fine-grained carbonate matrix, resembles a boudinage structure (Fig. 2F). Some of these quartz grains also contain an extremely high number of secondary fluid inclusion planes. All along the wells steeply dipping veins with an aperture of about 0.5–1 mm crosscut sub-horizontal S2 foliation. The host rock is uneven along the vein walls and optically does not indicate alteration. Vein filling minerals are similar along the wells, with a various proportion of the phases; pyrite, quartz and various carbonate phases.

Discussion

Remnants of the metamorphic evolution

Because of the strong deformation, the rock studied could not preserve much evidence for the details of its metamorphic evolution. Zoned feldspar grains with sericitic inclusions as well as euhedral accessory phases (apatite, zircon) of the uppermost zone are important textural features

of the orthogneiss common in the whole northern part of the SzD (M Tóth et al., 2002). Mineralogy and texture of the garnet replacing chlorite and calcite bearing pseudomorphs are identical to those described by M Tóth et al. (2002) characteristic of the region. Preserved snowball structure outlined by quartz inclusion trails in these structures suggests garnet of metamorphic origin instead of an igneous relic phase.

Samples studied show a homogeneous lithology along the two wells, which is identical to the common orthogneiss of the northern flank of the SzD.

Development of the shear zone

The significant grain size reduction towards the lowermost zone is caused by different deformation mechanisms, which depend on the rheology of the minerals involved at the given temperature and strain rate. The size of the hard mineral grains (such as feldspar and muscovite in part) can be reduced by brittle deformation, while different dynamic recrystallization processes transform quartz grains.

In the lower part of the shear zone mica fishes, asymmetric porphyroclasts and S3 shear band cleavage (SBC) show characteristic monoclinic appearance indicating a deformation with a dominant non-coaxial component. Mica fish may form by a combination of brittle and crystal-plastic processes (Lister et al., 1984). On microscopic scale the spacing between S3 cleavage domains is relative large (2-4 bands per thin sections). Based on the arrangement and shape of the S2 and S3 cleavages, they form an S/C fabric (Lister et al., 1984). The age relationship of the S-C-surfaces has been discussed by several authors (e.g. Berthé et al., 1979; Platt et al., 1980; Vernon et al., 1983). Berthé et al. (1979) suggest that the S/C-surfaces develop simultaneously, while others (e.g. Vernon et al. (1983)) concluded that the accumulation of finite strain first led to the development of foliation (the S-surfaces) and later (ongoing) deformation led to the formation of cross-cutting shear bands (the C-surfaces). Since in the studied samples the S3 (C) planes clearly crosscut the much more developed S2 (S) planes, we prefer the successive evolution model and use the S2-S3 terminology. Trails of mica flakes often surround recrystallized quartz ribbons on both sides, making recrystallization of quartz possible, but also restrict its change in external shape or form.

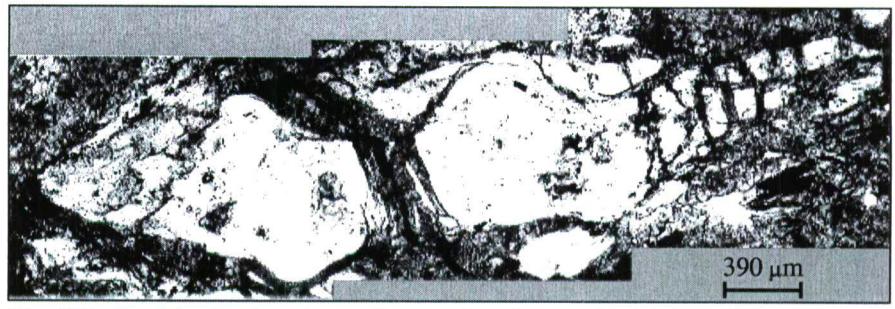

Fig. 2F. Combined microphoto of quartz boudinage effected by subsequent brittle deformation forming chocolate tablet structure.

After Passchier (1991b) S/C fabric is a common feature of strongly foliated extensional mylonites. The well-developed S-surfaces (S2) relative to the C-planes (S3) suggest that the rock is a Type I mylonite in the terminology of Lister et al. (1984). Since the shear zone boundary was not observed on the core material, a more exact specification of the SBC (Berthé et al., 1979a,b) is not possible. The shear bands in the study area are filled by chlorite±quartz±carbonate, which is consistent with McCaig's (1987) observations, namely that the shear band cleavage is usually indicative of retrograde metamorphic conditions.

The strongly elongated and flattened quartz grains usually show strong undulose extinction, which is probably caused by the interaction of diverse mechanisms. In addition to crystalplastic processes (dislocation creep, solid state diffusion) also pressure solution may form elongated quartz ribbons, especially because it is the favourable deformation mechanism of quartz at relatively low homologous temperature in the presence of water (Passchier et al., 1996). LT conditions can be deduced from the complicated quartz-to-quartz sutures (Kruhl et al., 1996) observed. Bulging might indicate grain boundary migration during the deformation (Passchier et al., 1996).

Softening, which is generally ascribed to nucleation and development of ductile shear zones is often related to fluid migration and infiltration (Ingles et al., 1999). Kerrich et al., (1988) suggest that meteoric water might penetrate down to 10-15 km along fault zones. Hydration alteration of strong mineral phases, such as feldspar, was probably a considerable softening process in the study area as well. The progressive grain size reduction is obvious downwards in the shear zone, which through the surface increase of the mineral grains might further promote the effect of hydration weakening. In the upper level of the shear zone the feldspar→mica alteration is the main hydration reaction, while biotite→chlorite becomes more intense towards the deeper levels. Further downwards chlorite→muscovite replacement is dominant. All of these hydration reactions lead to volume reduction (Wintsch et al., 1995), which enables further fluid migration into the shear zone (Rumble et al., 1983). The growth of phyllosilicates via feldspar replacement reactions is a widespread phenomenon in meteoric water-dominated failure systems (Wintsch et al., 1995). The feldspar consuming and clay mineral producing alteration is one of the most effective reactions, which can lower the strength of granitoid rocks. Thus, nucleation and recrystallization of the oriented phyllosilicate grains might further reduce the strength of the rock.

A thin biotite rim surrounds the garnet replacing pseudomorphs of the transition zone. Biotite, however is entirely missing from the fine-grained chlorite and carbonate bearing wings, which frame the pseudomorph on both ends. Such a structure suggests syn-kinematic recrystallization of the garnet replacing chlorite, and in this way the structure might be considered a stair-stepping, σ-type mantled porphyroclast. The presence of biotite

in the rim of the pseudomorph and its absence in the wings shows that the deformation proceeded below the biotite isograde. The presence of the clast forming minerals in the wings, on the other hand, suggests that garnet altered to biotite or chlorite prior to or simultaneously with the deformation. Undeformed structures of identical composition are widespread in the northern flank of the SzD and represent a garnet→chlorite→biotite reaction sequence (M Tóth et al., 2000).

The occurrence of carbonate patches parallel to the mylonitic foliation and in the external zone of the wings in the σ-clasts suggests that the fine-grained carbonate precipitated in the entire shear zone during the deformation process. This should correspond with the carbonate precipitated at the maximal elongation zone of the boudinaged quartz grains indicating the presence of carbonate during the ductile deformation.

This estimate agrees well with the presence of re- and neocrystallized quartz grains in absence of any trace of feldspar recrystallization as quartz begins to recrystallize above 270 °C, while feldspar behaves brittle below 450-500 °C (Voll, 1980). Feldspar grains generally exhibit limited ductility in low temperature (greenschist facies) mylonites and they fracture (or recrystallize) before exhibiting any marked elongation (White et al., 1980).

Based on the above microstructural observations we conclude that the lowermost part of the wells represent the most intensively deformed part of a mylonitic shear zone.

The non-continuous, en-echelon arrangement of the veins in the maximal strain zone suggests formation probably by tension, rather than shearing. The angles between the veins and the S2 show a consistent change in the chlorite-rich and chlorite-poor parts of the rock. The dip of the veins decreases abruptly where they crosscut the foliation. Leaving the phyllosilicate-rich plane they return to the original, steep dip. Several authors (Meschede, 1994; Colletta et al., 2002) describe the change in the dip of veins in strongly foliated rocks composing mineral zones of extremely different rheological properties.

On this basis vein formation is thought to be independent from the mylonitic deformation and its PTd properties and relative age constraints are out of scope of the present study.

Traces of brittle deformation observed on quartz boudins ("chocolate tablet structure") as well as the breccation of the mylonite suggest a late tectonic event connected probably to the exhumation of the shear zone. Stable isotopic composition of the carbonate cement of the breccia and investigation of the secondary fluid inclusions in quartz could help to estimate PT conditions of the subsequent brittle event.

Conclusions

The aim of this study was to interpret microstructural data of a wide ductile shear zone in the northern flank of the SzD. We showed that in the studied wells orthogneiss forms the basement of mineralogical and textural features identical to those described from the whole area previously. In addition to the early igneous history this rock type also encloses the remnants of multiphase metamorphic evolution. Retrogression of the orthogneiss led to the chloritization of garnet, while the often myrmekitic magmatic feldspar altered to sericite (M Tóth et al., 2002). Isometric garnet pseudomorphs are good evidence for low strain during the retrogression. The following progressive event well below 600 °C (M Tóth et al., 2000) resulted in formation of a secondary biotite in place of the chlorite and recrystalization of sericitized feldspar grains as fresh microcline (M Tóth et al., 2002). The fact that undeformed biotite does not appear in the recrystallized wings of the σ-clasts suggests that ductile deformation followed the thermal peak (Fig. 3). Probably due to the late uplift of the gneiss terrane, complicated brittle structures overprinted the mylonitic rocks.

The rock column studied exceeds 200 m in width from

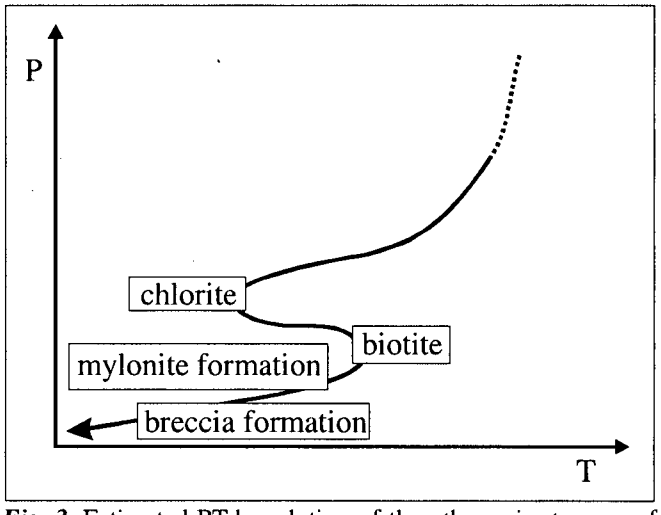

Fig. 3. Estimated PTd evolution of the othogneiss terrane of the northern SzD. Not to scale.

the moderately deformed gneiss down to the mylonitic centre of the shear zone suggesting a high strain rate during the deformation. This reason also infers that the ductile event studied is of fundamental importance in the metamorphic and deformation history of the northern SzD orthogneiss terrane. Keeping also the widespread brittle deformation structures in mind, one can state that the mylonite zone presented in this paper seems an excellent candidate as a fluid migration pathway that is worth being investigated further.

Acknowledgement

The project was financially supported by the Hungarian Research Found (grant no. OTKA F32792), the Hungarian Ministry of Culture (grant no. FKFP 0139/2001) and the János Bolyai Research Grant.

References

Berthé, D., Choukroune, P., Jegouzo, P. (1979): Orthogneiss, mylonite and non coaxial deformation of granites: the example of the South Amorican Shear–Zone. Journal of Structural Geology, **1**, 31-42.

Colletta, B., Piron, E., Marchal, D., Moretti, I. (2002): Gravitational folds and compressional structures related with normal faults in the Suez rift. (Abst.) EAGE 64th Conference and Exhibition, Florence. P073.

D. Lőrincz, K. (1996): Feszültségtér történet meghatározása szeizmikus szelvényeken azonosított többfázisú tektonizmus alapján, a Szolnoki flis öv nyugati peremén. Magyar Geofizika, **37**, 228-246.

INGLES, J., LAMOUROUX, C., SOULA, J., GUERRERO, N., DEBAT, P. (1999): Nucleation of ductile shear zone in a granodiorite under greenschist facies conditions, Néouvielle massif, Pyrenees, France. Journal of Structural Geology, **21**, 555-576.

KERRICH, R., KAMINENI, D. C. (1988): Characteristics and chronology of fracture – Fluid infiltration in the Archean, Eye Dashwa Lakes pluton, Superior Province: Evidence from H, C, O-isotopes and fluid inclusions. Contribution to Mineralogy and Petrology, **99**, 430-445.

KRUHL, J. H., NEGAN, M. (1996): The fractal shape of sutured quartz grain boundaries: application as a geothermometer. Geologische Rundschau, **85**, 38-43.

LISTER, G. S., SNOKE, Q. W. (1984): S-C Mylonites. Journal of Structural Geology, **6**, 617-638.

M. TÓTH, T., SCHUBERT, F., ZACHAR, J. (2000): Neogene exhumation of the Variscan Szeghalom Dome, Pannonian Basin, E. Hungary. Geological Journal, **35**, 265-284.

M. TÓTH, T., ZACHAR, J. (2002): Myrmekite-bearing gneiss from the Szeghalom Dome (Pannonian Basin, SE Hungary). Part II.: Origin and spatial relationships. Acta Mineralogia-Petrographica, this volume.

MCCAIG, A. M. (1987): Deformation and fluid-rock interaction in metasomatic dilatant shear bands. Tectonophysics, **135**, 121-132.

MESCHEDE, M. (1994): Methoden der Strukturgeologie. Ferdinand Enke Verlag Stuttgart. 169 pp.

PASSCHIER, C. W., TROUW, R. A. J. (1996): Microtectonics. Springer. 289 pp.

PLATT, J. P., VISSERS, R. L. M. (1980): Extensional structures in anisotropic rocks. Journal of Structural Geology, **2**, 397-410.

RUMBLE, D., III, SPEAR, F. S. (1983): Oxygene-isotope equilibration and permeability enhancement during regional metamorphism. Journal of the Geological Society, **140**, 619-628.

TÓTH, J., ALMÁSI, I. (2001): Interpretation of observed fluid potential patterns in a deep sedimentary basin under tectonic compression: Hungarian Great Plain, Pannonian Basin. Geofluids, **1**, 11-36.

VERNON, R. H., WILLIAMS, V. A., D'ARCY, W. F. (1983): Grain size reduction and foliation development in a deformed granite batholith. Tectonophysics, **92**, 123-146

VOLL, G. (1980): Ein querpr ofil durch die Schweizer Alpen vom Vierwaldstätter See zur Wurzelzone – Strukturen und jahre Entwicklung durch Deformationsmechanismen wichtiger minerale. N. Jb. Geol. Paläont, **160**, 321-335.

WHITE, S. H., BURROWS, S. E., CARRERAS, J., SHAW, N. D., HUMPHREYS, F. J. (1980): On mylonites in ductile shear zones. Journal of Structural Geology, **2**, 175-187.

WINTSCH, R. P., CHRISTOFFERSEN, R., KRONENBERG, A. K. (1995): Fluid-rock reaction weaking of fault zones. Journal of Geophysical Research, **100**, 13021-13032.

Received: November 18, 2001; accepted: June 19, 2002

Acta Mineralogica-Petrographica, Szeged 2001, Vol. 42, pp. 65-74

ACTA
Mineralogica
Petrographica

EFFECT OF THE GROUNDWATER FLOW ON TRACE ELEMENT DISTRIBUTION IN THE RIVER DANUBE DEPOSITS IN THE SOUTHERN PART OF THE PANNONIAN BASIN (HUNGARY)

ERIKA HRABOVSZKI

Department of Mineralogy, Geochemistry and Petrology, University of Szeged
H-6701 Szeged, P. O. Box 651, Hungary

ABSTRACT

Processes controlling the groundwater trace element composition were studied in the River Danube deposits. Cluster analysis based on trace element concentration was used to separate the different aquifer systems. Separation resulted two groups, which correspond to the midline and to the discharge area of the same water flow. Principal component and correlation analyis were used to determine the geochemical processes, which control the trace element distribution of the groundwater in these hydrological regions. Geochemical computer models helped to simulate the possible chemical processes. PHREEQE was used to model the chemical composition of the average midline water, and PHREEQM to simulate the processes taking place along the flow path of groundwater. In the midline area, the main processes controlling the trace element content are dissolution of calcite, dolomite, and Fe- Mn-oxides, aluminosilicate weathering, and As adsorption. In the discharge area, cation exchange, As desorption and organic matter decomposition play an important role in water chemistry.

Key words: hydrology, principal component- and cluster analysis, ion exchange, adsorption, weathering, dissolution, organic matter decomposition.

INTRODUCTION

Previous studies of the distribution of trace metals in natural waters have emphasised the importance of different geochemical processes controlling the trace element content such as dissolution and precipitation of carbonate minerals, feldspar weathering (Paces, 1973; Chou, Wollast 1984; Berner, 1981; Murphy, Helgeson, 1987) redox reactions, oxidation of organic materials, sorption and cation exchange (Chapelle, Knobel, 1983; Appelo et al., 1989; Hrabovszki, 1998).

According to Tóth (1990) in the recharge and in the discharge area of the same water flow system, different chemical processes can play an important role in the groundwater chemistry. The main chemical processes modifying the chemical composition of the groundwater are dissolution of minerals and oxidation in the recharge area, precipitation, reduction or water mixing in the discharge area. Groundwater flow influences hydrochemical patterns. In the direction of the water flow ion exchange has fundamental importance in water-rock interaction (Appelo, Postma, 1993). Along the flow path the distribution of some components may follow a chromatographic pattern because of the differences in the retardation for the various cations.

From tne hydrological point of view, the Pannon basin is a large (1000,000 km^2), non-uniform multilayer flow-system formed mainly during the late Tertiary and Quaternary periods (Erdélyi et al., 1972; Erdélyi, 1979). The system is composed of two flow regions: an intermediate flow regime in the Pleistocene sediments and a regional one in the deeper zone (2500 m). In the Pleistocene sediments of the Great Hungarian Plain two water types exist (Erdélyi, 1979). The coarser sediments contain a calcium- and magnesium-bicarbonate water type and in the finer grained sediments sodium-bicarbonate water is characteristic. In the Ca-Mg-HCO_3 type waters the concentration of the dissolved solids is lower than in the Na-HCO_3 type waters.

Geochemical computer models have been developed to calculate the distribution of species when minerals dissolve, different types of waters mix or ion exchange takes place in the system. In the present study PHREEQE (Parkhurst et al., 1990) was used to model the composition of the avarage water type, and PHREEQM (Nienhuis et al., 1993) to simulate ion exchange.

In an earlier study (Hrabovszki, Varsányi 1998), processes which controll the trace element concentrations of groundwaters in the Great Hungarian Plain were determined. These processes are: dissolution of carbonate minerals, ion exchange, oxidation, reduction, albite weathering and formation of secondary minerals. On the basis of the trace metal content (As, Fe, Mn, Zn^{2+}, Ba^{2+}, Sr^{2+}, Li^{+}, Si) the study area was divided into three units, which correspond to different hydrogeological regions: the River Körös basin, the River Maros alluvial fan and the River Danube deposits. The aim of the present work is to separate the aquifer system in the intermediate flow regions of the River Danube deposits on the basis of the trace chemical components of the groundwater, to establish the main processes controlling the chemical features of these elements in the groundwater of the different aquifers and to present the trace element pattern in the water flow direction.

GEOLOGICAL SETTINGS

The location of the studied area can be seen in Fig. 1. The geology of the River Danube deposits was described earlier (Hrabovszki, Varsányi, 1998).

Materials and Methods

In situ measurements and laboratory major and trace element analyses were used to establish the geochemical evolution of the groundwater in the studied aquifers. Groundwater samples from 52 water wells of different depths (174-605 m) from the River Danube deposits were collected, cooled and analyzed within 24 hours. Alkalinity, pH, Ca^{2+}, Mg^{2+}, Na^{+}, As, Fe, Mn, Zn^{2+}, Ba^{2+}, Sr^{2+}, Li^{+}, Si, Cl^{-} and chemical oxygen demand (COD) were determined (Hrabovszki, Varsányi, 1998).

22 core samples of 61-468 m depth were subjected to XRD analysis using a DRON-UM 1 X-ray diffractometer. X-ray studies show that sediments over the study area contain quartz, plagioclase, feldspar (mainly albite), calcite, dolomite, illite, chlorite and muscovite (Varsányi, Ó. Kovács, 1994).

The great number of the samples and parameters to be processed require a statistical approach. Classification of the water samples on the basis of the trace elements is one of the classical tasks of multivariate statistics (Marriott, 1974; Mardia et al., 1979). Cluster analysis (Le Maitre, 1982) was used to divide the water samples into groups. All variables were brought into the same range by scaling the values for each constituent. The similarity measure was the correlation coefficients. The groups of highest similarity were connected by the unweighted pair group average method. This algorithm results in clusters containing samples with close values. Principal component analysis and correlation analysis (Sváb, 1979) were applied to determine what chemical processes play important roles in the trace element distribution of the ground water in each cluster.

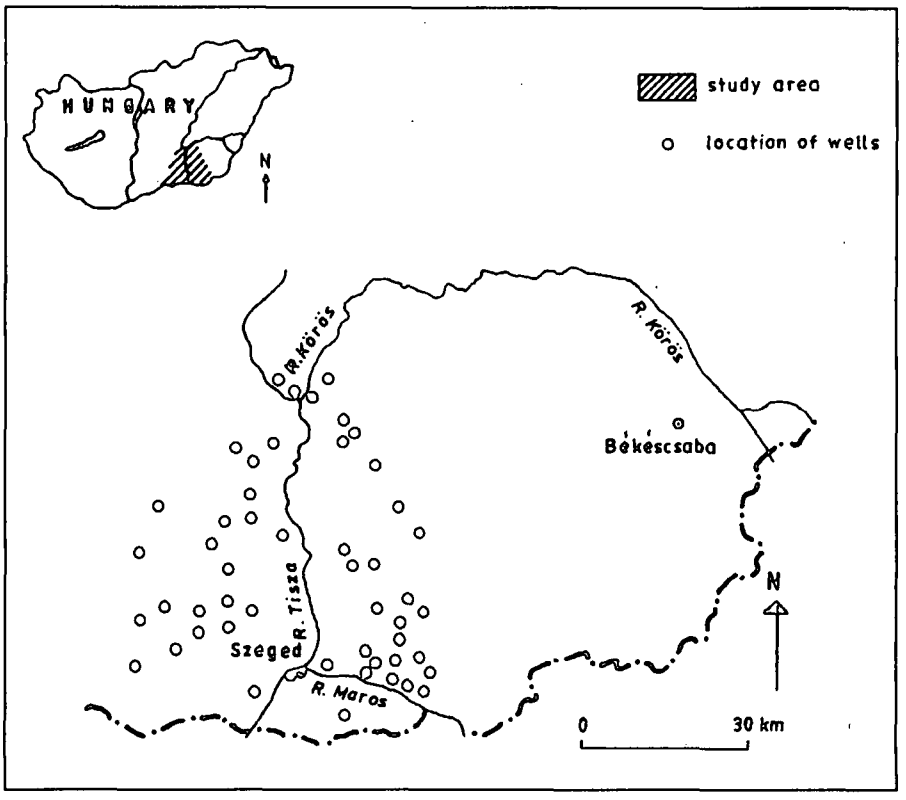

Fig. 1. Location of the water samples in the study area.

Results and Discussion

On the basis of the frequency distributions of the trace components (As, Fe, Mn, Zn^{2+}, Ba^{2+}, Sr^{2+}, Li^{+}, Si), it was established that the groundwater quality is not uniform throughout the study area. Samples represent more than one population. This possibly means that different processes can influence the distribution and mobility of the trace element composition in the groundwater from different depths or locations. In order to investigate geochemical processes which may influence the trace element distribution in groundwater of the study area, the first task was to separate the different aquifer systems from each other.

Cluster analysis of 52 water samples based on trace elements (As, Fe, Mn, Zn^{2+}, Ba^{2+}, Sr^{2+}, Li^{+}, Si) resulted in two groups, which are shown in Fig 2. Separation based on the distribution of major elements (Na^{2+}, Ca^{2+}, Mg^{2+}) gives very similar location of groups (Hrabovszki, Varsányi, 1998) to Group 1 and Group 2. Group 1 belongs to the throughflow (midline) area, Group 2 to the discharge area of the same groundwater flow system (Fig. 3). Comparing the mean valus of the major and trace element concentrations of the groups (Table 1), the throughflow area can be characterized by higher Ca^{2+}, Mg^{2+}, Ba^{2+}, Sr^{2+}, Fe, Mn, Si content, and lower Na^{+}, As, Li^{+} concentration. Erdélyi (1979) determined the potentiometric contours of the Pleistocene aquifers to the depth of 200-400 m. The potentiometric

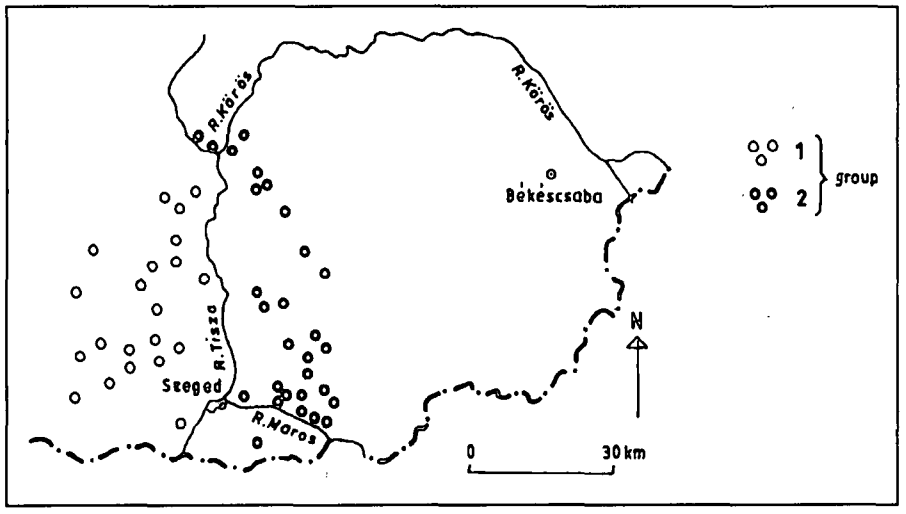

Fig. 2. Location of the groundwaters characterized by different water quality on the basis of the trace element content.

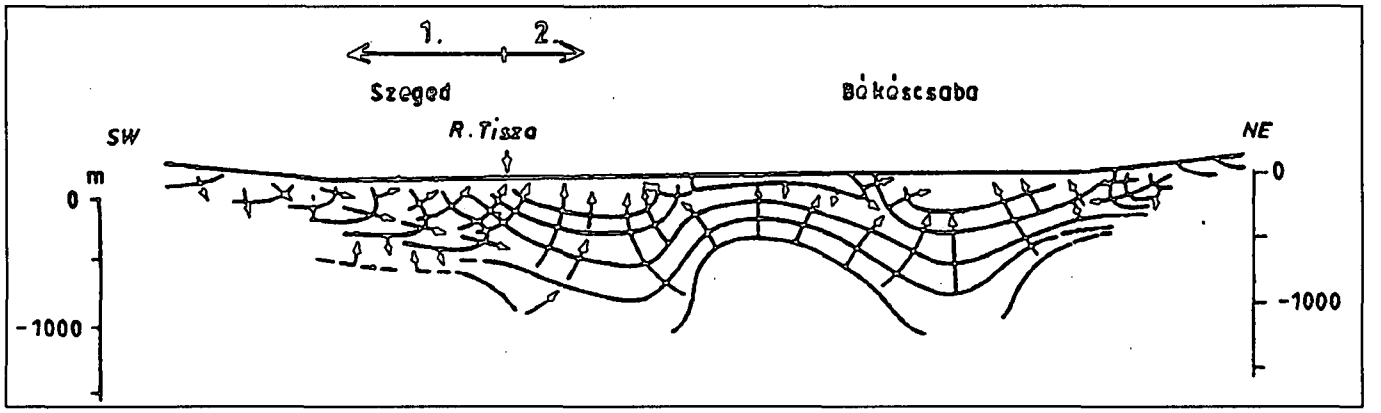

Fig. 3. The piezometric contours and water flow directions by Erdélyi (1976) with the location of the groups separated by cluster analysis.

contours indicate that in the generally flows from west to east in the RiverDanube deposits. In the study area from West to East – in the West-East water flow direction - Ba^{2+}, Sr^{2+}, Fe, Mn, Si content decreases, while As, Zn^{2+} and Li^{+} increase.

In order to determine what reactions occure between groundwater and sediments in each aquifer, principal component analysis was used. Only those chemical parameters can be used up for the calculation which distribution in each group is normal, therefore the second step was to study the normality of pH and alkalinity, COD, Ca^{2+}, Mg^{2+}, Na^{+}, As, Fe, Mn, Zn^{2+}, Ba^{2+}, Sr^{2+}, Li^{+}, Si concentration distribution in groups with Kolmogorov-test (Füst, 1997). According to the result of the Kolmogorov-test, the frequency distribution of pH and alkalinity, COD, Ca^{2+}, Mg^{2+}, Fe, Ba^{2+}, Sr^{2+}, Li^{+}, Si can be described as lognormal in Group 1. In Group 2. distribution of pH and COD, Ca^{2+}, Mg^{2+}, Na^{+}, As, Fe, Mn, Zn^{2+}, Ba^{2+}, Sr^{2+}, Li^{+}, Si concentration can be approached with lognormal distribution.

GEOCHEMISTRY OF THE TRACE ELEMENTS IN THE THROUGHFLOW AREA

In the Group 1. principal component analysis was carried out with the logarithmic value of pH and logarithmic transformed concentration of, Ca^{2+}, Mg^{2+}, Fe, Ba^{2+}, Sr^{2+}, Li^{+}, Si, alkalinity and COD. Results of the calculation are summarized in Table 2. In the first factor alkalinity, Mg^{2+}, Sr^{2+}, Ba^{2+} show the highest value. This factor also has some influence on Li^{+} content of the groundwater. On the basis of the correlation matrix (Table 3) Sr^{2+} displays good correlation with Na^{+}, Ba^{2+} and Mg^{2+}. Correlation between Mg^{2+} and Na^{+} is tighter ($r_{Mg^{2+}\text{-}Na^{+}} = 0{,}53$) than between Mg^{2+} and Ca^{2+} ($r_{Mg^{2+}\text{-}Ca^{2+}} = 0{,}28$). Ba^{2+} has positive correlation with Mg^{2+} and Na^{+} concentration. Correlation of Li^{+} content with Na^{+} and Ba^{2+} is moderate, but it is also positive.

The X-ray diffraction analysis showed the presence of albite, muscovite, illite, calcite and dolomite in the sediment. Albite dissolution and ion exchange on clay minerals are

Table 1. Mean chemical compositions and standard deviations in the groups.

		River Danube deposits							
		Group 1.				Group 2.			
		mean	s. d.	minimum	maximum	mean	s. d.	minimum	maximum
Alkalinity	mequ./l	5,23	0,45	4,50	6,10	6,42	2,06	5,00	13,90
COD	mg/l	1,79	0,66	0,80	3,50	2,56	0,90	1,30	4,60
pH		7,59	0,13	7,30	7,80	7,80	0,18	7,40	8,10
Cl^{-}	mmol/l	0,09	0,03	0,06	0,17	0,16	0,17	0,08	0,87
Na^{+}	mmol/l	0,95	0,22	0,60	1,38	3,55	3,50	1,17	6,58
Ca^{2+}	mmol/l	1,41	0,15	1,13	1,70	0,70	0,35	0,12	1,39
Mg^{2+}	mmol/l	0,94	0,11	0,79	1,15	0,53	0,28	0,08	1,13
Ba^{2+}	mmol/l	0,00110	0,00025	0,00051	0,00145	0,00082	0,00034	0,00020	0,00174
Sr^{2+}	mmol/l	0,00400	0,00070	0,00250	0,00540	0,00350	0,00170	0,00040	0,00600
As	mmol/l	0,00010	0,00010	0,00000	0,00035	0,00050	0,00040	0,00003	0,00173
Fe	mmol/l	0,00480	0,00200	0,00170	0,00106	0,00250	0,00180	0,00040	0,00830
Zn^{2+}	mmol/l	0,00014	0,00010	0,00000	0,00044	0,00018	0,00010	0,00006	0,00040
Mn	mmol/l	0,00080	0,00020	0,00052	0,00113	0,00065	0,00020	0,00015	0,00094
Li^{+}	mmol/l	0,00050	0,00020	0,00020	0,00130	0,00084	0,00040	0,00030	0,00210
Si	mmol/l	0,450	0,042	0,380	0,545	0,354	0,042	0,264	0,439
Al^{3+}	mmol/l	0,00				0,00			
T	^{0}C	20,5	2,5	16,0	26,0	24,1	3,5	18,0	30,0
$\log P_{co2}$		-2,14	0,13	-2,38	-1,89	-2,28	0,16	-2,56	-1,91
depth	m	313,8	80,0	200,0	500,0	354,4	104,0	174,0	605,0
No of sample		21				31			

thought to be the source of Na^+ in groundwaters. Fresh water is dominated by Ca^{2+} and HCO_3^- (Appelo, Postma, 1993). Cation exchangers take up Ca^{2+} from the water and release Na^+ if the Ca^{2+} concentration in the groundwater is relatively high to the concentration of Na^+ in the exchange position of clay minerals (Robertson, 1991), which assumes that the sediment was flushed by salt water before the fresh water intrusion. The result of the cation exhange the water quality changes from $Ca(HCO_3)_2$ to $NaHCO_3$. Na^+ does not show strong negative correlation with Ca^{2+} (Table 3), which suggests that not the ion exchange of Ca^{2+} for Na^+ but albit dissolution is likely to be the main process supplying Na^+ in the study area. The first step of the irreversible albit dissolution is the exchange of the Na^+ content of albit for H^+. The necessary H^+ is supplied by the reaction of CO_2 origined by organic matter decomposition and water. In the lattice

Table 2. Result of the principal component analysis for Group 1 (λ is Eigenvalue)

	I.	II.	III.	IV.
alkalinity	0,868	-0,007	0,200	0,050
pH	-0,118	0,316	-0,550	-0,580
COD	0,091	0,348	0,721	0,214
Ca^{2+}	0242	0,869	-0,284	0,189
Mg^{2+}	0,938	0,029	0,104	0,167
Fe	-0,302	-0,357	-0,063	0,640
Ba^{2+}	0,903	-0,123	-0,132	-0,130
Sr^{2+}	0,825	-0,435	0,212	0,083
Li^+	0,644	-0,183	0,336	-0,364
Si	0,223	0,890	-0,273	0,138
λ	3,766	2,135	1,209	1,034
λ%	46,26	26,22	14,82	12,70

Table 3. Correlation matrix of the chemical components of Group 1

	alk.	pH	COD	Na^+	Ca^{2+}	Mg^{2+}	As	Fe	Zn^{2+}	Mn	Ba^{2+}	Sr^{2+}	Li^+	Si
alk.	1,00													
pH	0,07	1,00												
COD	0,05	0,37	1,00											
Na^+	0,41	-0,39	-0,12	1,00										
Ca^{2+}	0,19	0,01	0,14	-0,32	1,00									
Mg^{2+}	0,87	-0,13	0,09	0,53	0,28	1,00								
As	0,12	0,09	-0,16	0,41	-0,71	-0,09	1,00							
Fe	-0,17	-0,13	-0,01	-0,08	-0,10	-0,23	0,07	1,00						
Zn^{2+}	-0,16	-0,23	0,20	-0,03	0,43	0,01	-0,35	0,26	1,00					
Mn	-0,46	-0,12	0,06	-0,55	0,49	-0,26	-0,74	0,16	0,31	1,00				
Ba^{2+}	0,66	-0,15	0,03	0,68	0,21	0,73	0,09	-0,33	0,12	-0,52	1,00			
Sr^{2+}	0,67	-0,17	0,10	0,86	-0,25	0,74	0,27	-0,18	-0,16	-0,51	0,71	1,00		
Li^+	0,08	-0,08	-0,36	0,33	0,33	0,12	0,22	-0,03	0,25	-0,24	0,40	0,1	1,00	
Si	0,18	0,02	0,18	-0,38	0,87	0,27	-0,73	-0,22	0,37	0,41	0,15	-0,25	0,08	1,00

of albit Mg^{2+} and Ba^{2+} does not occure (Koch, Sztrókay, 1967). Mg^{2+} can be found in the lattice of muskovite and illite. In muscovite and illite lattice Sr^{2+}, Ba^{2+}, in some cases Li^+ can substitute K^+. The results of the calculations indicate that different mineral phases are likely to dissolute at the same time in the study area. Na^+ is produced by irreversible albite dissolution, Sr^{2+}, Ba^{2+}, Li^+ concentration of the groundwater is probably determined by the dissolution of muscovite and illit. In the first factor pH correlates negatively with Mg^{2+}, Ba^{2+}, Sr^{2+} and Li^+ content, which suggests that increase in H^+ concentration of the water influences the dissolution rate of the mineral phases and Mg^{2+}, Ba^{2+}, Sr^{2+}, Li^+ and Na^+ content of the groundwater increases with decreasing pH.

The second factor contains Ca^{2+} and Si with the highest values. Ca^{2+} can came from the dissolution of calcite. Calcite dissolution is an equilibrium process which is controlled by the dissolved CO_2 originated from organic matter transformation (Appelo, Postma, 1993). In the study area Ca^{2+} concentration increases in the direction of the water flow (Fig. 4). The strong correlation between Ca^{2+} and Si ($r_{Si.Ca^{2+}}$ = 0,87) can be explained with the fact that change in H^+ concentration modifies not only Ca^{2+}, but also Si content of the groundwater. Si can be originated from irreversible feldspar weathering and dissolution of amorphous quartz (Grasselly, 1988). Solubility of amouphous quartz increases with increasing pH (Grasselly, 1988; Appelo, Postma,

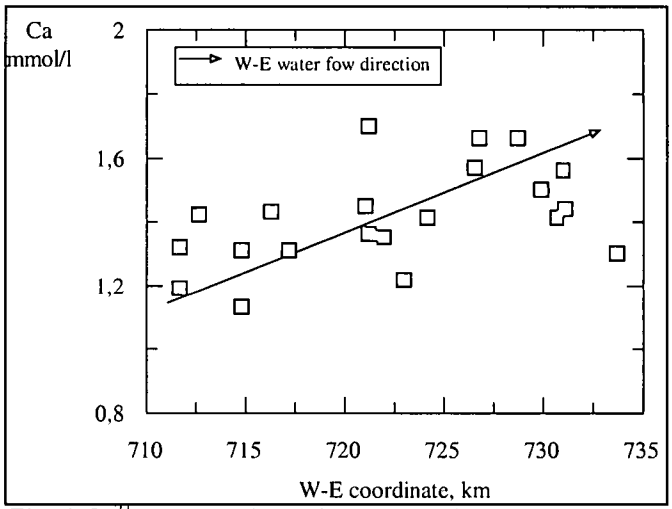

Fig. 4. Ca^{2+} concentration – distance graph.

1993). Since Si and Ca^{2+} concentration increases with decreasing pH, therefore Si content is probably controlled by the feldspar weathering not by the dissolution of quartz. Correlation between Si content and the temperature of the water samples cannot be found, therefore the feldspar weathering is controlled by only H^+ concentration of the groundwater. On the basis of the correlation matrix (Table 3) not only Si but also As displays correlation with Ca^{2+}. In natural waters As exists as $HAsO_4^{2-}$, $H_2AsO_4^-$, H_3AsO_4.

Table 4. Result of the principal component analysis for Group 2. (λ is Eigenvalue)

	I.	II.	III.	IV.
pH	-0,497	0,050	0,278	0,595
COD	-0,623	0,029	0,372	-0,432
Na^+	-0,0844	0,164	0,040	0,077
Ca^{2+}	0,960	-0,161	0,049	-0,026
Mg^{2+}	0,968	-0,021	0,063	-0,036
As	-0,543	-0,601	-0,059	0,149
Fe	0,191	-0,127	0,810	-0,348
Mn	0,420	-0,689	0,029	0,300
Zn^{2+}	0,207	0,271	0,508	-0,480
Ba^{2+}	0,930	0,139	0,132	0,126
Sr^{2+}	0,967	0,095	0,031	0,030
Li^+	-0,085	0,470	-0,050	0,101
Si	0,680	0,213	-0,243	-0,090
λ	6,097	1,277	1,222	1,040
λ%	63,27	13,25	12,68	10,80

Arsenic can be adsorbed as an oxianion on the surface of the sediment (clay), Fe-, Mn-oxyhydroxides and organic matters (Onishi, Sandell, 1955; Laxen, 1985). Arsenic concentration does not show correlation with Fe and COD content of the water (Table 3), but there is a negative correlation between As and Mn, Si. Considering all these above the clay content of the sediment may play an important role in As adsorption. The negative correlation between Ca^{2+} and As ($r_{As\text{-}Ca^{2+}}$ = -0,71) can be explained with the change in pH of the groundwater. According to the experimets by Balistrieri, Murray (1982), arsenic adsorption on the surface of sediments increases with increasing H^+ concentration, the solubility of calcite increases with decreasing pH. The negative correlation between As and Mn shows the change in H^+ concentration. Mn exists in sediments as Mn-oxyhydroxides. Solubility of Mn-oxyhydroxides depends on H^+ concentration of the water (Grasselly, 1988). Because of decreasing pH Mn-oxides dissolute from the sediment producing higher Mn content in the water, while As adsorption on clay minerals increases with decreasing pH.

In the third factor COD and pH can be found with the highest value. The connection between these components is negative, therefore this factor can be connected with organic matter decomposition. Transformation of organic matters produces not only CO_2, but also water soluble organic components. The concentration of the organic components in water is proportional to COD (Varsányi, 1985).

Fe displays negative correlation with pH in the fourth factor. Fe exists as Fe-oxyhydroxides in sediments. Solubility of Fe-oxides depends on the H^+ content of the water, dissolution of Fe-oxyhydroxides increases - similarly to Mn - with decreasing pH (Grasselly, 1988).

GEOCHEMISTRY OF THE TRACE ELEMENTS IN THE DISCHARGE AREA

According to the result of Kolmogorov-test, principal component analysis was carried out with logarithmic value of pH and the logarithmic transformed concentration of COD, Ca^{2+}, Mg^{2+}, Na^+, As, Fe, Mn, Zn^{2+}, Ba^{2+}, Sr^{2+}, Li^+, Si, which resulted four factors above 1,000 (Table 4). In the first factor Na^+ shows good negative correlation with Ca^{2+}, Mg^{2+}, Sr^{2+} and Ba^{2+}. On the basis of Fig. 5A-D concentration of Ca^{2+}, Mg^{2+}, Sr^{2+} and Ba^{2+} decreases, Na^+ content increases along the flow path. The large increase in Na^+ and loss of Ca^{2+} and Mg^{2+} along the water flow show the typical pattern of cation exchange (Appelo, Postma, 1993). Taking all above into consideration, Sr^{2+} and Ba^{2+} content of the groundwater is likely to be controlled by ion exchange in the discharge area. In the same factor pH and COD can be found with the same sign, therefore this connection cannot be explained by the degradation of organic matters. According to the computer simulation of Varsányi (1994), in the study area H^+ concentration of water decreases along the flow path. On the basis of the correlation matrix (Table 5), pH correlates negatively with Ca^{2+}, Mg^{2+}, Sr^2, Ba^{2+} and positively with Na^+, which suggests that H^+ can also take part in ion exchange resulting increase in pH in the direction of water flow. Si concentration shows negative correlation with COD and pH in the first factor (Table 4). Silica distribution in groundwater cannot only be controlled by dissolution/precipiation processes of SiO_2 but also formation of secondary aluminosilicates (Grasselly, 1988). Solubility of SiO_2 increases with decreasing H^+. In the study area, Si content in the groundwater decreases with increasing pH, which means that Si concentration of the groundwater is mainly controlled by the formation of secondary silicates.

$$2NaAlSi_3O_8 + 2H^+ + 9H_2O = Al_2Si_2O_5(OH)_4 + 2Na^+ + 4H_4SiO_4:$$
(albite) (kaolinite)

Table 5. Correlation matrix of the chemical components of Group 2

	alk.	pH	COD	Na^+	Ca^{2+}	Mg^{2+}	As	Fe	Zn^{2+}	Mn	Ba^{2+}	Sr^{2+}	Li^+	Si
alk.	1,00													
PH	0,09	1,00												
COD	0,59	0,09	1,00											
Na^+	0,42	0,43	0,55	1,00										
Ca^{2+}	-0,44	-0,56	-0,42	-0,92	1,00									
Mg^{2+}	-0,39	-0,49	-0,45	-0,93	0,96	1,00								
As	0,17	0,30	0,51	0,50	-0,41	-0,48	1,00							
Fe	-0,05	0,00	0,38	-0,08	0,18	0,13	0,25	1,00						
Zn^{2+}	-0,13	0,02	-0,02	-0,09	0,09	0,12	-0,17	0,08	1,00					
Mn	-0,55	-0,11	-0,20	-0,40	0,47	0,33	0,12	0,22	0,13	1,00				
Ba^{2+}	-0,31	-0,30	-0,53	-0,80	0,79	0,83	-0,59	0,09	0,23	0,33	1,00			
Sr^{2+}	-0,42	-0,45	-0,52	-0,94	0,89	0,94	-0,59	0,09	0,11	0,33	0,83	1,00		
Li^+	0,53	0,17	0,160	0,10	-0,21	-0,10	-0,20	-0,14	0,13	-0,47	0,06	0,03	1,00	
Si	-0,02	-0,46	-0,31	-0,69	0,76	0,78	-0,42	0,02	0,17	0,24	0,70	0,74	0,14	1,00

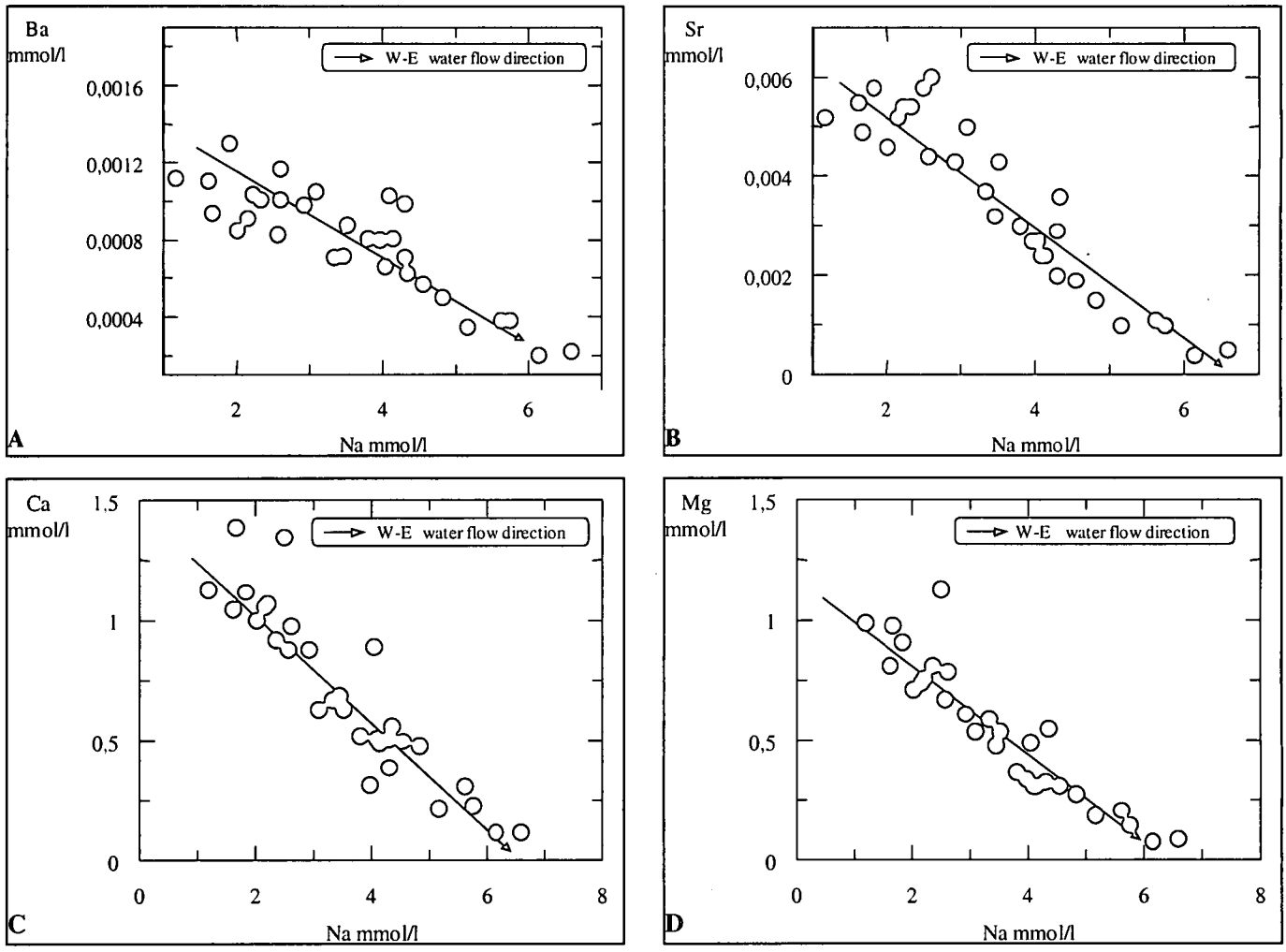

Fig. 5. Relationship between Na^+ concentration and **(A)** Ba^{2+}, **(B)** Sr^{2+}, **(C)** Ca^{2+}, **(D)** Mg^{2+}

In the first factor (Table 4) arsenic and pH display the same, negative sign. This suggests that anion adsorption, which depends on H^+ concentration of the aquatic system, may play a role. The extent of arsenic adsorption on the sedimentary rocks decreases with increasing pH (James, Healy, 1972; Balistrieri, Murray, 1982). Sediments under South Plain of Hungary have a high arsenic adsorption potential. The factors controlling the extent of the arsenic adsorption in this area are pH and the composition of the sediments such as organic matter, Fe-oxyhydroxide content and the rate of the clay fraction (Hrabovszki, 1995). The positive correlation between As and COD ($r_{As\text{-}COD} = 0{,}51$) means that degradation of organic matters in sediments can also controll arsenic content in waters. Arsenic can be adsorbed on the surface of organic matters in sediments as an oxianion (Onishi, Sandell, 1955, Laxen, 1985), and it goes into solution with the oxidative transformation of organic matters. The positive connection between Mn and As in the second factor suggests that Mn-oxyhydroxides of sediments can play a role in arsenic distribution of the groundwater. Mn-oxides can adsorb As on their surface (Takamatsu et al., 1985; Newman et al., 1985; Baistrieri, Murray, 1986). Oxidative deggradation of organic matters is carried out with O_2, NO_3^-, MnO_2, SO_4^{2-} in consecutive steps (Froehlich et al., 1979). Quantity of the burried organic matters can be brought in connection with the velocity of sedimentation (Wilson et al., 1985). At higher velocity of sedimentation the oxigen is consumed by organic matters and NO_3^-, MnO_2, and SO_4^{2-} become oxidizing substances. Mn-oxide is reduced and it goes into solution, which results the mobilization of arsenic. In the third factor Fe with Zn^{2+}, in the fourth factor Fe, Zn^{2+} and COD show positive correlation with each other and pH shows the highest value. Zn^{2+} adsorption on Fe-oxides plays an important role in Zn^{2+} distribution in natural waters (Johnson, 1986). Fe-oxyhydroxides can take part in the oxidative transformation of organic matters as oxidizing substances (Froechlich et al., 1979; Balistrieri, Murray, 1982). Fe^{3+} is reduced, Fe^{2+} goes into solution resulting mobilization of Zn^{2+}. Degradation of organic matters produces not only CO_2 but also water soluble organic components such as humic and fulvic acids (Varsányi, 1985). Concentration of these components corresponds to the increase in COD and decrease in pH.

COMPUTER SIMULATION OF PROCESSES

According to the results of the principal component analysis, different geochemical processes can control the trace metal distribution of groundwater in the midline and in the discharge area. Water quality is likely to be determined by dissolution of sediments in the midline area. The degree of dissolution depends on the quantity of the dissolved CO_2 in water, which is originated from the oxidative

transformation of organic matters. In the discharge area, Sr^{2+} and Ba^{2+} concentration similarly to Ca^{2+} and Mg^{2+} content seems to be controlled by cation exchange. To test the above hypotheses, forward method of geochemical modelling (Plummer, 1984) was used to perform the calculation. The first step of the modelling was to assume geochemical reactions in the water-rock system, then water quality was calculated by geochemical computer programs and compared to the measured data. Since in the midline and in the discharge area different geochemical processes are likely to control the water quality, 2-stage model for evolution of groundwater is suggested.

The first stage of simulation dealt with modelling the water composition of the midline area. The partial pressure of CO_2 used for the calculation, was $10^{-1.95}$ atm, which corresponds to Pco_2 in the root zone. The dissolution of calcite was considered to be the source of Ca^{2+}, therefore under open system conditions ($Pco_2 = 10^{1.95}$ = constans) the clean water was brought into equilibrium with calcite first. Albite dissolution is thought to be the source of Na^+ in this area. Since albit dissolution is an irreversible process, modelling this process in a thermodynamic way is impossible, therefore the irreversible albit dissolution was represented by adding 1,0 mmol/l Na^+ into thre solution. Assuming that the trace elements (Sr^{2+}, Ba^{2+}, Li^+, Si, As, Fe, Mn, Zn^{2+}) and Mg^{2+} go into solution by irreversible dissolution in the study area, irreversible dissolution of these elements was carried out by adding Sr^{2+} (0,004 mmol/l), Ba^{2+} (0,001 mmol/l), Li^+ (0,0005 mmol/l), Si (0,45 mmol/l), As (0,0001 mmol/l), Fe (0,005 mmol/l), Mn (0,0008 mmol/), Zn^{2+} (0,0015 mmol/l), Mg^{2+} (1,00 mmol/l) into the solution on the same CO_2 partial pressure. PHREEQE was used to perform the simulation of the water composition. In Table 6 the measured and the computed composition of the water show good agreement.

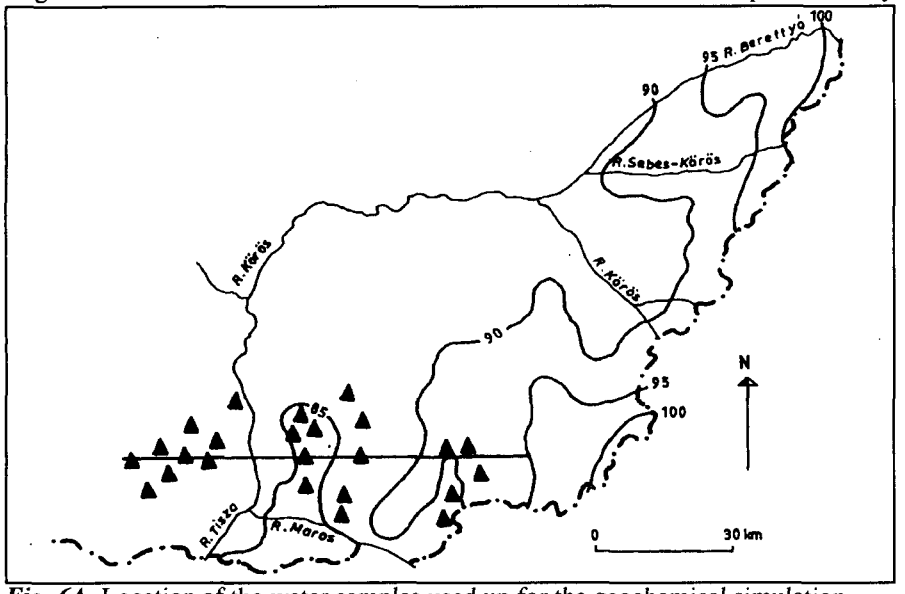

Fig. 6A. Location of the water samples used up for the geochemical simulation.

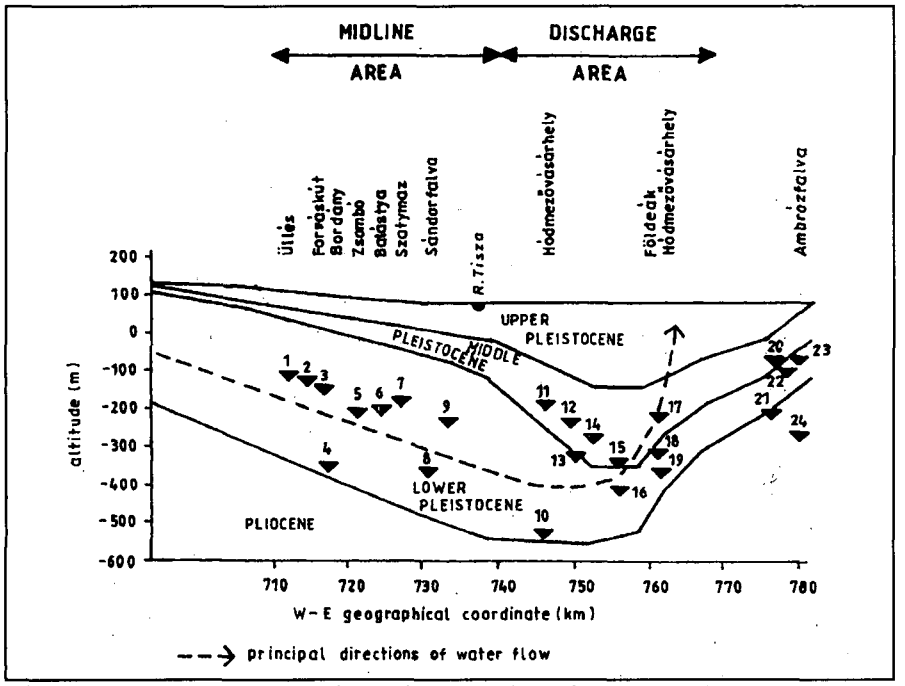

Fig. 6B. W-E cross-section and sampled sites along the cross section.

Table 6. Calculated and measured average water chemistry for Group 1.

		measured	simulate
alk	mequ./l	5,31	5,70
pH		7,59	7,50
Na^+	mmol/l	1,09	1,00
Ca^{2+}	mmol/l	1,39	1,30
Mg^{2+}	mmol/l	0,94	1,00
Ba^{2+}	mmol/l	0,0011	0,0010
Sr^{2+}	mmol/l	0,0038	0,0040
As	mmol/l	0,0001	0,0001
Fe	mmol/l	0,0047	0,0050
Zn^{2+}	mmol/l	0,0020	0,0015
Mn	mmol/l	0,0008	0,0008
Li^+	mmol/l	0,0005	0,0005
Si	mmol/l	0,4467	0,4500

The second stage was the simulation of cation exchange along the flow path in the discharge area. PHREEQM a combined geochemical and mixing model was used to simulate ion exchange. To develop the chromatographic pattern, displacement of initial water by flushing water is required (Appelo, Willemsen, 1987). The initial water forms an exchange complex on clay minerals, then the displacing water with different chemical composition flushes the initial pore water content and develops a new equilibrium between the flushing water and the exchanger resulting characteristic distribution of dissolved ions. In the discharge area, the large increase in Na^+ and the loss of Ba^{2+},Sr^{2+}, Ca^{2+} and Mg^{2+} display the typical pattern of cation exchange along the flow path (Fig. 5A-D). To model the cation exchange between Na^+ and Ba^{2+}, Sr^{2+}, Ca^{2+}, Mg^{2+}, 24 wells were chosen. The location of these wells can be seen in Fig. 6A-B.

Table 7. Chemical composition of the samples along the cross-section.

location	area	W-E coord	altitude	depth	alkalinity	COD	pH	T	Cl	Na^+	Ca^{2+}	Mg^{2+}
		km	m	m	meqv./l	mg/l		^0C	mmol/l	mmol/l	mmol/l	mmol/l
1. Üllés	midline	711,70	101	200,0	4,9	1,0	7,3	17	0,06	1,09	1,19	0,87
2. Zákány	midline	714,80	98	218,0	5,5	2,3	7,8	19	0,06	0,90	1,31	0,89
3. Forráskút	midline	716,30	94	245,0	5,3	1,9	7,7	19	0,06	0,84	1,43	0,97
4. Bordány	midline	717,20	82	437,0	5,3	0,8	7,6	24	0,08	1,25	1,31	0,98
5. Zsombó	midline	721,10	91	301,0	5,7	0,9	7,6	23	0,08	0,85	1,45	0,91
6. Balástya	midline	724,20	88	295,0	4,5	2,8	7,7	20	0,11	0,71	1,41	0,82
7. Szatymaz	midline	726,80	86	272,0	5,5	1,8	7,5	21	0,14	1,00	1,66	0,98
8. Sándorfalva	midline	730,70	84	460,0	5,0	3,5	7,7	26	0,08	0,90	1,41	0,89
9. Dóc	midline	733,00	83	300,0	5,0	1,8	7,4	20	0,08	1,38	1,30	0,89
10 .Hódmezővásárhely	discharge	746,00	78	605,0	5,4	2,1	7,9	30	0,08	3,07	0,73	0,54
11. Hódmezővásárhely	discharge	746,00	82	278,0	5,4	2,3	7,8	23	0,08	1,99	1,00	0,71
12. Hódmezővásárhely	discharge	749,20	82	324,0	5,2	2,0	7,8	21	0,08	2,15	1,06	0,74
13. Hódmezővásárhely	discharge	750,00	80	410,0	5,0	1,8	7,7	24	0,08	1,61	1,05	0,81
14. Ferencszállás	discharge	751,00	85	305,0	6,0	1,9	7,8	24	0,08	2,91	0,88	0,61
15. Kiszombor	discharge	756,50	85	420,0	6,2	1,6	7,6	25	0,11	4,13	0,49	0,31
16. Kiszombor	discharge	756,50	85	442,0	6,2	1,7	8,1	28	0,11	4,07	0,51	0,31
17. Hódmezővásárhely	discharge	757,60	82	300,0	5,9	2,6	8,0	22	0,11	5,14	0,22	0,19
18. Földeák	discharge	761,00	90	410,0	6,7	4,1	7,9	26	0,14	6,58	0,12	0,09
19. Hódmezővásárhely	discharge	761,60	84	450,0	7,7	3,3	8,3	27	0,08	7,75	0,11	0,09
20. Csanádalberti		778,00	86	156,0	16,4	10,0	8,1	23	0,39	14,80	0,33	0,34
21. Nagylak		778,60	84	292,0	15,2	8,5	7,9	23	0,37	14,64	0,50	0,52
22. Ambrózfalva		779,50	93	173,0	14,7	9,6	7,8	18	0,42	11,80	0,83	0,72
23. Csanádpalota		779,50	85	156,0	15,4	8,4	7,8	16	0,28	12,67	0,76	0,85
24. Pitvaros		780,30	87	341,0	14,5	10,7	8,0	24	0,90	13,90	0,38	0,30

Table 7 (continued)

	As	Fe	Zn^{2+}	Mn	Ba^{2+}	Li^+	Sr^{2+}	Si
	mmol/l	mmol/l	mmol/l	mmol/l	mmol/l	mmol/l	mmol/l	mmol/l
1.	0,0003	0,0056	0,0001	0,0006	0,0011	0,0005	0,0036	0,4010
2.	0,0004	0,0073	0,0000	0,0005	0,0010	0,0004	0,0034	0,4030
3.	0,0001	0,0058	0,0001	0,0006	0,0011	0,0006	0,0033	0,4610
4.	0,0002	0,0045	0,0002	0,0006	0,0013	0,0013	0,0041	0,4610
5.	0,0001	0,0032	0,0001	0,0007	0,0012	0,0006	0,0031	0,4690
6.	0,0001	0,0032	0,0004	0,0009	0,0008	0,0003	0,0027	0,4700
7.	0,0001	0,0081	0,0004	0,0009	0,0012	0,0006	0,0034	0,4630
8.	0,0001	0,0041	0,0002	0,0007	0,0012	0,0004	0,0034	0,4650
9.	0,0002	0,0042	0,0001	0,0007	0,0011	0,0005	0,0045	0,4120
10.	0,0001	0,0019	0,0001	0,0007	0,0011	0,0008	0,0050	0,3680
11.	0,0005	0,0018	0,0001	0,0009	0,0009	0,0006	0,0046	0,3500
12.	0,0004	0,0004	0,0001	0,0008	0,0009	0,0011	0,0052	0,3690
13.	0,0001	0,0025	0,0002	0,0008	0,0011	0,0006	0,0055	0,3920
14.	0,0004	0,0022	0,0001	0,0007	0,0010	0,0007	0,0043	0,3470
15.	0,0003	0,0031	0,0002	0,0005	0,0008	0,0007	0,0024	0,3260
16.	0,0002	0,0029	0,0002	0,0007	0,0010	0,0007	0,0024	0,3240
17.	0,0006	0,0021	0,0001	0,0005	0,0004	0,0006	0,0010	0,2820
18.	0,0004	0,0012	0,0000	0,0004	0,0002	0,0007	0,0005	0,2640
19.	0,0007	0,0037	0,0000	0,0003	0,0003	0,0006	0,0006	0,2720
20.	0,0001	0,0027	0,0002	0,0005	0,0008	0,0018	0,0027	0,3320
21.	0,0000	0,0033	0,0000	0,0004	0,0009	0,0017	0,0035	0,3650
22.	0,0005	0,0050	0,0010	0,0037	0,0010	0,0013	0,0049	0,3600
23.	0,0001	0,0060	0,0002	0,0007	0,0012	0,0015	0,0059	0,3280
24.	0,0001	0,0019	0,0006	0,0007	0,0007	0,0016	0,0015	0,3470

Table 7. contains the composition of the water samples. The distance from the begining (745 km coordinate) to the end of the flow line (765 km coordinate) is 20 km. The whole distance was divided into two layers and 10 cells for the calculation. Cell length is 2.0 km. The first layer consisting of 6 cells corresponds to the coarser grained sediment, the second layer consisting of 4 cells represents the finer grained sediment. Two layers have different cation exchange capacity (CEC). CEC value in the coarser sample (Bácsalmás, 132 m) 1.20 mequiv./100g, in the finer sample (Mindszent 476 m) 1.7 mequiv./100g (Varsányi, Ó. Kovács, 1996). Considering the bulk density of 2.6 g/cm^3 and the porosity of 30%, recalculation of CEC to mequiv./l gives 75 mequiv/l for the coarser grained sediment and 105 mequiv./l for the finer grained sediment. Since the original pore water of the River Danube deposits exchanged at the end of Pleistocene (Varsányi, 1994), the present water quality differs from the original water quality. To execute the

Table 8. Simulated concentrations along the cross-section.

cells	W-E	Ca^{2+}	Mg^{2+}	Na^{+}	Ba^{2+}	Sr^{2+}
	km	mmol/l	mmol/l	mmol/l	mmol/l	mmol/l
0.	727,5	1,20	1,00	1,00	0,0010	0,0040
1.	747,0	1,08	1,04	1,41	0,0014	0,0056
2.	749,0	0,97	0,97	1,80	0,0014	0,0056
3.	751,0	0,77	0,81	2,50	0,0012	0,0049
4.	753,0	0,52	0,54	3,60	0,0008	0,0034
5.	755,0	0,24	0,25	4,80	0,0004	0,0016
6.	757,0	0,12	0,12	5,40	0,0002	0,0008
7.	759,0	0,09	0,09	5,60	0,0002	0,0006
8.	761,0	0,09	0,09	5,90	0,0001	0,0006
9.	763,0	0,09	0,09	6,04	0,0002	0,0006
10.	765,0	0,09	0,09	6,20	0,0002	0,0006
11.	780,0	0,56	0,55	13,55	0,0009	0,0037

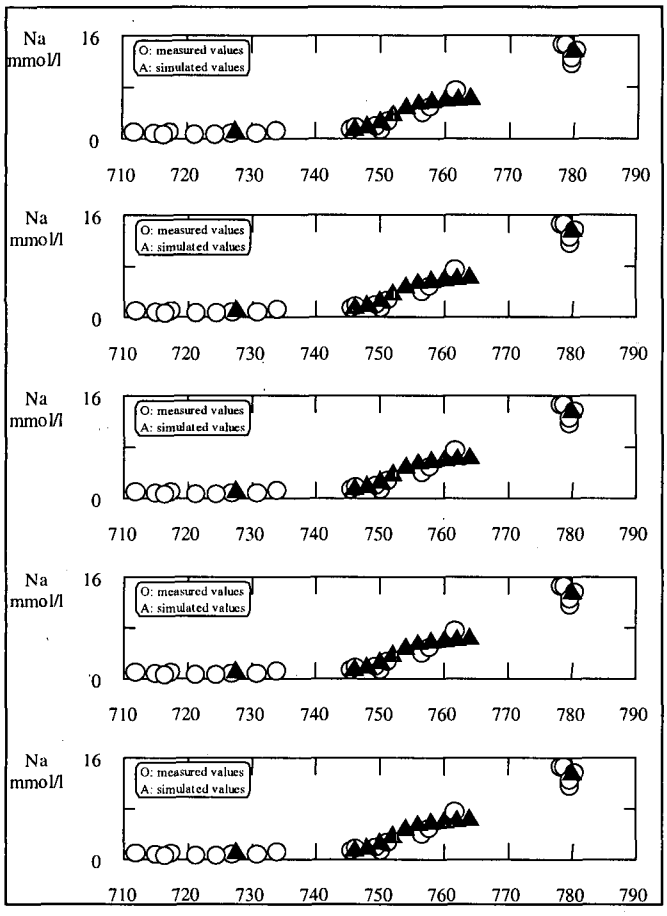

Fig. 7: Measured and simulated concentrations along the cross-section.

calculation it was necessary to know the composition of the original water. To obtain information about the original water chemistry, the water quality from an aquifer, where restricted water circulation is supposed, was chosen as initial water. This aquifer is located next to the River Danube deposits in the east part of the study area. Five water samples from this area were used to calculate the average composition of the initial water. The original pore water composition is characterized by high Na^{+} and COD concentration and low As, Fe, Mn content (Table 7, sample 20-24.). The chemical composition of the flushing water is that calculated with the help of PHREEQE at the first stage of the simulation. The whole pore volumes of cells was flushed out in 15 steps, dispersivity is 1300 m, and porosity 0.3. The ion exchange calculation was carried out by PHREEQM and the result of the calculation is summarized in Table 8. The flushing water quality corresponds to sample 0, and the initial water quality corresponds to sample 11. Along the cross section the measured and simulated concentration of Sr^{2+}, Ba^{2+}, Ca^{2+}, Mg^{2+} can be seen in Fig. 7. According to Fig. 7, in the midline area – between 710 and 745 km coordinate – there is no evidence for ion exchange. In the discharge area – between 745 and 765 km - the simulation follows quite well the pattern of concentration along the flow path, which gives an evidence for ion exchange of Sr^{2+} and Ba^{2+} for Na^{+}.

Conclusions

The groundwater chemistry does not show remarkable correlation with depth in the study area. The concentration of some studied chemical components (Sr^{2+}, Ba^{2+}, As, Si) changes in the direction of water flow.

The study area can be divided into two parts on the basis of trace components dissolved in water. Location of these groups corresponds to the midline and discharge area of the same water flow.

Geochemical processes controlling the trace element distribution are different in the midline and in the discharge area. In the midline area, the content of Sr^{2+}, Ba^{2+}, Li^{+} and Si is controlled by silicate weathering. Fe and Mn concentration in groundwater is determined by dissolution of Fe- and Mn-oxides. Weathering of the sediment depends on pH of the groundwater which is influenced by the partial pressure of CO_2 originated from organic matter transformation. Arsenic adsorption plays an important role in As distribution in water of this area. The factors controlling the extent of As adsorption are: pH, oxidative transformation of organic matters and dissolution of Mn-oxides besides the composition of the sediments (rate of the clay fraction, Fe-oxides content).

In the discharge area As content is controlled by two gechemical processes. One is As desorption from the surface of the sediments, which occurs because of increase in pH. The other is the transformation of organic matters, which influences indirectly As concentration throuhg the dissolution of Fe- and Mn-oxides.

Geochemical modelling gave an evidence for cation exchange. This process controls Sr^{2+}, and Ba^{2+} concentration in the discharge area.

Acnowledgements

The author wishes thank to I. Varsányi for the helpful discussions and the revision of the manuscript and E. Pál Molnár for the editorial handling.

References

Appelo C. A. J., Ponten J., Beekman H. E .(1989): Natural ion-chromatography during fresh-/sea water displacements aquifers: A hydrogeochemical model of the past. D. L. Miles (ed): Water-Rock Interaction, Proceedings of the 6th Water-Rock Interaction Symposium, Malvern, 23-28. A.A. Balkema, Rotterdam.

APPELO, C. A. J., POSTMA, D. (1993): Geochemistry, Groundwater and Pollution. A. A. Balkema.

APPELO, C. A. J., WILLEMSEN, A. (1987): Geochemical calculations and observations on salt water intrusions. Journal of Hydrology, **94**, 313-330.

ALTHAUS, E., TIRTADINATA, E. (1989): Dissolution of feldspar: The first step. Proceeding of the 6th International Symposium on Water - Rock Interaction, 15-17. Balkema, Rotterdam.

BALISTRIERI, L. S., MURRAY, J. W. (1982): The adsorption of Cu, Pb, Zn, Cd on goethit from major ion seawater. Geochim. Cosmochim. Acta, **46**, 1253 - 1265.

BALISTRIERI, L. S., MURRAY, J. W. (1986): The surface chemistry of sediments from Panama Basin. The influence of Mn oxides on metal adsorption. Geochim. Cosmochim. Acta, **50**, 2235-2243.

BERNER, R. A. (1981): Kinetics of weathering and diagenesis. Rewiews in Mineralogy, **8**, 111-135.

CHAPELLE, F., KNOBEL, L. L. (1983): Aqeous geochemistry and the exchangeable cation composition of glauconit in the Aquia aquifer, Mariland. Groundwater, **21**, 343-352.

CHOU, L., WOLLAST, R. (1984): Study of weathering of albite at room temperature and pressure with a fluidised bed reactor. Geochim. Cosmochim. Acta, **48**, 2205-2217.

ERDÉLYI, M., KOVÁCS, GY., KORIM, K., MAJOR, P. (1972): A felszín alatti vizek hidrológiája és hidrogeológiája. Nemzetközi hidrológiai továbbképző tanfolyam kézikönyve. VITUKI

ERDÉLYI, M. (1976): Outlines of the hydrodinamics and hydrochemistry of the Pannonian Basin. Geologica Hungarica, **20**, 287-309.

ERDÉLYI, M. (1979): A magyar medence hidrodinamikája. VITUKI közlemények, **18**.

FROEHLICH, P., KLINKHAMMER, G., BENDER, M., LUEDTKE, N. A., HEATH, G. R., CULLEN, D., DAUPHIN, P., HAMMOND, D., HARTMAN, B., MAYNARD, V. (1979): Early oxidation of organic matter in pelagic sediments of the eastern equatorial Atlantic suboxic diagenesis. Geochim. Cosmochim. Acta, **43**, 1075-1090.

FÜST, A. (1997): Geostatisztika. Kézirat. Eötvös Kiadó, Budapest.

GRASSELLY, GY. (1988): Ásványi nyersanyagok (Ásványtan II.) 190-196. Tankönyvkiadó, Budapest,.

HRABOVSZKI, E. (1995): Arzén adszorpció vizsgálata a Dél-Alföld üledékes kőzetein. Hidrol. Közl, **75**, 113-116.

HRABOVSZKI, E. (1998): A Dél-Alföld felszín alatti vizei. Hidrol. Közl. **78**, 223-230.

HRABOVSZKI, E., VARSÁNYI, I. (1998): Main and trace elements in groundwater from the quaternary sediments in the Southern Great Plain, Hungary. Acta Mineralogica-Petrographica, **39**, 151-167.

JAMES, R. O., HEALY, T. W. (1972): Adsorption of hydrolyzable metal ions at the oxid – water interface. Colloid Interface Sci., **40**(1), 42-81.

JOHNSON, C. A. (1986): The regulation of the trace element concentration in river and estuarin waters contaminated with acid mine drainage. The adsorption of Cu and Zn on amorphous Fe oxihydroxides. Geochim. Cosmochim. Acta, **50**, 2433-2438.

KOCH, S., SZTRÓKAY, K. I. (1967): Ásványtan I-II. Tankönyvkiadó, Budapest.

LAXEN, D. P. H. (1985): Trace metal adsorption /coprecipitation of hydrous ferric oxide under realistic conditions. Wat. Res., **19**, 1229-1236.

LEMAITRE R. W. (1982): Numerical petrology. Devl. Petrol., **8**. Elsevier.

MARDIA, K. V., KENT, J. T., BIBBY, J. M. (1979): Multivariate Analysis. Academic Press.

MARRIOTT, F. H. C. (1974): The interpretation of multiple observations. Academic Press.

MURPHY, W. M., HELGESON, H. C. (1987): Thermodynamic and kinetic constraints on the reaction rates among minerals and aqueous solution. III: Activated complexes and pH-dependence of the rates of feldspar, pyroxene, wollastonite, and olivine hydrolysis. Geochim. Cosmochim. Acta, **51**, 3137-3153.

NIENHUIS, P., APPELO, C. A. J., WILLEMSEN, G. (1993): PHREEQM, Adaptation of PHREEQE for use in mixing-cell flowtube.

NEWMAN, M. C., ALBERTS, J. J., GREENHUT, V. A. (1985): Geochemical factors complicating the use of AUFWUCHS to monitor bioaccumulation of arsenic, cadmium, chromium, copper and zinc. Wat. Res., **19**, 1157-1165.

ONISHI, H., SANDELL, E. B. (1955): Geochemistry of arsenic. Ceochim. Cosmochim. Acta., **7**, 1-33.

PACES, T. (1973): Steady-state kinetics and equilibrium between groundwater and granitic rock. Geochim. Cosmochim. Acta, **37**, 2641-2663.

PARKHURST, D. L., THORSTENSON, D. C., PLUMMER, L. N. (1990): PHREEQE - a computer program for geochemical calculation. U. S. Geological Survey. Water Resource Investigations. 80-96.

PLUMMER, L. N. (1984): Geochemical modelling: A comparison of Forward and Inverse methods. Proceedings in the first Canadian/American conference on Hydrogeology, Alberta, Canada.

RÓNAI, A. (1985): Az Alföld negyed időszaki földtana. Geologica Hungarica. Tom **21**, Inst. Geol. Hung. Budapest.

ROBERTSON, F. N. (1991). Geochemistry of groundwater in alluvial basins of Arizona and adjacent parts of Nevada, New Mexico and California. U. S. Geological Survey Professional Paper 1406-C.

SVÁB, B. J. (1979): Többváltozós módszerek a biometriában. Mezőgazdasági Kiadó, Budapest.

TAKAMATSU, T., KAWASHAMI, M., KOYAMA, M. (1985): The role of Mn^{2+} rich hydrous manganese oxide in the accumulation of arsenic in lake sediments. Wat. Res., **19**, 1029-1032.

TÓTH, J. (1990): Hydrogeology in petroleum exploration and basin analysis. Proceedings first Canadian / American conference on hydrogeology.

VARSÁNYI, I. (1985): Humic acids in subsurface waters from the southern Great Plain, Hungary. Acta Min. Petr., **XXVII**: 165-170.

VARÁNYI, I., Ó KOVÁCS, L. (1994): Combination of statistical methods with modelling mineral - water interaction: a study of groundwater in the Great Hungarian Plain. Appl. Geochem., **9**, 419-430.

VARSÁNYI, I. (1994): A Dél - Alföld felszín alatti vizei. Eredete, kémiai evolúció és vízmozgás a jelenlegi kémiai összetétel tükrében. Hidrol. Közl., **74**, 193-201.

VARÁNYI, I., Ó KOVÁCS, L. (1996): Chemical evolution of groundwater in River Danube deposits in the southern part of Pannonian Basin (Hungary). Ceochim. Cosmochim. Acta., **12**, 625-636.

WILSON, T. R. S., THOMSON, J., COLLEY, S., HYDES, D. J., HIGGS, N. C. (1985): Early organic diagenesis: The significance of progressive subsurface oxidation fronts in pelagic sediments. Geochim. Cosmochim. Acta, **49**, 811-822.

Received: September 12, 2001; accepted:May 29, 2002

INSTRUCTIONS FOR AUTHORS

General

Acta Mineralogica-Petrographica (AMP) publishes articles (papers longer than 4 printed pages but shorter than 16 pages, including figures and tables), notes (not longer than 4 pages, including figures and tables), and short communications (book reviews, short scientific notices, current research projects, comments on formerly published papers, and necrologies of 1 printed page) dealing with crystallography, mineralogy, ore deposits, petrology, volcanology, geochemistry and other applied topics related to the environment and archaeometry. Articles longer than the given extent can be published only with the prior agreement of the editorial board. Occasionally, in the form of supplement issues AMP publishes materials of conferences, or other events of scientific interest.

The journal accepts papers that represent new and original scientific results, which have not appeared elsewhere before, and are not in press either.

All articles and notes submitted to AMP are reviewed by two referees (short communications will be reviewed only by one referee) and are normally published in the order of acceptance, however, higher priority may be given to Hungarian researches and results coming from the Alpine-Carpathian-Dinaric region. Of course, the editorial board does accept papers dealing with other regions as well, let they be compiled either by Hungarian or foreign authors.

The manuscripts (prepared in harmony of the instructions below) must be submitted to the Editorial office in triplicate. All pages must carry the author's name, and must be numbered. At this stage (revision), original illustrations and photographs are not required, though, quality copies are needed. It is favourable, if printable manuscripts are sent on disk, as well. In these cases the use of Microsoft Word or any other IBM compatible editing programmes is suggested.

Language

The language of AMP is English.

Preparation of the Manuscript

The different parts of the manuscript need to meet the instructions below:

Title

The title has to be short and informative. No subtitles if possible. If the main title is too long, an additional shortened title is needed for the running head.

Author

The front page has to carry (under the main title) the name(s) (initials, surname), affiliation(s), current address(es), e-mail address(es) of the author(s).

Abstract and keywords

The abstract is required to be brief (max. 250 words), and has to highlight the aims and the results of the article. The abstracts of notes are alike (but max. 120 words). As far as possible, citations have to be avoided. In the near future the abstracts are going to be distributed in digital form, as well.

The abstract has to be followed by 4 to 10 keywords.

Text and citations

The format of the manuscripts is required to be: double-spacing (same for the abstract), text only on one side of the page, size 12 Times New Roman fonts. Margin width is 2.5 cm, except the left margin, which has to be 3.5 cm wide. Underlines and highlights ought not be used. Accents of Romanian, Slovakian, Czech, Croatian etc. characters must be marked on the manuscript clearly.

When compiling the paper an Introduction – Geological setting – Materials and Methods – Results – Conlclusions structure is suggested.

The form of citations is: the author's surname followed by the date of publication e.g. (Szederkényi, 1996). If there are more than two authors, after the first name the co-authors must be denoted as "et al.", e.g. (Roser et al., 1980).

References

The reference list can only consist of published papers, M.Sc., Ph.D. and D.Sc. theses, and papers in press.

Only works cited previously in the text can be put in the reference list.

Examples:

Szederkényi, T. (1996): Metamorphic formations and their correlation in the Hungarian part of Tisia Megaunit (Tisia Megaunit Terrane). Acta Mineralogica-Petrographica, **37**, 143-160.

Rosso, K. M., Bodnar, R. J. (1995): Microthermometric and Raman spectroscopic detection limits of CO_2 in fluid inclusions and the Raman spectroscopic characterization of CO_2. Geochimica et Cosmochimica Acta, **59**, 3961-3975.

Roser, B. P., Childs, C. W., Glasby, G. P. (1980): Manganese in New Zealand. In Varentsov, I. M., Grasselly, Gy. (eds.): Geology and Geochemistry of Manganese, Vol. II., 199-211. Akadémiai Kiadó, Budapest.

Nesse, W. D. (2000): Introduction to Mineralogy. Oxford University Press. 442 pp.

Pál-Molnár, E. (1998): Geology and petrology of the Ditró Syenite Massif with special respect to formation of hornblendites and diorites. Ph. D. thesis, University of Szeged, Szeged, Hungary. 219 pp.

The full titles of journals ought to be given. In case more works of the same author are published in the same year, then these has to be differentiated by using a, b, etc. after the date.

Illustrations

Finally, each figure, map, photograph, drawing, table has to be attached in three copies, they must be numbered and carry the name of the author on their reverse. All the illustrations ought to be printed on separate sheets, captions as well if possible. Foldout tables and maps are not accepted. In case an illustration is not presented in digital form then one of the copies has to be submitted as glossy photographic print suitable for direct reproduction. Photographs must be clear and sharp. The other two copies of the illustrations can be quality reproductions. Coloured figure, map or photograph can only be published at the expense of the author(s).

The width of the illustrations can be 56, 87, 118, or 180 mm. The maximum height is 240 mm (with caption).

All figures, maps, photographs and tables are placed in the text, hence, it is favourable if in case of whole page illustrations enough space is left on the bottom for inserting captions. In the final form the size of the fonts on the illustrations must be at least 1,5 mm, their outline must be 0,1 mm wide. Digital documents should be submitted in TIFF-, BMP- or JPG-format. The resolution of line-drawings must be 400 dpi, while that of photographs must be 600 dpi. The use of Corel Draw for drawing is appreciated.

Proofs and offprints

After revision the author(s) receive only the page-proof. The accepted and revised manuscripts need to be returned to the Editors either on disc, CD or as an e-mail attachment. Proofreading must be limited to the correction of typographical errors. If an illustration cannot be presented in digital form, it must be submitted as a high quality camera-ready print.

The author(s) will receive 25 free offprints. On payment of the full price, further offprints can be ordered when the corrected proofs are sent back.

Manuscripts for publication in the AMP should be submitted to:

Dr. Pál-Molnár Elemér
e-mail: palm@geo.u-szeged.hu
Phone: 00-36-62-544-683, Fax: 00-36-62-426-479
Department of Mineralogy, Geochemistry and Petrology
University of Szeged
P. O. Box 651
H-6701 Szeged, Hungary

Published in 450 copies/issue (300 in Hungary, 150 abroad).
Distributed by the Department of Mineralogy, Geochemistry and Petrology, University of Szeged, Szeged, Hungary.
Price of subscription to volume 42, 2001 (including Postage): HUF 3000.00 in Hungary, USD 15.00 in all other countries.

established in 1922

ACTA MINERALOGICA-PETROGRAPHICA

VOLUME 42 2001

HU ISSN 0365-8066

CONTENTS

Please note change of editorial staff

New Associatet Editor of AMP is Dr. Elemér Pál-Molnár

New editorial address is

Department of Mineralogy, Geochemistry and Petrology
University of Szeged
H-6701 Szeged, P. O. Box 651
Hungary

Printed in Hungary by Páskum Nyomda, H-7103 Szekszárd, P.O. Box 627